Regulation of neurogenesis termination during development

Matthew Charles Pahl
Milton, PA

B.S., Susquehanna University, 2012

A Dissertation presented to the Graduate Faculty of the University of Virginia in Candidacy for the Degree of Doctor of Philosophy

Department of Biology

University of Virginia

November 14, 2018

Sarah Siegrist (Advisor)	_____	_____
Barry Condron (First Reader)	_____	_____
Paul Adler	_____	_____
Christopher Deppmann	_____	_____
Robert Grainger	_____	_____
Adrian Halme (Dean's representative)	_____	_____

Project Summary:

A remarkable number of morphologically and functionally diverse neurons and glia make up the brain. All of these neurons are generated by the highly regulated asymmetric cell divisions of populations of neural stem cells, which are multi-potent self-renewing progenitors. As development approaches completion, neurogenesis becomes limited in some adult animals due in part to the depletion of neural stem cells. Restricting neurogenesis during development may protect the functioning of the adult brain as ectopic proliferation of neural stem cells can disrupt neural circuitry or act as seeds for tumorigenesis. To date, the molecular mechanisms that terminate cell divisions of neural stem cells are poorly understood.

Here, I describe our work characterizing factors that regulate the developmentally programmed elimination of a subset of *Drosophila* neural stem cells, termed neuroblasts, with the goal of understanding how neurogenesis becomes limited during brain development. Eight mushroom body neuroblasts generate the neurons that form the mushroom body, a structure important for some types of memory and learning. The mushroom body neuroblasts are eliminated relatively late in development by a combination of apoptosis and autophagy in late pupal stages.

We first examined the regulation of apoptosis in terminating MB neuroblast divisions. To identify genes that regulate the elimination of the MB neuroblasts, we conducted a directed RNAi screen to find cell-intrinsic regulators of MB neuroblast termination. We included candidate genes known to regulate

apoptosis, be specifically expressed in MB neuroblasts or other subtypes, and have putative binding sites near grim or sickle regulatory regions as determined by our bioinformatic analysis. From this screen, we identified 12 genes are required for the elimination of Drosophila neuroblasts.

We further characterized one gene identified from our screen, the steroid hormone-induced transcription factor E93, which down regulates PI3-kinase to activate autophagy for MB neuroblast elimination. Expression of E93 is restricted to late-staged MB neuroblasts by the cell-intrinsic temporal factors Imp and Syp. We found evidence that systemic ecdysone signaling increases E93 levels for termination. Altogether, E93 functions as a late-acting temporal factor that integrates extrinsic hormonal developmental timing cues with neuroblast intrinsic temporal state to precisely time the termination of neurogenesis during development.

Taken together, my project provides important mechanistic insight into how systemic signaling and cell intrinsic temporal progression of neural stem cells coordinates their elimination to ensure proper neural circuit formation.

Acknowledgements:

I have a great deal of gratitude to many people who assisted me over the course of this work. First, I would like to thank my advisor Sarah Siegrist for her patient guidance, excellent technical skills, and continuous support over the years. I like to thank the members of my committee: Drs. Barry Condron, Paul Adler, Robert Grainger, Chris Deppmann, and Adrian Halme for their time and valuable input. I especially want to thank Barry and Chris for the enthusiasm they bring to the Biology Department.

I have been extreme fortunate to have great lab mates. I would like to acknowledge Dr. Conor Sipe for valuable feedback. I thank the fellow past and present Siegrist lab graduate students: Xin Yuan, Chhavi Sood, Ausrfuggaman Nahid, and Emily Ross for always providing a sense of comradery.

I am especially glad to thank Dr. Susan Doyle, who worked closely on experiments with me throughout the majority of my graduate work. Susie's passion for science and optimism is inspirational. I am extremely grateful to have such a great friend and colleague during my time in graduate school.

I also would like to thank my friends and family for their support over the years. In particular I would like to thank Sumanth Manohar for years of great discussions. I also want to thank Olga Askinazi and Matt Scheffer. I thank my dad and brother for their unconditional support. I thank my mother for everything she did to raise me. Lastly, I would like to thank my amazing wife Chun for her unwavering support and patience.

Abbreviations

Dac: Daschund
Dpn: Deadpan
E93: Ecdysone induced protein 93F
EcR: Ecdysone Receptor
Ey: Eyeless
GFP: Green fluorescent protein
Grh: Grainyhead
Hb: Hunchback
Imp: Insulin-like growth factor 2 mRNA binding protein
Kr: Kruppel
MB: Mushroom body
miRHG: microRNA targeting reaper, hid, and grim
Oc: occeliless
PCNA: Proliferating cell nuclear antigen
Pdm: POU domain member
RFP: Red fluorescent protein
Rx: Retinal homeobox
Scrib: Scribble
Skl: Sickle
Syp: Syncrip
Tll: Tailless
UAS: Upstream activating sequence

Table of contents:

Chapter 1

General Introduction

Restriction of neurogenesis in development

The human brain is comprised of approximately 100 billion neurons that form the circuits responsible for coordinating behavior. The assembly of the adult neural circuitry requires the generation of an incredible number of highly specialized neuronal subtypes, which form stereotyped connections that are maintained throughout ones lifetime. The majority of these neurons are generated by the asymmetric cell divisions of multipotent self-renewing neural stem cells. With few exceptions, the entire set of neurons is generated during development, after which neurogenesis becomes restricted to specific regions of the brain. In this dissertation, I investigate the molecular mechanisms that restrict neurogenesis during development.

Adult neurogenesis often becomes restricted to only a few regions of the brain in mammals or can be completely absent in other species (Cayre et al. 2002; Bhardwaj et al. 2006; Eriksson et al. 1998). Restriction of neurogenesis to development may protect the proper size and structure of the adult brain, as aberrant neurogenesis may lead to disruption of the existing neural circuitry, interfering with the proper function of the central nervous system (Chenn & Walsh 2011; Goffart et al. 2013). Ectopic neurogenesis has been linked to several neurological disorders, including autism (Hazlett & Poe 2011; Marchetto et al. 2017; Reif et al. 2007; Valvo et al. 2013). In addition ectopic neural stem cells may act as seeds for tumorigenesis (Chesler 2012).

One consequence of restricting neurogenesis is that it limits central nervous system regeneration in response to injury or degenerative diseases. In some animals, neurogenesis continues in many regions of the central nervous system throughout adulthood, and as a consequence displays incredible capacities for regeneration. For example, axolotls and salamanders can fully regenerate their spinal cord and large regions their brain (Tazaki et al. 2017; Amamoto et al. 2016). In humans, neurogenesis becomes limited to the dentate gyrus of the adult hippocampus, although this has recently been controversial (Sorrells et al. 2018; Boldrini et al. 2018). Understanding the mechanisms that either restrict or facilitate adult neurogenesis is important for designing future stem cell therapies aimed at improving neural regeneration. In addition basic understanding of the mechanisms that regulate neurogenesis may help with designing treatments to diseases where it becomes misregulated.

In this chapter, I will review the molecular mechanisms that underlie the regulation of neural stem cell proliferation which determine when neurogenesis terminates, focusing on *Drosophila* neuroblasts as a model.

Drosophila **neuroblasts as a model for studying how neurogenesis terminates**

The central nervous system in *Drosophila* is an ideal model system to uncover the molecular mechanisms that regulate neural stem cell behavior and the termination of neurogenesis during development. In addition to exceptional genetic tools, *Drosophila* neural stem cells, called neuroblasts, display several

characteristics that facilitate tracking individual lineages over time. A defined number of neuroblasts are specified in stereotypical positions during embryogenesis and are easily distinguished by their large size and expression of molecular markers (Homem et al. 2015). In the central brain, 200 (100 per lobe) neuroblasts generate approximately 30,000 neurons over the course of development (Simpson 2009). Additionally the timing of termination in individual lineages has been rigorously established.

No neurogenesis occurs in adult *Drosophila*, as neuroblasts are eliminated from the central nervous system before adult stages (Von Trotha et al. 2009; Siegrist et al. 2010; Kao et al. 2012). The divisions of neuroblasts terminate through either terminal differentiation, after a final division that leads to a loss of the capacity to self renew, or through programmed cell death (Bello et al. 2003; Maurange, Cheng & Alex P. Gould 2008; Siegrist et al. 2010; Kuert et al. 2012).

Balancing of self-renewal and differentiation by asymmetric cell division

During development, neuroblasts balance self-renewal and differentiation in order to ensure that a sufficient number of neurons are generated for proper functioning of the adult central nervous system, while also avoiding overgrowth or tumorigenesis (Knoblich 2008). Asymmetric cell division is the key mechanism that segregates cell fate determinants to ensure that one daughter will inherit stem cell-like qualities.

In *Drosophila* neuroblasts, asymmetric distribution of cortical cell fate determinants ensures that a division produces two molecularly distinct daughter

cells. One retains stem cell like properties, while the other receives the cell fate determinates that drive it to differentiate into a ganglion mother cell (GMC), which will subsequently divide once to generate two neurons and/or glia (Fig 1.2). To segregate cell fate determinates, neuroblasts polarize to form distinct apical and basal cortical domains. Inheritance of basal factors fates a daughter cell to differentiate into a GMC. The cortical polarity factors that orchestrate asymmetric fate determination are summarized in Table 1.1. The apical protein complex aPKC/Bazooka/Par6 phosphorylates Miranda and Numb to restrict their localization to the basal cortex (Smith et al. 2007; Atwood & Prehoda 2009). Miranda is an adapter protein that binds to the differentiation factors Prospero (Pros) and Brain tumor (Brat) to ensure their basal localization (Spana & Doe 1995; Bello 2006; C. Y. Lee, Wilkinson, et al. 2006; Ikeshima-Kataoka et al. 1997).

During asymmetric cell division in *Drosophila* neuroblasts, the spindle is oriented to generate a plane of division orthogonal to cortical polarity factors. The roles of individual proteins in asymmetric cell division in *Drosophila* neuroblasts are summarized Table 1.1. The apical protein inscutable is recruited by the Par complex and binds to partner of inscutable (Pins) (Nipper et al. 2007; Yu et al. 2000; Kraut et al. 1996). Pins acts as an adapter to recruit Mud, the *Drosophila* homolog of NuMa, which stabilizes microtubule asters to orient the spindle (Izumi et al. 2006; Siller et al. 2006; Nipper et al. 2007). Genetic perturbations of this asymmetric division machinery can result in either microcephaly or tumorigenesis (Kelsom & Lu 2012). Inheriting the apical proteins or loss of differentiation factors

leads to ectopic divisions that result in two daughter cells with neuroblast-like characteristics, leading to an tumorigenic phenotype (C. Lee et al. 2006; Chia et al. 2008). Conversely, failure to repress differentiation factors leads to premature loss of neuroblasts and microcephaly (Choksi et al. 2006).

Spatial patterning in neuroblasts

Neuroblasts are a heterogeneous population of cells; individual neuroblasts have distinct molecular identities that determine the sequence of neurons they will generate. Neuroblasts adopt unique spatial identities when specified in the embryonic neural ectoderm (Hartenstein & Wodarz 2013). Lineage-specific spatial factors regulate the types of neurons and glia that are generated, as well as regulate when they terminate cell divisions (Prokop et al. 1998; Bello et al. 2003; Maurange, Cheng & Alex P. Gould 2008).

Neuroblasts delaminate in several waves during embryonic stages from specific regions in the neuroectoderm, where they express combinations of positional factors based on their location (Hartenstein & Campos-Ortega 1984; Doe 1992). In both the brain and ventral nerve cord, morphogen gradients promote expression of columnar genes, which specify dorsal-ventral identity (Jussen et al. 2016; Skeath 1998). Gap and segment polarity genes as well as homeotic transcription factors pattern neuroblasts along the anterior-posterior axis (Urbach & Technau 2004; Urbach & Technau 2003; Doe 1992).

Neuroblast spatial identity integrates with external signaling to yield different responses to the same developmental cues. In late embryogenesis,

most neuroblasts exit the cell cycle into quiescence or undergo apoptosis depending on their position within the central nervous system (Truman & Bate M 1988). Most of the neuroblasts in the gnathal and ventral nerve chord segments terminate neurogenesis by undergoing apoptosis in late embryonic stages (Peterson et al. 2002; Bello et al. 2003), while in the central brain and thoracic ventral nerve cord neuroblasts exit the cell cycle and enter quiescence (Ito & Hotta 1992; Truman & Bate M 1988; Tsuji et al. 2008).

Spatial determination of Mushroom body neuroblasts

The mushroom body neuroblasts (MB neuroblasts) are a subset of neuroblasts that are the focus of this dissertation. The eight (four per lobe) MB neuroblasts are the last neuroblasts to terminate cell divisions (Fig 1.1) (Truman & Bate M 1988; Ito & Hotta 1992). They are located on the dorsal surface of the central brain and divide consistently to generate neurons, which form a paired structure important for memory and learning (Heisenberg 1998). MB neuroblasts proliferate continuously throughout development (Fig 1.1) (Truman et al. 1994; Ito & Hotta 1992).

MB neuroblasts delaminate from a defined region of the procephalic neuroectoderm (Noveen et al. 2000a; Kunz et al. 2012). MB neuroblasts and their progeny express molecular markers that distinguish them from other neuroblasts including: Eyeless (Ey), Retinal homeobox (Rx), Tailless (Tll), and Dachshund (Dac) (Urbach 2003; Urbach & Technau 2004; Noveen et al. 2000b; Kunz et al. 2012). Two of these transcription factors, Tll and Rx are necessary for

the extended neurogenesis that occurs in pupal phases (Kraft et al. 2016; Kurusu et al. 2009).

Developmental timing and Temporal patterning in neuroblasts

In addition to spatial patterning, neuroblasts adopt different molecular identities over the course of development. This is accomplished via temporal factors, defined as temporally expressed genes whose mutant phenotype results in cell fates associated with an ectopic time in development. Sequential expression of temporal factors determines the types of neurons generated and when they exit the cell cycle (Maurange, Cheng & Alex P. Gould 2008; Isshiki et al. 2001; Tsuji et al. 2008). The molecular mechanisms that regulate temporal patterning are best understood in the embryonic nervous system.

Temporal patterning in embryonic neuroblasts

Temporal patterning is best characterized in the embryonic *Drosophila* ventral nerve cord neuroblasts, where a gene regulatory network known as the "temporal transcription factor cascade" determines the types of neurons produced by each neuroblast (Brody & Odenwald 2000; Isshiki et al. 2001). The core transcription factor cascade involves a sequential expression of Hunchback (Hb) -> Kruppel (Kr) -> Pdm1/2 -> Castor (Cas) -> Grainyhead (Grh) (Brody & Odenwald 2000; Isshiki et al. 2001). Most embryonic neuroblasts progress through the same cascade, but there is variation among individual neuroblast lineages, where a temporal window may be skipped or added (Kao et al. 2012).

Progression through the cascade is ensured by feedback and feed-forward, where some later factors inhibit expression of earlier factors (Figure 1.3). Misexpression of temporal transcription factors has shown that feedback repression delimits discrete temporal windows during development. Kr is repressed by Pdm1/2 in some lineages (Grosskortenhaus et al. 2006; Tran & Doe 2008), while Pdm1/2 is directly repressed by Cas (Grosskortenhaus et al. 2006; Tran & Doe 2008; Tsuji et al. 2008), and Cas is repressed by Grh (Baumgardt et al. 2009). Progression through the embryonic temporal cascade occurs in a cell intrinsic manner as embryonic neuroblasts still express later factors after being dissociated and cultured in isolation (Grosskortenhaus et al. 2005).

This leads to a model in which general activation is coupled with feedback repression to bring about the observed temporal transcription factor cascade. The transcription factor seven-up (ortholog of COUP-TFI/II) is transiently expressed in early embryonic stages to transition neuroblasts from the *Hb* to *Kr* temporal window (Mettler et al. 2006). The cis-regulatory elements that control the expression the temporal transcription factors have begun to be examined in detail (Kuzin et al. 2012; Ross et al. 2015; Hirono et al. 2012; Kuzin et al. 2018).

The core temporal transcription factors interact with other gene regulatory mechanisms to properly organize the nervous system. Additional epigenetic mechanisms regulate neuroblast competence to generate different neurons in response to the core temporal transcription factor cascade. After NBs lose competence, they are unable to generate early born neurons in response to

misexpression of earlier temporal factors (Kohwi et al. 2013; Cleary & Doe 2006). The early competence transitions are mediated through global changes in chromatin structure (Kohwi et al. 2013; Touma et al. 2012). This added layer of regulation progressively restricts the types of neurons and glia generated during development.

The temporal transition factor program times when neuroblasts exit the cell cycle during embryonic stages (Fig 1.1). In the central brain and thoracic ventral nerve cord lineages, the late factors Cas and Grh are required for neuroblast entry into quiescence (Tsuji et al. 2008; Cenci & Gould 2005). In contrast, the same temporal factors promote programmed cell death in the ventral segments (Cenci & Gould 2005; Maurange, Cheng & Alex P Gould 2008).

Cell cycle exit via apoptosis or quiescence in embryonic neuroblasts

Most neuroblasts exit the cell cycle during two developmental windows. The first occurs during late embryogenesis, where neuroblasts in the abdominal ventral nerve cord and gnathal segments undergo apoptosis, and neuroblasts in the central brain and thoracic ventral nerve cord enter a state of quiescence (Bello et al. 2003; Cenci & Gould 2005; Tsuji et al. 2008).

Most neuroblasts in the abdominal ventral cord and gnathal segments undergo programmed cell death in late embryonic stages (Fig. 1.1) (Peterson et al. 2002; Kuert, Philipp A et al. 2014). Programmed cell death is a highly conserved process that eliminates damaged or unnecessary cells during development. The pro-apoptotic genes, reaper (rpr), grim, and sickle (skl) are

necessary for programmed cell death during Drosophila embryogenesis (White et al. 1994).

Spatial and temporal identity cues integrate directly to coordinate the timing of apoptosis in embryonic neuroblasts. Expression of Rpr, Grim, and Skl is regulated by the reappearance of homeotic genes in late embryonic stages (Bello et al. 2003; Urbach et al. 2012). Abdominal-A (Abd-A) in the abdominal ventral nerve cord and Deformed (Dfd) in the gnathnal segment promote expression of reaper, grim, and sickle (Ying Tan et al. 2011; Bello et al. 2003; Arya et al. 2015). Abd-A and Dfd regulate their transcription by binding to a long distance regulatory element located approximately 30 kb upstream of grim in a region termed the neuroblast regulatory region (Ying Tan et al. 2011). This regulatory region is necessary for expression of grim and rpr in neuroblasts at late embryonic stages (Ying Tan et al. 2011; Arya et al. 2015; Liu et al. 2011; Khandelwal et al. 2017). In addition to homeotic genes, the last factor in the embryonic transcription factor cascade, Grh, promotes apoptosis in the abdominal lineages by cooperatively binding with Abd-A to promote expression of Reaper and Grim (Cenci & Gould 2005; Khandelwal et al. 2017).

Extrinsic regulation postembryonic neuroblast proliferation

Regulation of neuroblast behavior is more complex in post embryonic stages, as individual neuroblasts generate hundreds of progeny and must respond appropriately to extrinsic cues such as the nutritional state of the animal and developmental hormones (Yamanaka et al. 2013). The nutritional state is

primarily sensed by the insulin PI3-Kinase pathway (Britton et al. 2002). Neuroblasts also respond to changes in ecdysone, a steroid hormone that is the primary systemic signal that coordinates developmental timing in *Drosophila* (Yamanaka et al. 2013). I will briefly describe some of the cell-extrinsic cues that regulate neuroblast proliferation during development.

PI3 Kinase regulates cell cycle exit and entry

Neuroblasts, like most stem cells, can exit the cell cycle in response to developmental or environmental cues (Cheung & Rando 2013). With the exception of the MB and one lateral neuroblasts, neuroblasts enter quiescence in late embryogenesis once they have reached the last temporal window in their intrinsic temporal series (Truman & Bate M 1988; Tsuji et al. 2008). During this stage, neuroblasts transiently express low levels of nuclear Pros and a protein pseudokinase called Tribbles, which promotes cell cycle exit (Lai & Doe 2014; Li et al. 2017; Otsuki & Brand 2018). In the ventral nerve cord, each neuroblast stereotypically arrests proliferation at the G1 or G2 phase of the cell cycle, which may affect how quickly neuroblasts resume proliferation in larval stages (Otsuki & Brand 2018). Once the larvae hatches and begins feeding, a nutrient-sensing pathway regulates neuroblast exit from quiescence (Britton & Edgar 1998). Dietary amino acids are sensed by the fat body, the *Drosophila* adipose tissue analog, which activates Tor signaling, which in turn promotes the release of an uncharacterized mitogen into the hemolymph (Britton & Edgar 1998; Sousa-Nunes et al. 2011). In response to this mitogen, insulin signaling activates the

PI3-kinase pathway in neuroblasts (Spéder & Brand 2018; Chell & Brand 2010; Sousa-Nunes et al. 2011). Important downstream targets of PI3-kinase signaling for reactivation include a set of spindle matrix proteins (Chromator, Megator, Skeletor, and EAST) that also prevent accumulation of Pros in the nucleus to keep neuroblasts engaged in the cell cycle (Li et al. 2017).

In early larval stages, neuroblasts are capable of exiting the cell cycle if deprived of amino acids during early larval stages (Sipe & Siegrist 2017). After the larva reaches critical weight, a developmental checkpoint where sufficient nutrients have been acquired to commit to metamorphosis, non-MB neuroblasts become insensitive to nutrient deprivation, allowing the brain to preferentially grow at the expense of other organs (Cheng et al. 2011). The brain sparing mechanism involves activation of PI3-Kinase by the Anaplastic lymphoma kinase receptor (Alk) and its ligand jellybelly, which bypass reductions in insulin signaling to maintain elevated PI3-Kinase levels in neuroblasts (Cheng et al. 2011).

MB neuroblasts do not enter quiescence during embryonic stages or in response to nutrient withdrawal (Britton & Edgar 1998; Cheng et al. 2011; Sipe & Siegrist 2017). The transcription factor Eyeless (Ey), a Pax6 family member predominantly expressed in MB neuroblasts, is necessary and sufficient for neuroblast proliferation under nutrient withdrawal at early stages of development (Sipe & Siegrist 2017). Unlike the brain sparing mechanism seen after critical weight, MB neuroblast proliferation under nutrient restriction is independent of PI3-Kinase signaling (Sipe & Siegrist 2017; Cheng et al. 2011). Interestingly, MB

neuroblasts terminate divisions in late pupal stages and are sensitive to the levels of PI3-kinase (Siegrist et al. 2010). This suggests that MB neuroblasts transition from PI3-kinase insensitive to PI3-kinase sensitive over the course of development.

Ecdysone signaling

Drosophila neuroblasts respond to systemic changes in the primary developmental steroid hormone ecdysone, which is important for regulating neuroblast temporal identity and terminating non-MB neuroblasts in early pupal stages (Syed et al. 2017b; Homem et al. 2015).

Sequential pulses of ecdysone time developmental transitions such as the sequential larval molts and pupation (Yamanaka et al. 2013). Ecdysone is synthesized from dietary cholesterol in an endocrine organ known as the ring gland and secreted systemically into the hemolymph (Yamanaka et al. 2015). In peripheral tissue, ecdysone is converted to 20-hydroecdysone (20-E), which is the biologically active form (Petryk et al. 2003). 20-E is transported into target cells by a transporter where it binds ecdysone receptor (EcR), a nuclear receptor that binds DNA as a heterodimer with Usp (*RXR* in vertebrates) (Yamanaka et al. 2013; Haga-yamanaka et al. 2018). Like many nuclear receptors, in the absence of ecdysone, EcR recruits co-repressors to repress expression of its target genes (Mirth et al. 2009). Most effectors of ecdysone signaling are not directly regulated by EcR, but are instead controlled by a cascade of ecdysone-responsive transcription factors (Gauhar et al. 2009). These include the early response

genes broad, ecdysone induced protein 74EF, and ecdysone inducible protein 93F (E93) (Thummel 2001).

In the periphery, ecdysone signaling suppresses growth and promotes elimination of larval tissues during metamorphosis (Jiang et al. 2000). Early during pupariation, ecdysone-dependent degeneration or remodeling occurs in several larval tissues including the salivary glands, midgut, and fat body (Lee et al. 2000). A post-pupal pulse of ecdysone promotes transcription of genes involved programmed cell death and autophagy (Thummel 2001). In other tissues, ecdysone signaling promotes maturation of the tissue (Mou et al. 2012; Uyehara et al. 2017). One way this is accomplished is by ecdysone inducible proteins modifying the chromatin state of developmentally regulatory elements, allowing other transcription factors to access these elements only at certain stages of development (Pavlopoulos & Akam 2011; Uyehara et al. 2017).

Extrinisic and intrinsic regulation of temporal patterning in post-embryonic neuroblasts

Ecdsyone signals promote a transition in the temporal identity of larval CNS neuroblasts. In a subset of neuroblasts and most other central brain lineages, ecdysone represses early temporal identity factors, which include Imp, Lin28, and Chinmo, and promotes transition to late temporal identity genes such as Syp, Broad, and E93 (Fig 1.5) (Syed et al. 2017b). Ecdysone receptor (EcR) itself is temporally regulated by expression of the earlier temporal factor Seven up (Svp).

Two RNA binding proteins, IGF-II mRNA binding protein (Imp) and Syncrip (Syp) form a regulatory cassette that regulates neuroblast temporal identity in post embryonic development (Liu et al. 2015; Ren et al. 2017; Syed et al. 2017b). Imp levels are high early in development and gradually decrease, whereas Syp is expressed at higher later in development. Imp and Syp mutually repress one another to form an opposing temporal gradient (Liu et al. 2015).

An early switch from Cas to Svp expression precedes the transition through the Imp/Syp temporal cassette (Syed et al. 2017b; Ren et al. 2017). Svp drives this transition in part by regulating expression of the EcR in neuroblasts. EcR in turn represses expression of early factors such as Imp, Chinmo, and Lin28, while simultaneously promoting expression of the late factors Syp, Broad, and E93 (Fig.1.5) (Syed et al. 2017a). Thus, an intrinsic temporal transcription factor cascade regulates neuroblast competence to respond to ecdysone by directly regulating the timing of its receptor expression (Syed et al. 2017a). Thus, intrinsic signals time when neuroblasts are competent to respond to the extrinsic signals that drive neuroblast progression through the temporal series.

Temporal patterning in MB neuroblasts

MB neuroblast lineages are also temporally patterned. During larval and pupal development, MB neuroblasts sequentially generate four morphologically distinct classes of neurons. The early-born γ neurons, middle-born α’/β’ neurons, and late-born pioneer α/β and α/β neurons, which send their projections into distinct regions that comprise the five MB lobes (Fig 1.6) (Lee & Luo 1999; Ito et

al. 1997). The temporal factors Imp and Syp govern temporal identity in MB neuroblasts. Loss of Syp or over expression of Imp keeps MB neuroblasts in the early temporal window where they generate γ neurons at the expense of the later α’/β’ neurons, pioneer α/β neurons, and α/β neurons, conversely loss of Imp or misexpression of Syp leads to increased numbers of α/β neurons at the expense of earlier born types (Liu et al. 2015).

A target of Imp and Syp is the transcription factor Chinmo in GMCs and neurons (Liu et al. 2015). Early-born γ neurons express high levels of chinmo, while α’/β’ neurons have lower levels, and pioneer α/β, and α/β neurons lack expression altogether (Zhu et al. 2006; Wu et al. 2012). The opposing gradients of Imp/Syp in the neuroblasts are inherited by the mushroom body neurons where they promote temporal identity of the neurons by regulating levels of chinmo (Liu et al. 2015). In addition to Imp and Syp, ecdysone signaling suppresses chinmo by promoting expression of the let-7 miRNA in GMCs, which promotes the transition from α’/β’ -> pioneer α/β neurons (Kucherenko et al. 2012; Wu et al. 2012).

Termination of neurogenesis in *Drosophila*

Neuroblasts stop dividing in a spatially and temporally determined manner during development (Fig. 1.1). Adult neurogenesis does not occur in the *Drosophila* CNS as all neuroblasts are eliminated through apoptosis or terminal differentiation during development (Siegrist et al. 2010; Von Trotha et al. 2009; Kato et al. 2009). The majority of neuroblasts in the central brain and thoracic

ventral nerve cord terminates cell divisions in pupal stages (Pinto-Teixeira et al. 2016; Ito & Hotta 1992; Truman & Bate M 1988).

Whether a neuroblast is eliminated by programmed cell death or terminal differentiation is determined in a lineage determined manner (Maurange, Cheng & Alex P Gould 2008; Siegrist et al. 2010). Apoptosis is regulated by a set of proapoptotic genes that relieve inhibition of caspases (Fuchs & Steller 2011). Terminal differentiation is the result of a symmetric division, which segregates differentiation factors to both daughter cells, leading to the neuroblast to exit the cell cycle and differentiate. Most non-MB neuroblasts are eliminated in early to mid pupal stages, while the MB neuroblasts are eliminated later, approximately ten hours before the eclosion.

Termination of MB neuroblasts

MB neuroblasts are eliminated in late pupal stages by a combination of apoptotic and autophagic cell death (Siegrist et al. 2010). Reduced levels of PI3-kinase signaling leads to a failure of MB neuroblast regrowth after each division, causing them to reduce in size. This decrease in size precedes apoptosis induced by the pro-apoptotic genes in the reaper locus (Siegrist et al. 2010). Inhibition of apoptosis alone allows MB neuroblasts to persist transiently in adult stages before they are eliminated by a secondary autophagic cell death mechanism (Siegrist et al. 2010) (Fig. 1.7). However, the cell-intrinsic factors that promote MB neuroblast termination are not currently known.

Terminal differentiation of central brain and thoracic neuroblasts

Increased ecdysone levels during pupation terminate non-MB neuroblast proliferation. In response to increased levels of ecdysone, EcR and the mediator complex cooperate to regulate the expression of a set of metabolic genes (Homem et al. 2014). This change in gene expression switches the neuroblast from a metabolic state of high glycolysis to oxidative phosphorylation (Homem et al. 2014). In larval stages neuroblasts renew their volume after each division to maintain a constant cell size. This change in metabolism leads to a failure of neuroblast regrowth, causing them to gradually become smaller (Siegrist et al. 2010; Chell & Brand 2010; Homem et al. 2014). Following this change in growth, non-MB neuroblasts are thought to exit the cell cycle due to a loss of the ability to properly segregate differentiation factors, ultimately bringing about terminal differentiation (Homem et al. 2014).

Most neuroblasts in the central brain and thoracic ventral nerve cord are thought to be eliminated by a final symmetric division that leads to terminal differentiation of both daughters (Maurange, Cheng & Alex P. Gould 2008). Factors required for differentiation, including Pros and Nerfin-1, localize to the nucleus following a terminal cell division in early to mid pupal phases (Maurange, Cheng & Alex P. Gould 2008; Froldi et al. 2015). Nerfin+, Pros- but not Nerfin-, Pros+ neuroblasts are present when neuroblasts begin to be eliminated, suggesting that Nerfin-1 may act upstream of Pros (Froldi et al. 2015). Misexpression of either Pros or Nerfin-1 reduces the number of neuroblasts in larval brains (Froldi et al. 2015; Maurange, Cheng & Alex P. Gould 2008).

However, Pros and Nerfin-1 loss-of-function experiments are challenging to interpret, as inhibition of either results in the formation of tumors due to reversion of the GMC or neuronal progeny back into neuroblasts (Betschinger et al. 2006; Bowman et al. 2008; Shaw et al. 2018; Froldi et al. 2015; Choksi et al. 2006). A clear loss-of-function mutant for NB termination is unlikely to be obtained since there is not currently any method to inhibit Pros specifically in the NB without affecting the progeny.

Similar to the embryonic lineages, temporal identity is a key regulator of the timing of neuroblast termination (Maurange, Cheng & Alex P. Gould 2008; Chai et al. 2013; Yang et al. 2017). Mutations in embryonic temporal factors causes neuroblasts persist past their normal elimination time (Narbonne-Reveau et al. 2016; Maurange, Cheng & Alex P. Gould 2008). Of particular interest are two heterochronically expressed RNA-binding proteins, Imp and Syp, that regulate temporal identity and control when neurogenesis terminates (Liu et al. 2015; Ren et al. 2017; Syed et al. 2017b; Yang et al. 2017). Syp is required for their termination while Imp is necessary for neuroblast survival (Yang et al. 2017).

The Imp/Syp gradient appears to reflect the length of neurogenesis in individual lineages, as MB neuroblasts display a longer Imp+ window (Liu et al. 2015). In non-MB neuroblasts, Syp regulates termination by promoting stability of Pros and hence terminal differentiation (Yang et al. 2017). Imp protects MB neuroblasts from the ecdysone-induced shift in metabolism by directly regulating the expression of several mediator complex subunits. This changes sensitivity to

the ecdysone cue, which normally triggers the metabolic shift that causes neuroblasts to undergo reductive cell size divisions (Yang et al. 2017).

The extended neurogenesis observed in MB neuroblasts correlates with a delayed transition from Imp to Syp temporal window compared to non-MB neuroblasts (Liu et al. 2015). Imp may prevent the ecdysone dependent metabolic shift in the MB neuroblast lineage by repressing components of the mediator complex, (Yang et al. 2017). Coordination of temporal identity with termination may ensure that each neuroblast completes its lineage of neurons and glia.

Similarities with vertebrate neural stem cells

Mammalian neurogenesis shares a remarkable number of similarities with neurogenesis in *Drosophila*. Neural stem cells in vertebrates are specified from a neuroepithelium that first undergoes symmetric followed by asymmetric divisions. Once specified apical progenitors or radial glial cells begin expressing glial markers (Noctor et al. 2002). In the mammalian cortex, radial glia cells are located in the ventricular zone and extend processes that span the developing cortical layers.

Radial glia cells undergo asymmetrical divisions to generate neurons and glia (Florio & Huttner 2014). Following initial rounds of symmetric divisions, the radial glia begin to divide asymmetrically, where one daughter differentiates into a neuron or glial cell (Gao et al. 2014). Rather than undergoing the orthogonal divisions observed in *Drosophila* neuroblasts, radial glia divisions are oblique

with respect to the apical and basal processes. Following asymmetric division, one daughter inherits the basal process and will remain a radial glia cell, while the other lacking it goes on to differentiate (Dwyer et al. 2016). The basal process allows contact with the ventricle, exposing it to insulin-like growth factor 2 which promotes proliferation and survival of radial glia (Shitamukai et al. 2011; Lehtinen et al. 2011).

Like *Drosophila*, vertebrate neural stem cells also sequentially generate distinct neurons and glia in a chronological sequence (Soula et al. 2001). During mouse neurodevelopment, clonal analysis has demonstrated that individual radial glial cells generate neurons that sequentially contribute to multiple cortical layers (Frantz et al. 1994; Frantz & McConnell 1996; Gao et al. 2014). Orderly generation of different neuronal cell types is also observed in the developing retina, hindbrain, and spinal cord. Homologs of the temporal factors Hunchback and Castor also regulate temporal patterning in the mammalian cortex and retina (Alsiö et al. 2015; Mattar et al. 2015). Therefore, progression through a set of temporal factors is a fundamental feature of neural development (Kessaris et al. 2001; Soula et al. 2001; Livesey et al. 2001).

Comparatively less is known about the molecular mechanisms behind the termination of neural stem cell proliferation in mammals. Orthologs of Pros and Nerfin-1 are thought to play a role in cell cycle exit and terminal differentiation (Zhang et al. 2009; Dyer et al. 2003). Prox1, the vertebrate ortholog of Pros, promotes cell cycle exit in the developing retina in mice (Dyer et al. 2003). Similarly the vertebrate paralog of Nerfin-1, insulinoma-associated protein 1

(Insm1), is expressed in basal dividing neural progenitors that terminally differentiate into neurons (Farkas et al. 2008). Similar to neuroblasts, insulin-like growth factor 2 from the cerebral spinal fluid to promote proliferation and progenitor survival of radial glial cells (Yu et al. 2008; Popken et al. 2004). Although similarities exist, the lack of unambiguous molecular markers and cellular heterogeneity currently limit investigation into the ultimate fate of mammalian neural stem cells.

Neural stem cell proliferation becomes restricted in both *Drosophila* and mammals. Using the MB neuroblast lineage in *Drosophila* as a model, this thesis investigates the molecular mechanisms that govern neural stem cell decisions to terminate proliferation, leading to a better understanding of how neurogenesis becomes restricted as development completes. In chapter 1, I describe results from investigating pro-apoptotic genes *reaper, grim, hid,* and *skl*. In Chapter 2, I describe the results of a directed RNAi screen that identified several genes that are required for termination of neurogenesis. In chapter 3, I describe the role one of the genes identified from our RNAi screen; E93, which cooperates with two temporally, expressed RNA binding proteins to regulate neuroblast termination.

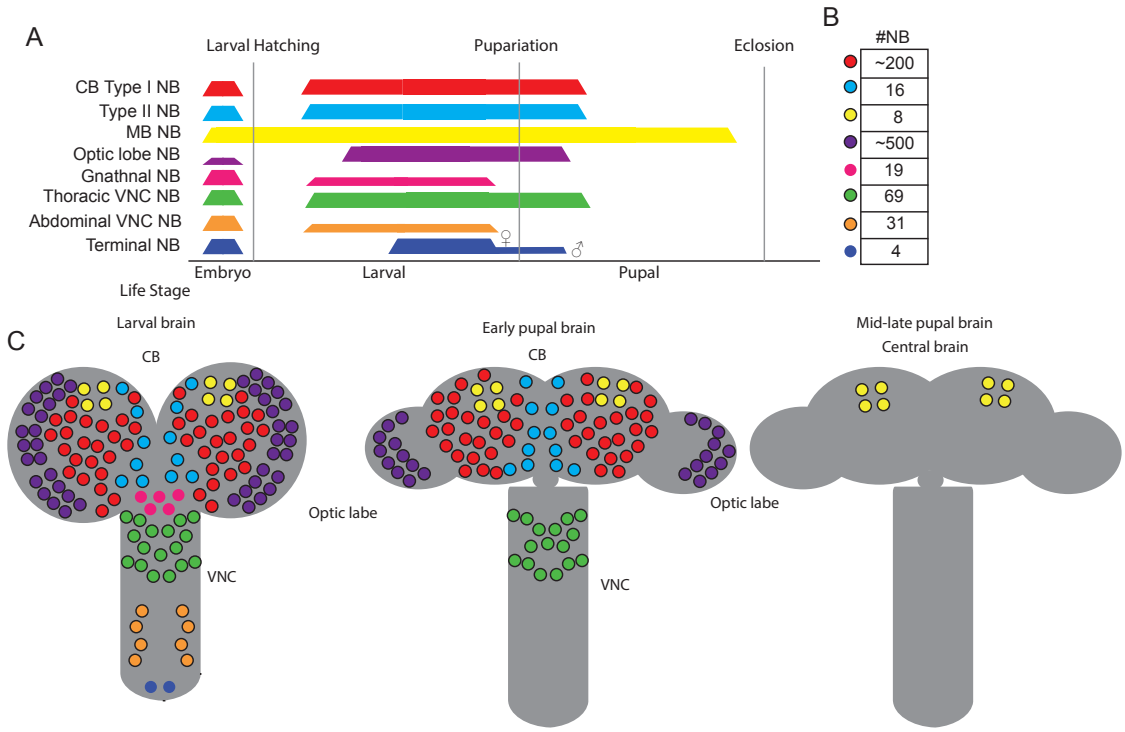

Figure 1.1. Summary of pattern of neurogenesis in *Drosophila*. (A) The timing of proliferation reported for identified NB subsets over the course of development. CB (central Brain), NB (neuroblast), MB (mushroom body), VNC (ventral nerve cord). Adapted from (Truman & Bate M 1988; Maurange & Gould 2005; Pinto-Teixeira et al. 2016; Truman et al. 1994). (B) The approximate number of neuroblasts during larval stages. The number of optic lobe neuroblasts represents the approximate number present in the prepupal stage (Lanet et al. 2013). (C) Spatial representation of changes in the neuroblast subtypes over time. Colors are as in panel A. Not to scale.

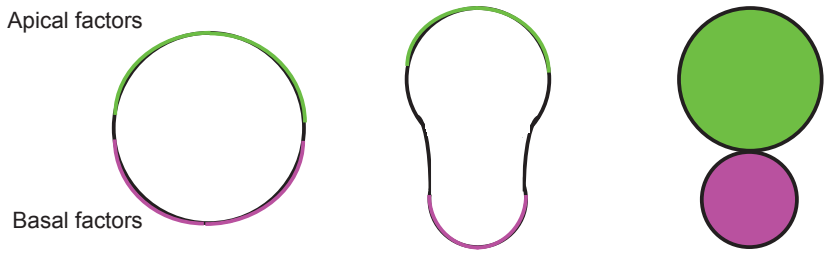

Figure 1.2: Asymmetric cell division in *Drosophila* neuroblasts. Neuroblasts segregate cell fate determinants to the apical and basal membrane and divide orthogonally relative to the polarity axis as they undergo self-renewing asymmetric cell divisions. This process results in one cell retaining neuroblast characteristics (green) and the other inheriting factors promoting differentiation into a ganglion mother cell (GMC; purple), which subsequently divides once to generate neurons and/or glia.

Table 1.1 Proteins involved in asymmetric cell division. Updated and modified from (Kelsom and Lu, 2012).

Protein name	Function	Localization during ACD	Loss of function	Human Ortholog	Reference
Numb	Differentiation of neurons/glia	Basal cortex	Overproliferation	*NUMB/ NUMBL*	(C. Y. Lee, Andersen, et al. 2006; Wang et al. 2006)
Pon	Localizing numb	Basal cortex	Loss of Numb localization	No ortholog	(Wang et al. 2007)
Brat	Regulates prospero localization	Basal cortex	Overproliferation	*TRIM3*	(Bello 2006)
Miranda	Localization of basal proteins	Basal cortex	Mislocalization of basal protein; overproliferation	No ortholog	(Shen et al. 1997; Shen et al. 1998)
Prospero	Differentiation of neurons/glia	Basal cortex	Overproliferation	*PROX1 /PROX2*	(Spana & Doe 1995)
Staufen	Localization of Prospero mRNA	Basal cortex	Delocalization of Prospero mRNA	*STAU1 /STAU2*	(Broadus et al. 1998; Shen et al. 1998; Jiang et al. 2011; Li et al. 1997)
Pins, Galphai, Loco	Spindle orientation; localization of basal proteins	Apical cortex	Failure to self renew	*GPSM1/GPSM2*	(Schaefer et al. 2000; Siegrist & Doe 2005; C. Y. Lee, Robinson, et al. 2006; Nipper et al. 2007)
Inscutable	G proteins to Par complex	Apical cortex	Localization of basal proteins; Spindle orientation	*INSC*	(Kraut et al. 1996)
aPKC, Bazooka/Par 3, Par6	Apical and basal polarity maintenance	Apical Cortex	Underproliferation	*PRKCI/PRKCZ, PARD3/PARD3B, PARD6G/PARD6 B/PARD6A*	(Rolls et al. 2003)
Mud	Spindle orientation	Centrosome and cortex	Spindle misoriented; Overproliferation	*NUMA1*	(Bowman et al. 2006; Nipper et al. 2007; Siller & Doe 2009; Rebollo et al. 2007)
Lethal 2 giant larvae, discs large, Scribble	Localization of basal proteins; Spindle positioning	Apical Cortex	Mislocalization of basal proteins; overproliferation	*LLGL1/LLGL2, DLG1, DLG2, DLG3, DLG4, SCRIB1*	(Albertson & Doe 2003)

Protein name	Function	Localization during ACD	Loss of function	Human Ortholog	Reference
Aurora A	Apical basal polarity	Centrosome and Cytoplasm	Overgrowth Spindle misoriented Mislocalized aPKC and Numb	*AURKA, AURKB, AURKC*	(Berdnik & Knoblich 2002; C. Y. Lee, Andersen, et al. 2006; Wang et al. 2006)
Polo	Spindle orientation	Centrosome and Cytoplasm	Overgrowth (catalytic subunit)	*PLK1, PLK2, PLK3, PLK4, PLK5*	(Wang et al. 2007; Llamazares et al. 1991)
PP2A	Spindle orientation	Cytoplasm	Misoriented spindle, mislocalization of aPKC	PPP2CA, PPP2CB	(Chabu & Doe 2009; Wang et al. 2009)
Dpn	NB identity/self-renewal	Cytoplasm	Loss of NBs	*HES1*	(Bier et al. 1992; Zhu et al. 2012)
Warts	Localization of Mud to the apical membrane	Cytoplasm, enriched at apical cortex	Misoriented spindle	*LATS1, LATS2*	(Dewey, Sanchez and Johnston, 2015; Keder et al., 2015)
Zif	Apical basal polarity	Cytoplasm	Overproliferation	No ortholog	(Chang et al. 2010)

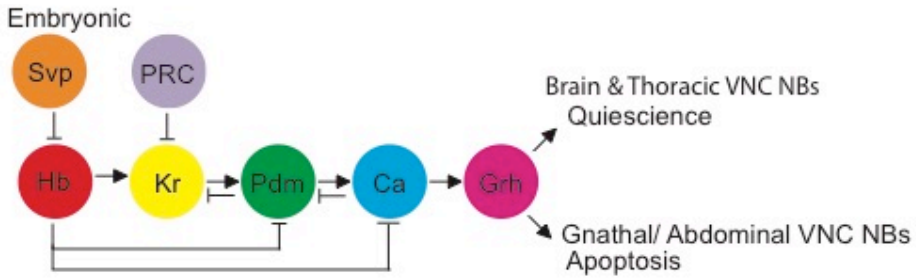

Figure 1.4: **A temporal transcription factor cascade regulates developmental timing in embryonic neuroblasts.** The canonical embryonic temporal transcription factor cascade as described in ventral nerve cord neuroblasts (Brody & Odenwald 2000; Isshiki et al. 2001; Touma et al. 2012; Kambadur et al. 1998; Cleary et al. 2006; Tsuji et al. 2008; Benito-Sipos et al. 2010; Tran & Doe 2008; Baumgardt et al. 2009; Stratmann & Thor 2017). Hunchback (Hb), Kruppel (Kr), POU domain 1/2 (Pdm), Castor (Cas), Grainyhead (Grh), Svp (Seven up), Polycomb repressive complex (PRC).

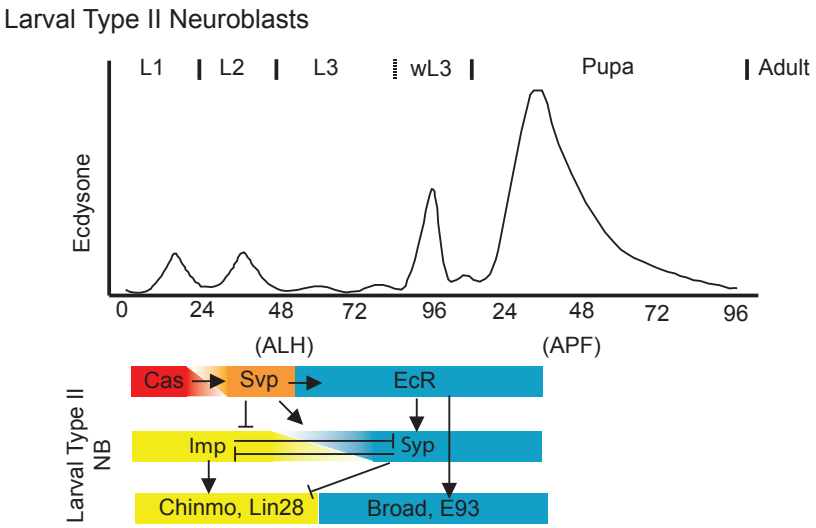

Figure 1.5: Factors that govern temporal patterning in larval neuroblasts. The graph at top shows the pattern of ecdysone pulses over development (modified from Truman *et al.*, 1994). The diagram at bottom shows the timing of the temporal transcription factor windows in Type II neuroblasts and other central brain lineages (Syed et al. 2017b; Ren et al. 2017).

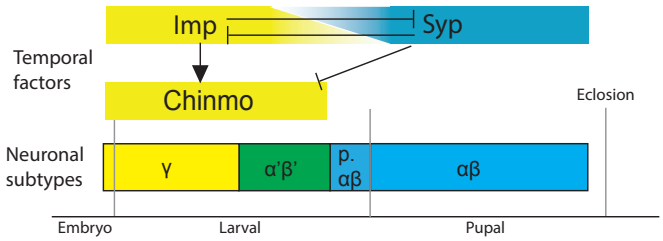

Figure 1.6: Imp and Syncrip regulate Chinmo to promote switching of daughter cell fate in the MB neuroblast lineage. Imp/Syp form an opposing gradient and in turn regulate expression of the zinc-finger transcription factor Chinmo (Zhu et al. 2006; Liu et al. 2015). Levels of Chinmo determine the class of MB neuron produced by the MB neuroblast. Early-born gamma neurons express high levels of Chinmo, while later born α'/β', pioneer α/β, and α/β express lower levels.

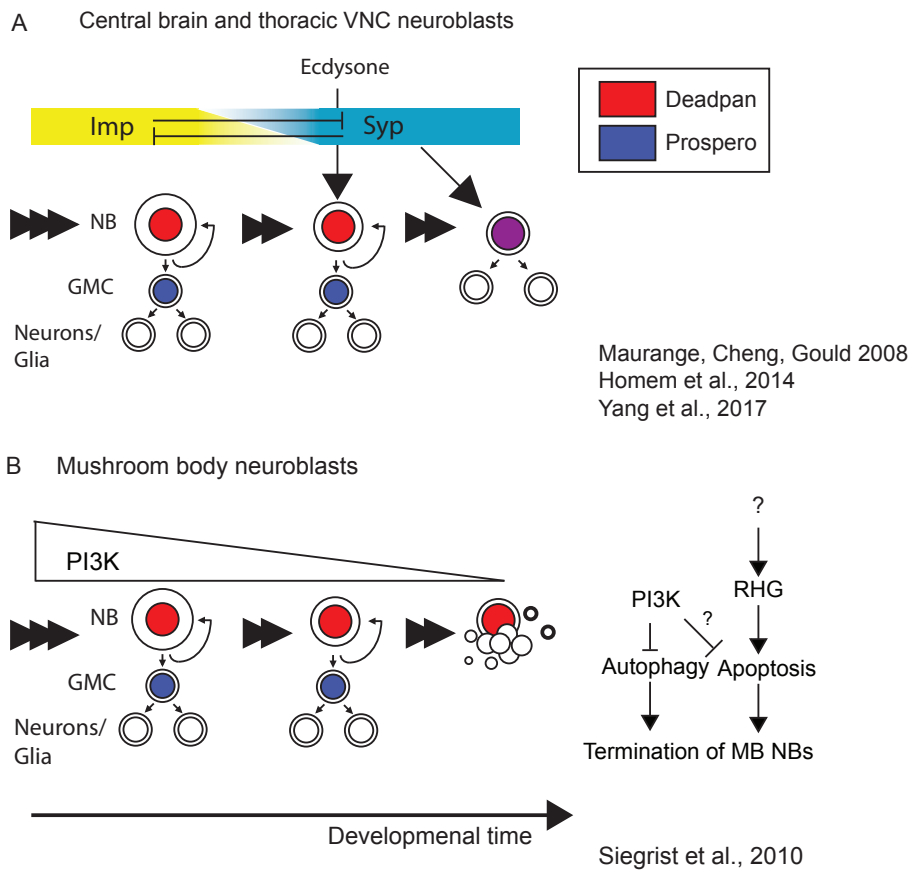

Figure 1.7: Two mechanisms for eliminating central brain neuroblasts during development. (A) Non-MB neuroblasts in the central brain and thoracic segments of the ventral nerve cord undergo terminal division in response to an ecdysone pulse that occurs within an Imp-/Syp+ temporal window (Homem et al. 2014; Yang et al. 2017). Reduced growth in MB neuroblasts gradually leads to nuclear accumulation of the differentiation factor Prospero, which results in terminal symmetric division (Maurange, Cheng & Alex P. Gould 2008). B) Mushroom body neuroblasts undergo apoptosis following a reduction in levels of PI3-kinase signaling (Siegrist et al. 2010). The proapoptotic genes reaper, grim, hid, and sickle are required MB neuroblast apoptosis. Apoptosis and autophagy act in parallel to regulate when MB neuroblasts terminate divisions.

Chapter 2

Directed screen for regulators of MB neuroblast elimination

Abstract:

Proliferation of neural stem cells is regulated in a spatial and temporal manner during development. We use *Drosophila* to study the molecular mechanisms that regulate how neurogenesis terminates once development completes. To identify cell intrinsic factors that regulate the termination of neurogenesis, we initiated a directed RNAi screen to identify genes that regulate the elimination of the mushroom body neuroblasts (MB neuroblasts). We knocked down the expression of candidate regulators in neuroblasts and assayed for premature loss or ectopic persistence of MB neuroblasts. In this screen, we identified eight transcription factors that affected the timing of MB neuroblast elimination. In addition, we found several genes that affect the elimination of other neuroblasts. We began to characterize the role of several genes implicated in our screen. One of the genes we identified, the *Pax6* ortholog, Eyeless (Ey), is required to promote autophagy before MB neurogenesis terminates. We also identified another transcription factor, E93, from this screen, which is discussed in Chapter 3.

Introduction:

Neurogenesis is regulated both spatially and temporally during development. This is due in part to decreasing numbers of actively proliferating neural stem cells as development approaches completion. We use *Drosophila*

melanogaster as a model system to study how neurogenesis becomes restricted during development. In *Drosophila*, all neural stem cells (called neuroblasts) are eliminated from the central nervous system, and no new neurons are generated (Siegrist et al. 2010; Kao et al. 2012; Von Trotha et al. 2009). Neuroblasts are eliminated in a spatially and temporally defined manner. The majority of central brain neuroblasts are eliminated during early pupal phases by either terminal differentiation or apoptosis (Truman & Bate M 1988; Ito & Hotta 1992; Siegrist et al. 2010; Maurange, Cheng & Alex P Gould 2008; Chai et al. 2013; Homem et al. 2014; Yang et al. 2017).

The mushroom body neuroblasts (MB neuroblasts) are a subset of neuroblasts that continue cell divisions until 96 hours APF several days longer than other central brain neuroblasts (non-MB neuroblasts) which are eliminated by 30 APF (Truman & Bate M 1988; Ito & Hotta 1992; Siegrist et al. 2010). MB neuroblasts are eliminated during late pupal phases by a combination of apoptosis and autophagy (Siegrist et al. 2010). Inhibition of either pathway results in a temporary delay of elimination, while inhibition of both pathways promote long-term survival (Siegrist et al. 2010). Prior to their elimination MB neuroblasts undergo reductive cell divisions and gradually reduce in cell size due to lower levels of PI3-kinase signaling (Siegrist et al. 2010). However, the cell-intrinsic factors that regulate the timing of MB neuroblast elimination remain unclear.

In this chapter, I will describe the results from our directed RNAi screen for genes that regulate MB neuroblast termination. Additionally, I will describe the initial characterization one of the genes identified in our screen.

Results:

To better understand the molecular mechanisms that determine when MB neuroblast terminate, we conducted a directed RNAi screen against a set of candidate genes that we identified through a combination of bioinformatic analysis and their ascribed functions in the literature.

Identification of candidate genes

To identify genes that act as intrinsic regulators of MB neuroblast elimination, we took a candidate gene approach. As grim and sickle are required for MB neuroblast apoptosis (Siegrist et al. 2010; Appendix), we were interested in identifying transcriptional regulators. Additionally, we wanted to include other genes already known to regulate the transcription of programmed cell death genes or those that are expressed in MB neuroblasts. We combined the two approaches to generate a list of candidates for our directed screen.

We first identified and curated candidate cis-regulatory elements located near grim and sickle within the genome. These regulatory regions had been shown to be bound by multiple transcription factors at different developmental stages in a previous whole-organism chromatin profiling study (Moorman et al.

2006). We selected 45 of these putative regulatory elements as possible regulators based on their proximity to the transcription start sites of *grim* and *skl*.

Cis-regulatory elements are often evolutionarily conserved (Visel et al. 2007). To narrow down the genomic regions to include in our analysis, we identified evolutionarily conserved regions within the set of 45 putative regulatory elements using the program EvoprinterHD. EvoprinterHD identifies evolutionarily conserved regions within a sequence by performing pairwise BLAST alignments on closely related species (Odenwald et al. 2005). We filtered our sequences to those conserved from seven Drosophilids, including *Drosophila melanogaster*.

We scanned the list of conserved sequences to identify potential transcription factor binding motifs using the R package, PWMEnrich. This package uses position weight matrices to calculate a score based on their similarity to known transcription factor binding motifs (Jayaram et al. 2016). We used a precompiled database of transcription factor binding motifs that were generated by the FlyFactorSurvey (Christensen et al. 2012), representing 358 out of 708 transcription factors in *Drosophila* (Rhee et al. 2014). From this analysis, we identified 91 candidate transcription factors (see Appendix).

In addition to our bioinformatics analysis, we also included genes that were previously described as regulating apoptosis, such as homeodomain containing genes, temporal identity genes, genes reported to bind near *grim* and *sickle* from the modEncode project, and genes known to be expressed in MB neuroblasts (Négre et al. 2011) (Appendix). Taken together we compiled a list of 152 candidate genes from both approaches (Fig 2.1). Fifteen of these

transcription factors showed overlap between the two approaches (Broad, Daughterless, Kruppel, Longitudinals lacking, Methoprene tolerent, Occeliless, Retinal homeobox, Sex combs reduced, Snail, Supressor of hairless, Tailless, Taiman, Visual system homeobox 2, and Zerknullt).

Screen results

To screen for intrinsic factors required for MB neuroblasts elimination, we used the GAL4/UAS system to knockdown expression of candidate genes in neuroblasts (Brand & Perrimon 1993). We drove expression of *UAS-RNAi* lines from the TRiP collection in neuroblasts using *worGAL4* with *UASDcr2* and *tubGAL80ts* (Albertson 2004; Perkins et al. 2015) (Fig 2.1). We assayed for the presence of neuroblasts at 72 hours after pupal formation (APF) and in 1-day-old adult brains by labeling for the neuroblast marker Deadpan (Dpn) and expression of the S-phase marker *pcna:GFP*. We defined premature loss as a brain having less than four MB neuroblasts at 72 hours APF and persistence as the presence of MB neuroblasts in early adult stages. We screened 69 of the 152 predicted candidates (Table 2.1, see appendix) and identified 13 genes that affect the timing of neuroblast termination (Table 2.2).

Knockdown of the transcription factors Eyeless, Grainyhead, Occeliless, Retinal Homeobox (Rx), Ultrabithorax (Ubx), or Yorkie (Yki) resulted in ectopic persistence of MB neuroblasts into adult stages. Conversely, knockdown of the bHLH transcription factor Mitf or mod(mdg4), a component of an insulator complex, resulted in premature loss of MB neuroblasts. Each of these genes was

included on the list derived from the literature. E93, Mitf, Oc, and Rx were also included as possible regulators of *grim* or *sickle* in our bioinformatics analysis.

Several genes in our screen affected termination of non-MB neuroblasts. Knockdown of Notch or Delta resulted in the ectopic persistence of some non-MB neuroblasts. The persistent non-MB neuroblast phenotype was more penetrant with knockdown of Delta than Notch. Knockdown of transcription factor Scarecrow (Scro), a homeodomain domain containing protein with high sequence similarity to the columnar gene Ventral neuroblasts defective (Vnd), resulted in ectopic persistence of non-MB neuroblasts located on the dosal surface of the brain or occasionally in the optic lobe. Thus, our screen identified multiple genes that are involved in terminating neurogenesis of different subsets of neuroblasts.

Initial characterization of the role of Ey in terminating MB neuroblasts

One candidate chosen for further characterization was the transcription factor Ey, an ortholog of the vertebrate Pax6. We included Ey in our screen as it was known to be expressed predominantly in MB neuroblasts (Noveen et al. 2000a; Kurusu et al. 2000; Callaerts et al. 2001).

Our initial results showed that some MB neuroblasts persist in *worGAL4, UASeyRNAi* brains, suggesting that Ey may promote the elimination of MB neuroblasts. To confirm the reproducibility of this phenotype, we again knocked down expression of Ey using *worGAL4* to drive expression of *UASeyRNAi* (HMS00489) in all neuroblasts (Sipe & Siegrist 2017; Bayraktar & Doe 2013). As

expected, MB neuroblasts were not observed in adult control brains (Fig 2.3 A,B; quantified in C). However, *worGAL4, UASeyRNAi* animals averaged 0.33 neuroblasts per brain hemisphere (n= 47) persisting in 1 day-old adults (Fig 2.3 A-C). We confirmed this result using a second RNAi line that targets a different coding exon (JF025501) (Fig 2.3C). We also looked earlier in development and found fewer than four MB neuroblasts in some animals (average = 3.83 at 48hr APF). We conclude that Ey promotes survival of MB neuroblasts early in development but also has a late function to promote their termination.

Cell size is an indicator of growth signaling in neuroblasts since it becomes restricted as they terminate cell division (Siegrist et al. 2010; Chell & Brand 2010; Yang et al. 2017; Homem et al. 2015). We measured the diameter of control and *worGAL4, UASeyRNAi* MB neuroblasts at 48hr APF and in 1-day-old adults and found that cell size was not statistically different from control animals at either stage. These data suggest that growth is not reduced in *worGal4, UASeyRNAi* MB neuroblasts.

MB neuroblasts generate neurons that send projections which terminate into five distinct lobes of the mushroom body (Lee & Luo 1999). We assayed the size of the mushroom body structure using Fas2 antibody staining, and observed it is reduced in adult animals. This reduction is consistent with previous results obtained from *ey* mutants (Callaerts et al. 2001; Kurusu et al. 2000). Although MB neuroblast elimination is delayed, we observed a reduction in the gross size of the mushroom body lobes, suggesting that could Ey have different roles early and late in MB neurogenesis.

Eyeless acts late in MB elimination

Ey is known to be expressed at low levels in the MB neuroblasts and at higher levels in their neuronal progeny (Noveen et al. 2000b; Callaerts et al. 2001; Kurusu et al. 2000). In the abdominal ventral nerve cord neuroblasts, the homeotic gene Abd-A also is weakly expressed in neuroblasts and becomes upregulated just prior to their elimination (Bello et al. 2003). We wanted to test if Ey levels similarly increase during pupal development prior to MB elimination. Therefore, we assayed expression of Ey in MB neuroblasts throughout pupal stages. We did not detect an obvious change in levels by immunofluorescence (Fig 2.4), suggesting that Ey expression is not temporally regulated in MB neuroblasts.

Given that Ey is expressed throughout development, we wondered if Ey has a specific late role required for the elimination of MB neuroblasts. To test this possibility, we used a temperature sensitive tubGal80 (*tubGal80ts*) to confine Ey knockdown to late pupal stages (McGuire et al. 2003). Due to early eclosion time, we dissected brains at 120hr APF (approximately 30 hours after most animals eclosed under this temperature regime). With knockdown of Ey late, we observed on average 0.79 MB neuroblasts per lobe (Fig 2.5 C quantified in D), we did not observed MB neuroblasts in control animals at any of the stages assayed (Fig 2.5 B, quantified in D). In addition we assayed one-week and two-week old adult brains for the presence of MB neuroblasts. We found an average of 0.32 and

0.14 persisting MB neuroblasts, respectively. Thus, we concluded that Ey is required late to eliminate MB neuroblasts.

Ey acts in parallel to proapoptotic genes

We next asked how Ey promotes elimination of MB neuroblasts. Apoptosis and autophagy are two pathways that act in parallel to eliminate MB neuroblasts, with long-term persistence requiring inhibition of both pathways (Siegrist et al. 2010). To test whether Ey was acting through autophagy or apoptosis we co-expressed *UASeyRNAi* with (1) an artificial microRNA that targets the proapoptotic genes Reaper, Hid, or Grim or (2) a dominant negative Atg1 (*UASAtg1DN*) and assayed for long-term persistence of MB neuroblasts in two-week-old animals (Siegrist et al. 2010; Scott et al. 2007). We observed that some MB neuroblasts persist in two-week-old *worGAL4, UASmiRHG, UASeyRNAi* brains but none were present in *worGAL4, UASeyRNAi, UASAtg1DN* brains (Fig 2.6 A,B quantified in C). We conclude that Ey acts in parallel with proapoptotic genes possibly through autophagy to regulate termination in MB neuroblasts.

Ey promotes autophagy in MB neuroblasts

Since Ey acts in parallel to Reaper, Hid, and Grim, we tested whether it is required for autophagy in MB neuroblasts by expressing *UAS-GFP-mCherry-Atg8*. This reporter for autophagic flux is a fusion protein between a pH-sensitive GFP, pH-insensitive mCherry, and Atg8 (LC3 in mammals), a core component of the autophagosome throughout its maturation (Kimura et al. 2007; Jacomin and

Nezis, 2016). Due to the changes in pH during autophagosome maturation, early autophagosomes are labeled by both GFP and RFP, while mature autophagolysosomes are labeled by only RPF. When we assayed the autophagy reporter in Ey knockdown, we observed a reduction the number of puncta in MB neuroblasts compared to controls (Fig. 2.6 D-K, quantified in L). In addition, we saw a lower percentage of RFP+GFP- autolysosomes, suggesting that autophagic flux is also inhibited (Fig 2.6 K). From this data we conclude that Ey is required for autophagy shortly before MB neuroblasts are eliminated by apoptosis.

Discussion:

From our RNAi screen, we identified several genes that regulate MB neuroblast elimination. Of particular interest, knockdown of the transcription factors Ey, Rx, or Oc allowed some MB neuroblasts to persist into adult stages (Fig 3.1 A,B,C). As MB neuroblasts are known to express Ey, Rx, and Oc, these transcription factors may give MB neuroblasts competence to respond to a temporal cue to terminate MB neuroblast proliferation, analogous to the role of Abd-A in the ventral nerve cord (Bello et al. 2003; Kunz et al. 2012; Urbach 2003). Abd-A is expressed shortly before abdominal ventral nerve cord neuroblast undergoes apoptosis (Bello et al. 2003; Arya et al. 2015).

Initial characterization of Ey in terminating MB Neuroblasts

We chose to characterize the role of Ey in eliminating MB neuroblasts in more detail as Ey is known to be expressed in MB neuroblasts (Noveen et al. 2000b; Kurusu et al. 2000; Callaerts et al. 2001). We found that it acts in parallel to the proapoptotic genes by promoting autophagy (Fig 2.6).

Eyeless is the ortholog of the vertebrate *PAX6* gene (Quiring et al. 1994). PAX6 is expressed in cortical neural progenitors in the ventricular zone and is required to keep them engaged in the cell cycle (Gotz et al. 1998). Dose dependent effects of PAX6 determine whether neural stem cells self renewal or undergo neurogenic divisions that prematurely deplete the stem cell pool (Sansom et al. 2009). To our knowledge there is not a known role for PAX6 to regulate autophagy.

How does Ey promote proliferation and neurogenesis early while terminating neurogenesis late? One possibility is that Ey is necessary to provide competence to receive or respond to extracellular signals. Another possibility is that the progression of neuroblasts through the temporal identity program could result in a change in its activity. Further characterization of the genes that Ey interacts with will be necessary to address this question.

We experienced difficultly replicating several of our initial analyses of some RNAi lines. We did not observe MB neuroblasts in 1-day-old adults when we knocked down Grh, Rx, or Oc using a *worGAL4* line lacking *tubGal80ts* or *UASDicer*. One possibility is that like Ey, these genes may regulate autophagy rather than apoptosis, which has a weaker affect on neuroblast persistence than inhibition of genes in the apoptotic pathway (Siegrist et al. 2010). We have

preliminary data with the autophagic flux reporter that supports the idea of the hypothesis that Rx and Oc may promote autophagy.

Knockdown of Notch/Delta and Scarecrow allow subsets of non-MB neuroblasts to persist

During our screen, we also identified some RNAi lines which resulted in the persistence of non-MB neuroblasts, including Notch and Delta. Knockdown of Delta resulted in the most penetrant neuroblast persistence phenotype from the screen (Fig 2.2E). The Notch signaling pathway is a critical regulator of multiple cell fate decisions during development. Notch signaling regulates programmed cell death in the ventral nerve cord and optic lobe in coordination with temporal factors (Khandelwal et al. 2017; Li et al. 2013; Arya et al. 2015). It will be interesting to investigate how Notch and Delta regulate elimination of non-MB neuroblasts.

We also identified one gene that currently does not have a described role in *Drosophila* neurogenesis (Fig 2.2D). Scarecrow (Scro) is a member of the NK family of homeodomain transcription factors, with high sequence similarity to the the dorsal-ventral patterning gene, Vnd (Zaffran et al. 2000). *NKX2.1,* the vertebrate homolog of *scro,* is also thought to play a role in dorsal-ventral patterning in the developing brain (Sussel et al. 1999). *NKX2.1* is expressed in neural progenitors in the medial ganglionic eminences, which contributes interneurons to all of the layers of the cortex (Butt et al. 2005). *NKX2.1* is required for the temporal specification of a subset neurons generated by these

progenitors, as well as for their proper migration into the cortex (Butt et al. 2008; Nóbrega-Pereira et al. 2008). However *NKX2.1* is not known to participate in the termination of neurogenesis.

Scro was previously reported to be expressed in the larval optic lobe and a subset cells in the central brain (Zaffran et al. 2000). In *worGAL4, UASscroRNAi* brains, we observed that a subset of Dpn+ non-MB neuroblasts located in the dorsal medial region of the CNS persisted into adult stages. These ectopic neuroblasts are stereotypically located on the dorsal medial surface and occasionally in the optic lobe (Fig. 2.2D.), which raises the possibility that Scro may be involved in eliminating a particular lineage of neuroblasts. Characterizing which lineages of neuroblasts are affected in *worGAL4, UASscroRNAi* will be important to explore this further. Taken together, the results from our screen provide a valuable resource to build upon. Investigating these genes will lead to new mechanistic insights as to how cell-intrinsic factors promote neural stem cell elimination and the termination of neurogenesis.

Materials and Methods:

Fly husbandry and genetics: All experiments were conducted at 25C on a 12-hour light dark cycle and using a standard Bloomington diet. The following stocks were used: *worGAL4, UASDcr2; pcnaGFP, tubGal80ts, worGAL4 (II), UASeyRNAi (HMS00489;III), worGAL4; UASeyRNAi, UASey (Uwe Walldorf), worGAL4, UASmiRHG, UASAtg1DN (3), worGAL4, UASGFPmcherryAtg8 (3), UASGFPmcherryAtg8 (3), UAS-TriP* RNAi lines (see table 2.1). For the screen

Virgin females *worGAL4, UASDcr2; PCNAGFP, tubGal80ts* files were crossed to males of selected RNAi lines from the TriP collection (Perkins et al. 2015). The progeny from this cross were raised at 25ºC until the desired time point (Table 3.1)

Immunohistochemistry: Temperature shift: For the temperature shift experiment, embryos were collected and kept at 18°C. White pupae then shifted to 29°C at 24 hours after pupal formation (APF) until the indicated time they were assayed. Adult flies eclosed at approximately 90 hours APF under this paradigm.

Immunofluorescence and confocal microscopy: Brains were dissected, fixed, and stained as described previously (Siegrist et al., 2010; Doyle et al., 2017; Sipe and Siegrist, 2017). Images were acquired using an upright Leica SP8 confocal microscope with a 63x 1.4NA oil immersion objective and analyzed using Imaris and ImageJ software. Figures were assembled using Adobe Photoshop and Illustrator software. The following antibodies were used rat anti-Deadpan (1:10), rabbit anti-Scribble (1:1000), mouse anti-Discs Large (1:40; DSHB), rabbit and chicken anti-GFP (1:1000), rabbit anti-Eyeless (1:1000; a kind gift from Uwe Walldorf). Appropriate secondary antibodies were used (Fisher; see Appendix).

Prediction of candidate transcription factors

To identify regions of interest near grim and skl we selected 45 regions with known transcription factor colocalization during development in Drosophila (HOT spots) (Moorman et al. 2006; Négre et al. 2011). We identified conserved sequences from these ~1-3kb regions using EvoprinterHD (Odenwald et al. 2005). We curated the sequences that were conserved in *D. melanogaster, D. simulans D. sechellia, D. erecta, D. yakuba, D. permilis, and D. pseudoobsura* and identified transcription factor binding sites within the conserved sequences using the *R* package PWMEnrich (Jin et al. 2013). Sequences were compared to the position weight matrices (PWMs) of transcription factors from the FlyFactorSurvey and the score compared to a pre-computed background distribution to determine statistical significance (Christensen et al. 2012). A stringent threshold of $p < 0.0001$ was used as the cutoff.

Acknowledgements:

We thank Uwe Walldorf for sharing the anti-Ey (Rabbit) antibody. We thank the Bloomington stock center and TriP collection for providing transgenic flies.

Table 2.1: A list of RNAi tested for presence of persisting MB neuroblasts

Gene	Symbol	CG	RNAi line	Type
abdominal a	abd-A	CG11648	JF03167	TF
abdominal b	abd-B	CG11648	HMJ03133	TF
abnormal chemosensory jump 6	acj6	CG9151	HMS02207	TF
Antennapedia	Antp	CG1028	JF02754	TF
apterous	ap	CG8376	HMS02207	TF
Broad	br	CG11491	HMS00042	TF
C-terminal Binding Protein	CtBP	CG7583	JF01291	Chromatin modifier
castor	cas	CG2102	HMS01180	TF
CG4238	CG4238	CG4238	GL00505	TF
crocodile	croc	CG5069	HMS01122	TF
Cut	cut	CG11387	HMS00924	TF
Dacshund	dac	CG4952	HMS01435	TF
daughterless	da	CG5102	JF02092	TF
Deformed	Dfd	CG2189	HMC03094	TF
Dichete	D	CG5893	HMS01150	TF
Discs overgrown	Dco	CG2048	HM04075	Kinase
dorsal	dl	CG6667	HMS00727	TF
Dorsal Related Immunity Factor	Dif	CG6794	HM05191	TF
earmuff	erm	CG31670	HMC03062	TF
Ecdysone Receptor	EcR	CG1765	HMC03114	TF
Ecdysone Responsive Protein 74 EF	Eip74EF	CG32180	JF02515	TF
Epidermal Growth factor receptor	EGFR	CG10079	HMS05003	Receptor
Eyeless	ey	CG1464	HMS00489	TF
eyes absent	eya	CG9554	HMS04515	TF/phosphatase
forkhead	fkh	CG10002	HMS00882	TF
ftz transcription factor 1	ftz-f1	CG4059	HMS00019	TF
gooseberry-neuro	gsb-n	CG2692	JF02915	TF
Grainyhead	grh	CG42311	HMS02446	TF
Hairless	H	CG5460	HMS01182	TF
hairy	h	CG6494	HMS01313	Chromatin modifer
Hormone Receptor 39	HR39	CG8676	HMS00018	TF
Hunchback	hb	CG9786	HMS01183	TF
Kruppel	Kr	CG3340	HMS01106	TF
longitudinals lacking	lola	CG12052	GLV21086	TF
Max	Max	CG9648	HMS02018	TF
Medea	Med	CG1775	JF02218	TF

Methoprene tolerant	Met	CG1705	HMJ23518	TF
Mitf	Mitf	CG43369	HMS02712	TF
mod(mdg4)	mod(mdg4)	CG32491	HMS01538	Chromatin modifer
Myc	dm	CG10798	HMS01538	TF
nanos	nos	CG5637	HMS00785	RNA binding protein
nervous fingers 1	nerfin-1	CG13906	HMC04083	TF
Notch	N	CG3936	HMS00001	Receptor
Ocelliless (Orthodentricle)	oc	CG12154	HMS01314	TF
Optix	Optix	CG18455	HMC03993	TF
Relish	Rel	CG11992	HMS01538	TF
Retinal Homeobox	Rx	CG10052	HMC03995	TF
scarecrow	scro	CG17594	HMS00828	TF
senseless	sens	CG32120	HMC03997	TF
Seven-up	svp	CG11502	JF03105	TF
Sine Oculis	so	CG11121	HMS01441	TF
snail	sna	CG3956	HMS01252	TF
Stat92E	Stat92E	CG4257	HMS00035	TF
Supressor Hairless	Su(H)	CG3497	HM05110	TF
Tailless	tll	CG1378	JF02545, HMS01316	TF
Taiman	tai	CG13109	HMS00673	TF
tao	tao	CG14217	HMS02333	Kinase
torso	tor	CG1389	HMS00021	Receptor
Transforming Growth Factor Beta Activated Kinase	Tak1	CG18492	HMC06368	Kinase
Trithoraxlike	Trl	CG33261	HMS02188	Chromatin modifer
twin of eyeless	toy	CG11186	HMS00544	TF
Ultrabithorax	Ubx	CG10388	HMS01403	TF
Ultraspircle	usp	CG4380	HMS01620	TF
Ventral Veins Lacking	vvl	CG10037	HMC03058	TF
Visual System Homeobox 1	Vsx1	CG4136	HMC03085	TF
Visual System Homeobox 2	Vsx2	CG33980	JF02121	TF
yorkie	yki	CG4005	HMS00041	TF
Zernkuilt	zen	CG1046	HMS01109	TF

Table 2.2 Genes identified in the screen.

Gene	RNAi line	Gene/TF Family	NB Phenotype
Delta	HMS01309	Signaling	Non-MB NB persist
E93	HMC04773	Wing Helix	MB NB persist
eyeless	HMS00489	HTH & Homeodomain	MB NB persist
grainyhead	HMS02446	bHLH	MB NB persist
longitudinals lacking	GLV21086	BTB-Zinc Finger Domain	Unknown Dpn+ cells
Mitf	HMS02712	bHLH	MB NB lost early
Modifier of (mdg4)	HMS00849	BTB-Zinc Finger Domain	MB NB lost early
Myc	HMS01538	Transcription Factor	MB and non-MB neuroblasts loss/persist
Notch	HMS00001	Transcription factor binding	Non-MB NB persist
occeliless	HMS01314	Homeodomain	MB NB persist
Retinal homeobox	HMC03995	Homeodomain	MB NB persist
Scarecrow	HMS00828	Homeodomain	Non-MB NB persistence (Dorsal)
Ultrabithorax	HMS01403	Homeodomain	MB NB persist
Yorkie	HMS00041	Transcripition factor binding	MB NB persist

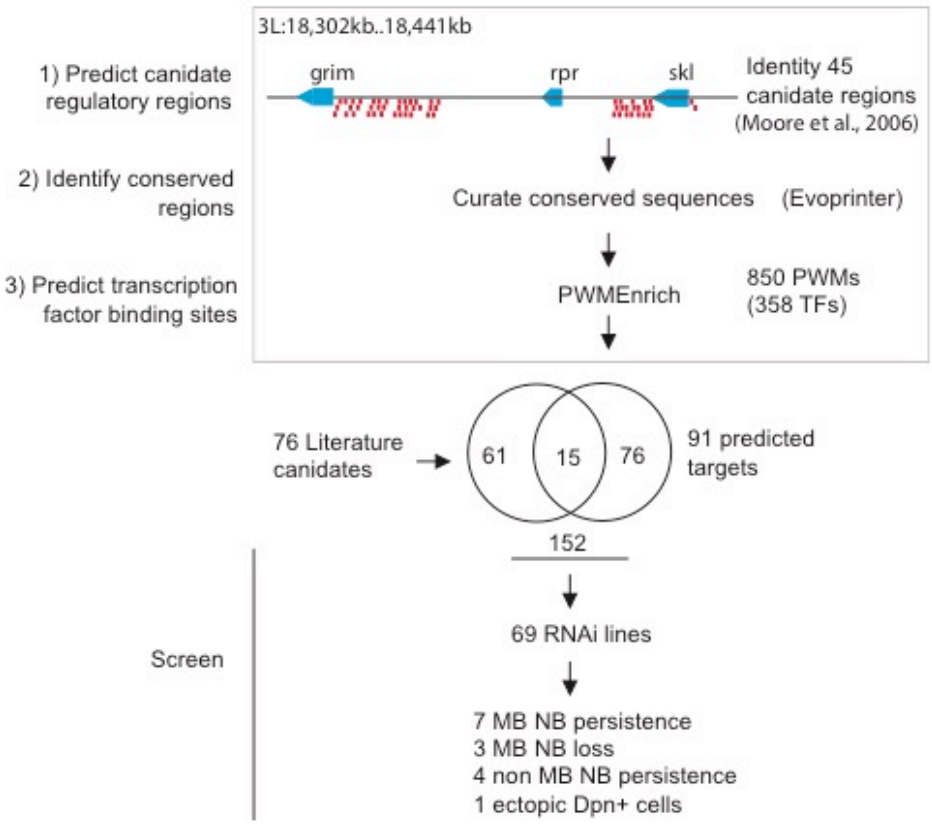

Figure 2.1. Selection of candidate genes and screen summary. We screened a combination of genes predicted to bind near *grim* and *skl*. (1) We first identified candidate regulatory regions from transcription factor HOT spots, which are regions that are known to bind multiple transcription factors (Red lines) (Moorman et al. 2006). (2) Next we identified evolutionarily conserved sequences using Evoprinter, which compares different Drosophilids (Odenwald et al. 2005). We predicted 91 target genes using this approach. In addition, we included 76 candidates from the literature known to regulate programmed cell death (Homeotic genes, ecdysone signaling genes, transcription factors with evidence to bind proapoptotic genes) or to be expressed in MB neuroblasts. In total, we assembled 152 candidate genes. We crossed 69 UAS-driven RNAi lines from the

TRiP collection to flies containing the tissue-specific reporter worniuGAL4 (Perkins et al. 2015). From this screen, we identified 14 RNAi lines that resulted in either premature loss or persistence of neuroblasts.

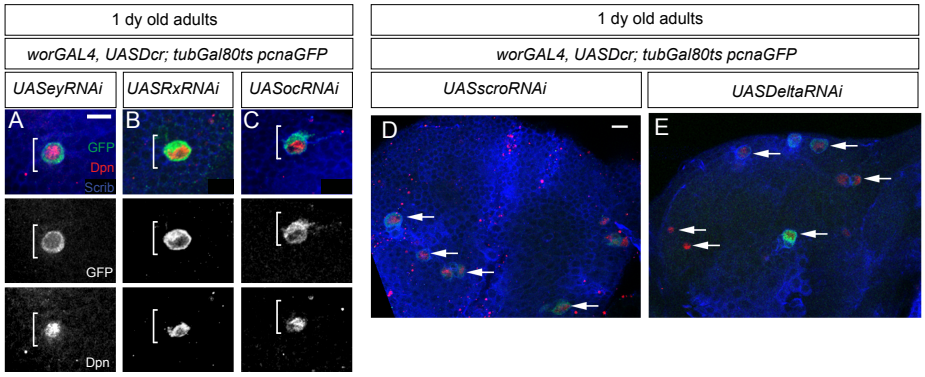

Figure 2.2: Examples of genes identified from the screen. (A-C) Color overlays of several RNAi lines where we found one-day old MB neuroblasts persist into adult stages. MB neuroblasts were observed with knockdown of Ey (A), Rx (B), and Oc (C). Single channel images are shown below. (D-E) Z-projections of one-day old brain hemispheres from *UASscroRNAi* and *UASDeltaRNAi* animals labeled with GFP, Dpn, and Scribble. Arrows indicate Dpn+ cells. Scale bar = 10 μm.

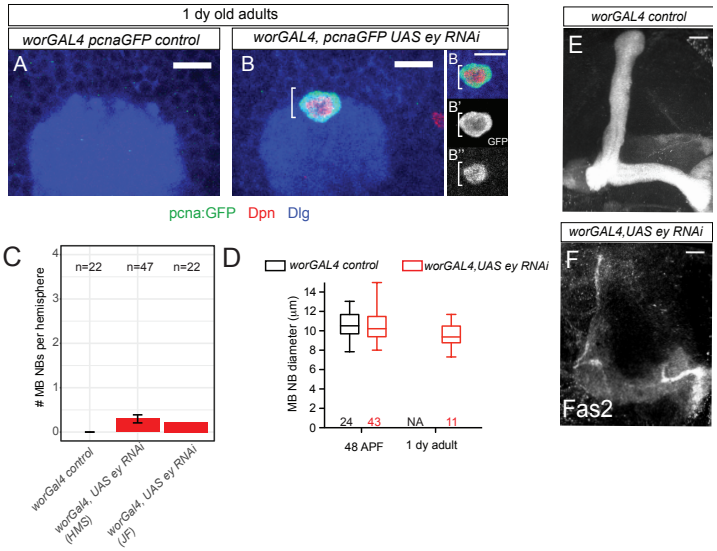

Figure 2.3: Knockdown of Ey allows MB NBs to persist into adult stages. (A-B) Z projections of the dorsal surface of control and *UASeyRNAi* animals. Brackets indicate MB neuroblasts labeled with antibodies against Dpn (red), GFP (green), and the membrane marker Dlg (blue). The MB calyx is marked strongly with Dlg and is used as a landmark. (C) Quantification of the average number MB neuroblasts per lobe in one-day-old adults. (D) Box plots of MB neuroblast diameters for indicated genotypes and times. (E-F) Z-projection of the ventral surface of a one-day-old adult brains, showing the MB lobes labeled with Fas2. Scale bar = 10 μm.

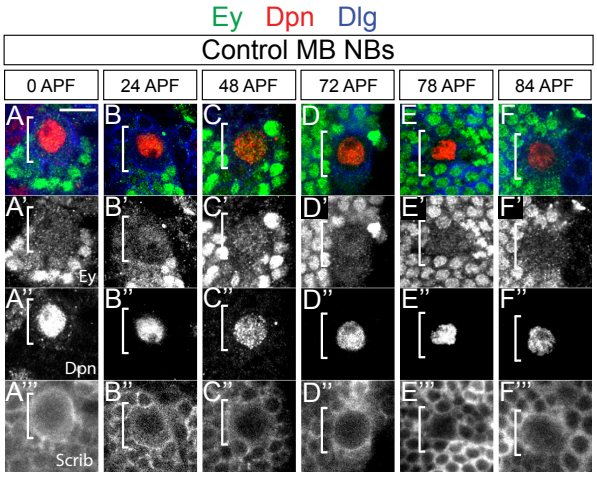

Figure 2.4. Ey is expressed in MB neuroblasts during pupal development

(A-F) Colored overlay with greyscale images below of control neuroblasts from the indicated time points (above), labeled with markers indicated within panel A and at top. Scale bar = 10μm.

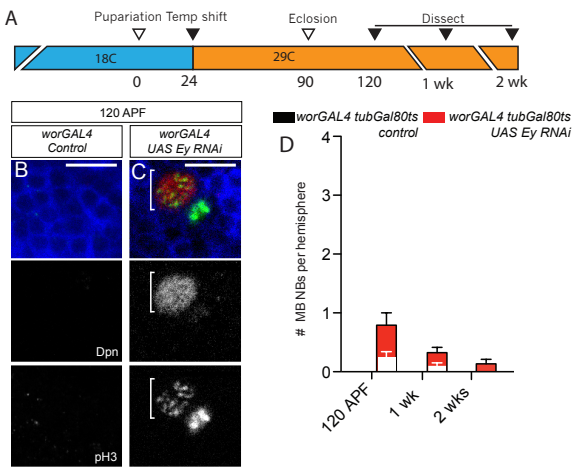

Figure 2.5 Ey is required late to terminate MB neuroblast

(A) Schematic of the temperature shift paradigm. To restrict knockdown of Ey to late developmental stages, we used a temperature sensitive GAL80. When animals are raised 18°C, GAL80 is active repressing GAL4 mediated expression of *UAS-eyRNAi*. When shifted to 29°C GAL80 is inactivated, and Ey expression is knocked down. (B, C) Single images control (B) and *worGal4, tubGAL80ts, UASeyRNAi* (C) of persisting MB neuroblasts in adult animals under this paradigm. (D) Quantification of the number of persisting MB neuroblasts at the indicated time points (120 hours occurs approximately 30 hours after eclosion under this paradigm). White bars indicate the number of MB neuroblasts marked with the mitotic marker pH3.

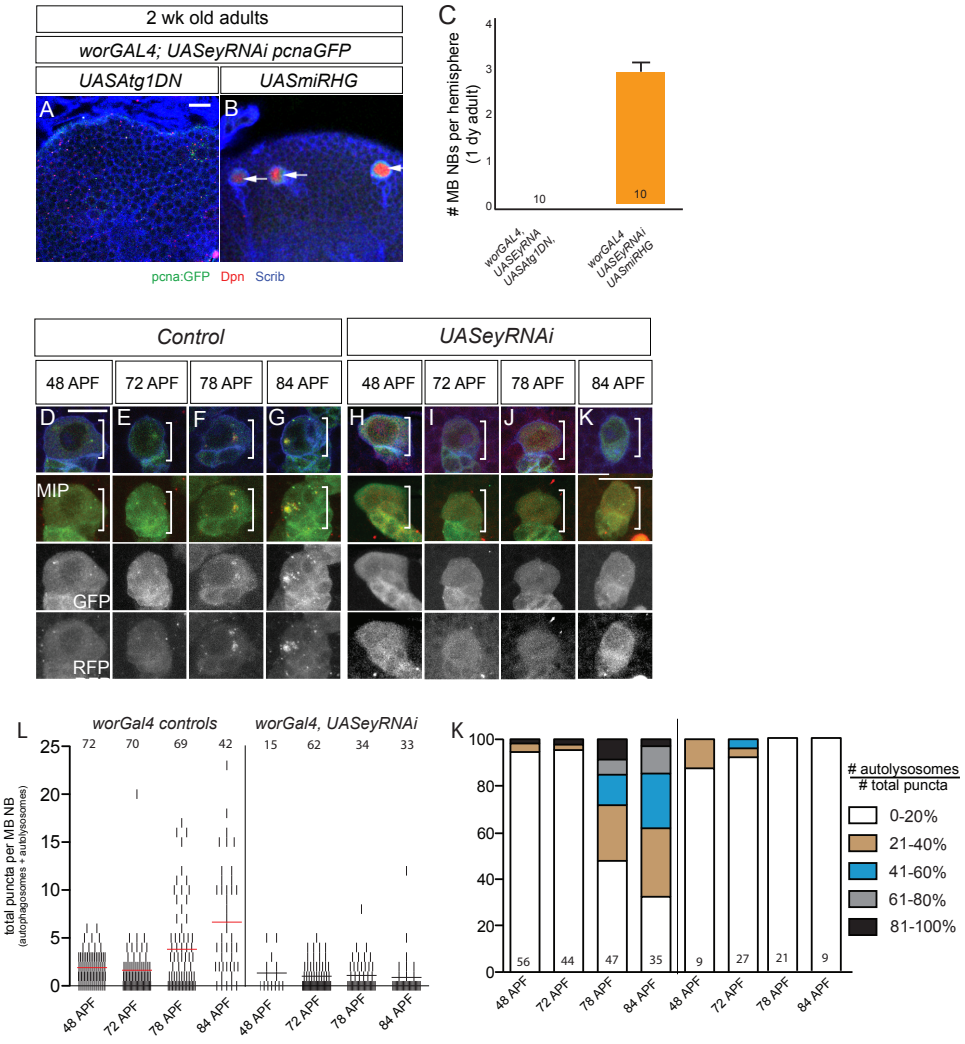

Fig 2.6 Ey is required for autophagy in MB neuroblasts. (A-B) Confocal images of the dorsal surface of one brain hemisphere from two-week-old animals of the indicated genotype. Arrows indicate MB neuroblasts, labeled with antibodies against Dpn (red), GFP (green), (D-K) Top, colored overlay of MB neuroblasts (white brackets) at indicated times and genotypes co-expressing the autophagy reporter *UAS-GFP-mCh-Atg8*. Below, colored overlay of maximum intensity projection of MB neuroblast above, single channel greyscale images

below. Scale bar = 10 μm. (L) Quantification of autophagosomes and autolysosomes. Black tics represent individual MB neuroblasts. Total number of MB neuroblasts assayed is indicated at the top of each column, red lines denote mean. (M) Distribution of percentages of autolysosomes relative to the total number of puncta in MB neuroblasts over time.

Chapter 3

E93 is a late acting temporal factor that integrates neuroblast intrinsic state with developmental time to terminate neurogenesis via autophagy

Matthew Pahl, Susan Doyle, and Sarah Siegrist

Under review

SUMMARY

Most neurogenesis occurs during development, driven by the cell divisions of neural stem cells. We use Drosophila to understand how neurogenesis terminates once development is complete, a process critical for neural circuit formation. We identified E93, a steroid hormone-induced transcription factor that downregulates PI3-kinase to activate autophagy for mushroom body (MB) neuroblast elimination. MB neurogenesis prolongs into adulthood when E93 is reduced and terminates prematurely when E93 is overexpressed. Cell intrinsic Imp/Syp temporal factors restrict E93 expression to late-staged MB neuroblasts, while extrinsic steroid hormone receptor (EcR) activation boosts E93 levels for termination. Imp/Syp form a temporal cassette with E93 that links early neurogenesis with termination: Imp promotes early neurogenesis by inhibiting Syp, and Syp promotes termination by inhibiting Imp and positively regulating E93. Altogether, E93 functions as a late acting temporal factor integrating extrinsic hormonal developmental timing cues with neuroblast intrinsic temporal state to precisely time neurogenesis ending during development.

KEYWORDS

neural stem cell, neurogenesis, autophagy, temporal factors, steroid hormone, mushroom body, PI3-kinase, neuroblast, E93, ecdysone

INTRODUCTION

Neurogenesis starts and stops in a spatially and temporally defined manner. Most neurogenesis occurs during development, but in some animals, new neurons are also produced throughout adulthood. Unlike developmental neurogenesis, adult neurogenesis is relatively restricted. Only certain neuron types are produced in only some brain regions (reviewed in Gonçalves et al. 2016; Lim & Alvarez-buylla 2016). For example, adult rodents produce new olfactory bulb neurons in the SVZ for odor detection, while primates produce new hippocampal neurons important for memory and learning. However, the extent of adult neurogenesis in primates, including humans, is uncertain (Boldrini et al. 2018; Sorrells et al. 2018). Equally important to continuing neurogenesis is to stop it once development is complete. This is because prolonged or ectopic neurogenesis leads to defects in the neural circuitry, which is now associated with autism, mental illness, and neurodegenerative disease (reviewed in Schoenfeld & Cameron 2015; Winner & Winkler 2007; Hazlett & Poe 2011).

We use Drosophila as a model to understand how extrinsic factors, local and systemic, integrate with neural stem cell intrinsic factors to control timing and mechanism of neurogenesis termination during development. Like mammals, neurons in the Drosophila brain are generated directly from the asymmetric divisions of neural stem cells, known as Type I neuroblasts in

Drosophila, or indirectly from a transit amplifying daughter cell, produced by a Type II neuroblast (Doe 2008; Brand & Livesey 2011; Kang & Reichert 2015; Homem et al. 2015). In Drosophila, neurogenesis completes during development and no new neurons are produced during adulthood (Kato et al. 2009; Von Trotha et al. 2009; Siegrist et al. 2010). This is because all neuroblasts are eliminated by terminal differentiation or apoptosis before adulthood (Maurange, Cheng & Alex P Gould 2008; Siegrist et al. 2010; Chai et al. 2013; Homem et al. 2014). Most Type I and all Type II neuroblasts stop dividing during early pupal stages, except for mushroom body neuroblasts (MB neuroblasts), a Type I subset, that produces neurons important for memory and learning (summarized in Fig. 1A). MB neuroblasts, which reside on the dorsal brain surface superficial to the MB calyx, continue dividing several days longer, until late pupal stages, and undergo apoptosis shortly before animals emerge from their pupal case as adults (Truman & Bate M 1988; Ito & Hotta 1992; Siegrist et al. 2010) .

Yet, independent of when neuroblasts terminate or whether they differentiate or undergo apoptosis, all neuroblasts undergo a period of reduced growth and proliferation prior to their disappearance, suggesting this reduced growth triggers neuroblast elimination (Maurange, Cheng & Alex P Gould 2008; Siegrist et al. 2010; Chai et al. 2013; Homem et al. 2014). In Type I and Type II neuroblasts that terminate early, reductions in cell growth and proliferation are caused by transcriptional changes in metabolic enzymes, likely induced by systemic increases in the steroid hormone ecdysone (Homem et al.,

2014). While in MB neuroblasts, reductions in growth and proliferation are due to decreased levels of PI3-kinase activity (Siegrist et al. 2010). Growth-inhibited MB neuroblasts are then primed for elimination by apoptosis (Siegrist et al. 2010). However, blocking MB neuroblast apoptosis alone is not sufficient to prevent their elimination, because downregulation of PI3-kinase activates autophagy in parallel to ensure MB neuroblast removal and termination of neurogenesis. Importantly, when both autophagy and apoptosis are inhibited together, MB neuroblasts persist long term and continually generate new neurons during adulthood, some of which incorporate into existing neural structures and others which mis-project axons elsewhere (Siegrist et al. 2010).

While PI3-kinase levels affect timing of MB neurogenesis termination, it remains unclear how PI3-kinase is regulated. PI3-kinase activity is nutrient regulated in many cell types, including MB neuroblasts (Sipe & Siegrist 2017), while in the salivary gland and fat body, increasing systemic ecdysone triggers reductions in levels of PI3-kinase activity (Rusten et al. 2004; Berry & Baehrecke 2007; Colombani & Le 2010). Two intrinsic neuroblast temporal factors, Imp (IgF-II mRNA binding protein) and Syp (Syncrip), also regulate timing of MB neurogenesis termination (Liu et al. 2015; Yang et al. 2017). When Imp is knocked down, MB neurogenesis terminates prematurely and when Syp is knocked down, MB neurogenesis prolongs into adulthood. Imp and Syp, both RNA binding proteins, are expressed in opposing temporal gradients in all neuroblasts, with Imp expressed at high levels first, followed by high Syp later (Liu et al. 2015; Ren et al. 2017; Syed et al. 2017b). Whether

PI3- kinase interacts with Imp/Syp to control neurogenesis timing is not known, however it was recently shown that ecdysone is required for the Imp to Syp temporal switch in Type II neuroblasts (Syed et al. 2017b) This raises the possibility that an ecdysone-induced temporal switch could also regulate PI3-kinase levels in MB neuroblasts and time neurogenesis ending during development.

To reveal the mechanism of how MB neuroblasts terminate cell divisions during development, we carried out a large-scale targeted RNAi screen. We identified Ecdysone- induced protein 93F (referred to as E93), a pipsqueak transcription factor family member, first characterized as an ecdysone response gene required for autophagy of larval tissues during metamorphosis(Baehrecke & Thummel 1995; Lee et al. 2000; Lee & Baehrecke 2001). More recently, it has been shown that E93 is also expressed in Type II neuroblasts in response to ecdysone, and in the wing, where E93 modifies chromatin accessibility at temporally regulated enhancers (Syed et al. 2017b; Uyehara et al. 2017). Here, we find that E93 down regulates PI3-kinase levels in MB neuroblasts to induce autophagy for MB neuroblast elimination. In the absence of E93, PI3-kinase levels remain high, autophagy fails, and neurogenesis continues into adulthood. E93 expression correlates with timing of neurogenesis termination, both occur late, and if E93 is overexpressed constitutively, neurogenesis terminates prematurely. We find that Imp/Syp temporal factors restrict E93 expression to late developmental stages, while EcR activation regulated by systemic hormone conditions induces E93 to high

levels required for neurogenesis termination. Altered Imp/Syp temporal factor expression as well as reduced EcR activation cause neurogenesis to either prolong into adulthood or terminate prematurely. By integrating the neuroblast intrinsic temporal state with extrinsic systemic hormonal cues, E93-dependent regulation of PI3-kinase provides a mechanism for neurogenesis termination to be synchronized with timing of animal development. This ensures that the adult mushroom body contains an appropriate number of molecularly and functionally distinct neuron types necessary for animal behavior.

RESULTS

E93 functions cell autonomously to eliminate MB neuroblasts during pupal development We carried out a candidate RNAi screen to identify genes required to eliminate MB neuroblasts and terminate neurogenesis during development. We screened factors known to be expressed in MB neuroblasts and factors known to initiate apoptosis and/or regulate autophagy. Candidate *UAS-RNAi* lines were crossed to *worGAL4*, and brains of one-day old adults were screened for presence of persisting neuroblasts. We identified the ecdysone-induced protein 93F (Eip93F in Flybase), hereafter referred to as E93. Following constitutive knock down of E93 in all NBs (*worGAL4, UAS-E93RNAi* #HMC04773), we observed on average, 3.5 persisting MB neuroblasts per brain hemisphere (Fig. 3.1B,C, n=50 brain hemispheres) in adult animals, whereas 0 MB neuroblasts were observed in control animals (n>50, data not shown)(Siegrist et al. 2010; Doyle et al. 2017). MB neuroblasts were positively

identified based on Deadpan (Dpn) and *pcna:GFP* (S-phase activity) reporter expression and location, on the dorsal brain surface superficial to the MB calyx (Fig. 3.1B) (Siegrist et al. 2010; Doyle et al. 2017). We tested a second RNAi line (#KK108140) which targets a different E93 protein coding exon and observed a similar but less penetrant phenotype (Fig. 1C and Figure S1. Related to Figure 1). Next, we used *OK107Gal4* to restrict E93 knockdown to MB neuroblasts and their neuron progeny. Again, MB neuroblasts were observed on the dorsal surface (average 2.4 per brain hemisphere, n=19 brain hemispheres), whereas control animals had no MB neuroblasts (Fig. 3.1C). We conclude that E93 is required for MB neuroblast elimination and termination of MB neurogenesis during development.

To determine whether E93 is sufficient for early induction of MB neurogenesis termination, we over-expressed a wild type version of E93 in all neuroblasts throughout development (*worGAL4,UAS-E93 WT*). MB neuroblasts normally terminate divisions between 78-90 hours APF (after pupal formation), whereas other Type I and Type II neuroblasts (referred to as non-MB neuroblasts) terminate divisions much earlier (Fig. 3.1A). Following E93 overexpression, MB neuroblasts were not present at 48 hours APF (n=15 brain hemispheres), indicating that E93 overexpression eliminates MB neuroblasts prematurely. Consistent with this conclusion, we found that the adult mushroom body neuropil was dramatically reduced in E93 overexpressing animals compared to controls, with the majority of late-born, FasII-positive α/β MB neuron types missing (Fig. 3.1G,H, and data not

shown). We conclude that E93 is both necessary and sufficient for termination of MB neurogenesis.

To determine when E93 is required during development, we used a heat-shock inducible GAL4 flip out cassette to control timing of *E93RNAi* expression and E93 inactivation (Fig. 3.1D)(Del Valle Rodríguez et al. 2012). Freshly hatched larvae (0 hours after larval hatching, ALH) and newly formed pupae (0 hours APF) were heat shocked to produce Flippase, which mediates excision of an FRT-flanked STOP codon (Fig 3.1D). After STOP excision, GAL4 is produced, driven by the actin promoter, and *UAS-E93RNAi* expressed in some cells, including MB neuroblasts. MB neuroblast *E93RNAi* expressing clones were positively identified based upon co-expression of a *UAS-RFP* reporter, which is weak in MB neuroblasts but strong in their neuron progeny, and Eyeless (Ey), a transcription factor that specifically marks MB neuroblasts and their neuron progeny (Fig. 3.1E and data not shown) (Kurusu et al. 2000; Noveen et al. 2000a; Callaerts et al. 2001; Sipe & Siegrist 2017). Following either heat shock regime (0 hrs. ALH or 0 hrs. APF), all MB neuroblast *E93RNAi* clones in adult animals had one Dpn- positive neuroblast and no Dpn positive cells were observed outside the *E93RNAi* clone (Fig. 3.1E,F). This suggests that E93 is required for MB neuroblast elimination during pupal stages and functions in a cell autonomous manner. To further define when E93 is required, we heat shocked pupae even later, at 24 or 48 hours APF. Again, all MB neuroblast *E93RNA*i clones in adult animals had one Dpn positive neuroblast, whereas control clones

had no neuroblasts (Fig. 3.1F). We conclude that E93 is required late in development to eliminate MB neuroblasts and terminate MB neurogenesis.

MB neuroblasts express E93 during later pupal development

Type II and some Type I neuroblasts express E93 during later stages of larval development (Syed et al. 2017b). We asked whether E93 is also temporally expressed in MB neuroblasts. In brains of wildtype larvae at 96 hours ALH, we observed E93 in Type I and Type II neuroblasts as reported (Fig. 3.2A, asterisks and 2B), but not in MB neuroblasts (Fig. 3.2A, arrows and 3.2C). Next, we examined MB neuroblasts during pupal stages. In wild type brains at 36 hours APF, E93 was observed in MB neuroblasts and their neuron progeny, but not earlier at 24 hours APF (Fig. 3.2D,E). We found that once expressed, MB neuroblasts maintain E93 throughout pupal development, until their elimination via apoptosis (Fig. 3.2F,G, and data not shown). This is consistent with results from our heat shock experiments demonstrating that E93 is required in late pupae for MB neuroblast elimination. To ensure specificity of the E93 antibody, we used the GAL4 flip out cassette again to generate MB neuroblast *E93RNAi* clones. Compared to control clones, *E93RNAi* clones had dramatically reduced E93 protein levels in both MB neuroblasts and their neuron progeny (Fig. 3.2H,I, and quantified in 3.6B). We conclude that E93 is expressed in MB neuroblasts during the latter half of pupal development, which includes the time when MB neuroblasts normally terminate their cell divisions.

E93 down regulates growth, proliferation and levels of PI3-kinase in MB neuroblasts

MB neuroblasts undergo a period of reduced growth and proliferation, due in part to reductions in levels of PI3-kinase activity prior to their elimination via apoptosis (Siegrist et al. 2010). Failure to downregulate PI3-kinase activity on time could allow *E93RNAi* MB neuroblasts to persist into adulthood (Siegrist et al. 2010). We used the mitosis specific marker phospho- Histone H3 (PHH3) to assay *E93RNAi* MB neuroblast proliferation and the plasma membrane markers Scribble (Scrib) or Discs-large (Dlg) to measure MB neuroblast size. Compared to control MB neuroblasts, which undergo significant decreases in size and proliferation after 72 hours APF prior to their elimination (Siegrist et al. 2010), *E93RNAi* MB neuroblasts remained large and mitotically active, even in one-day old adults (Fig. 3.3A,B). Next, we assayed subcellular localization of the transcription factor Foxo, a downstream effector and readout for levels of PI3-kinase activity (Junger et al. 2003; Puig & Tjian 2005; Puig & Tjian 2006). When PI3-kinase is active, Foxo remains cytoplasmic, and when PI3-kinase is inactive, Foxo relocates to the nucleus to regulate gene expression. At 48 hours APF, midway through pupal development, when MB neuroblasts are still large and actively proliferating, Foxo was mostly cytoplasmic in both control and *E93RNAi* MB neuroblast clones (Fig. 3.3C,D, quantified in H). But from 78-90 hours APF, after MB neuroblasts reduce their growth and proliferation (Siegrist et al. 2010), nuclear Foxo was increased in control but not in *E93RNAi* MB neuroblasts clones (Fig. 3.3E,F, quantified in H). Foxo remained mostly

cytoplasmic in *E93RNAi* MB neuroblast clones throughout pupal development and became nuclear only in adult animals (Fig. 3.3G, quantified in H). We also assayed total Foxo protein levels and found reductions over time in control clones, but not in *E93RNAi* MB neuroblast clones (Fig. 3.3I). We conclude that E93 is required to downregulate growth, proliferation and levels of PI3-kinase activity in MB neuroblasts in a timely manner, which could allow *E93RNAi* MB neuroblasts to persist into adulthood.

To test this possibility, we overexpressed the regulatory subunit of PI3-kinase, *UAS- dp60*, to reduce levels of PI3-kinase activity in *E93RNAi* MB neuroblasts (Weinkove et al. 1999). Essentially no MB neuroblasts were found in brains of one-day old adults (Fig. 3.3J). To determine whether absence of *dp60, E93RNAi* MB neuroblasts in adults correlates with reductions in MB neuroblast growth, we assayed MB neuroblast size at 72 hours APF when *dp60, E93RNAi* MB neuroblasts were still present (Fig. 3.3O). Compared to control and *E93RNAi* MB neuroblasts, *dp60, E93RNAi* MB neuroblasts were significantly smaller, similar to *dp60* MB neuroblasts which terminate prematurely (Fig. 3.3K-P). We conclude that E93 downregulates PI3- kinase to reduce MB neuroblast growth for termination of neurogenesis during development.

PI3-kinase is typically regulated in a nutrient dependent manner through binding of ligand to either InR (insulin-like tyrosine kinase receptor) or Alk (anaplastic lymphoma kinase receptor) in *Drosophila* (Brogiolo et al. 2001; Cheng et al. 2011). We co-expressed *UAS- InRRNAi* or *UAS-AlkRNAi* with

UAS-E93RNAi to knock down InR or Alk with E93 in MB neuroblasts. Relatively large sized MB neuroblasts were still observed in both *InRRNAi*, *E93RNAi* and *AlkRNAi*, *E93RNAi* double knock adult animals (Figure S2A-E. Related to Figure 3.3). We conclude that E93 downregulates PI3-kinase independent of InR and Alk, two known upstream regulators of canonical PI3-kinase signaling.

E93 is required for autophagy and functions in parallel to the pro-apoptotic regulators to terminate MB neurogenesis

Both apoptosis and autophagy are required to eliminate MB neuroblasts and terminate MB neurogenesis (Siegrist et al., 2010). Only by blocking both together can MB neuroblasts persist long-term into adulthood and continually produce new neurons (Siegrist et al., 2010). The pro- apoptotic genes, *reaper*, *hid*, and *grim* (RHG) are required for MB neuroblast apoptosis, however it remains unclear what regulates MB neuroblast autophagy. E93 is reported to induce autophagy of the salivary gland and midgut (Lee et al. 2000; Lee & Baehrecke 2001), therefore we asked whether E93 also induces MB neuroblast autophagy. We used the autophagic flux reporter, *UAS-GFP-mCherry-Atg8*, driven by *worGAL4*, to visualize autophagosome formation in control MB neuroblasts (Kimura et al. 2007; Jacomin and Nezis, 2016). *UAS-GFP-mCherry-Atg8* is a fusion between pH-sensitive GFP, pH-insensitive mCherry, and Atg8, a core component of the initiating phagophore, autophagosome, and final acidic autolysosome (Fig. 3.4M, schematic). From 48 to 72 hours APF, 90% of control MB neuroblasts have 1 or 2 autophagosomes (yellow puncta,

white arrow), reflecting basal autophagy (Fig. 3.4A,J,K and Figure S3A. Related to Figure 3.4). After 72 hours APF, when PI3-kinase activity declines and MB neuroblast growth and proliferation ceases, we found a dramatic increase in the number and size of autophagosomes (yellow puncta) and autolysosomes (red puncta, white arrowhead) in MB neuroblasts (Fig. 3.4C,E,J,K and Figure S3A. Related to Figure 4). In addition, autophagic flux, the change over time of autolysosomes to total puncta number (autophagosomes plus autolysosomes), increased (Fig. 3.4K). Both results suggest that increased autophagy and flux contribute to MB neuroblast elimination via autophagy.

Next, we assayed autophagy in *E93RNAi* MB neuroblasts using the same autophagy flux reporter. From 72 to 84 hours APF, *E93RNAi* MB neuroblasts had significantly fewer autophagosomes (yellow puncta) and autolysosomes (red puncta) compared to control MB neuroblasts at the same developmental stage (Fig. 3.4B,D,F,J,K and Figure S3A. Related to Figure 3.4). By adulthood however, autophagosome and autolysosome number did increase in some *E93RNAi* MB neuroblasts, suggesting that autophagy onset is delayed, which could be due to delayed reductions in PI3-kinase levels (Fig. 3.4G,J,K and Figure S3A. Related to Figure 3.4). To test this, we co-expressed *UAS-dp60* and *UAS-GFP-Atg8* (a standard non-flux autophagy reporter) in *E93RNAi* MB neuroblasts. At 72 hours APF, more autophagosomes were observed in *dp60, E93RNAi* MB neuroblasts compared to control or *E93RNAi* MB neuroblasts (Fig. 3.4A,B,H,I and quantified in L).

We conclude that E93 is required to initiate MB neuroblast autophagy via downregulation of PI3-kinase.

Next, we examined *E93RNAi* adult brains to determine when *E93RNAi* MB neuroblasts terminate cell divisions and whether E93 induced autophagy is required for MB neuroblast elimination. We examined brains of three-day old *E93RNAi* adults and found no MB neuroblasts present (Fig. 3.5A,D, n=20 brain hemispheres), which suggests presence of a back-up pathway for MB neuroblast removal (Siegrist et al. 2010). This compensatory pathway is likely apoptotic cell death. Therefore, we co-expressed *UAS-miRHG*, a synthetic microRNA that inhibits the pro- apoptotic genes Reaper, Hid, and Grim, in *E93RNAi* MB neuroblasts (Siegrist et al. 2010). In *E93RNAi, miRHG* adults, MB neuroblasts were found in brains of one-week and even two-week old adults, whereas no MB neuroblasts were found in *miRHG* adults at either of these times (Fig. 3.5B-D) (Siegrist et al. 2010). We conclude that E93 is required for autophagy and functions in parallel to the pro-apoptotic RHG pathway to eliminate MB neuroblasts and terminate MB neurogenesis.

EcR and Imp/Syp temporal factors regulate E93 expression in MB neuroblasts

The steroid hormone ecdysone regulates E93 expression in the salivary gland, midgut, and in Type II neuroblasts (Syed et al. 2017a) (Lee et al., 2002; Syed et al., 2017b). Ecdysone is released by series of pulses from the prothoracic gland into the circulating hemolymph and converted to active

20- hydroxyecdysone in peripheral tissues (Petryk et al. 2003). As a systemic factor, 20-hydroxyecdysone triggers major developmental transitions, including larval molting and pupation. (Fig. 3.6A, schematic) (Truman et al. 1994; King-Jones & Thummel 2005; Yamanaka et al. 2013). Because 20-hydroxyecdysone levels change over time, ecdysone signaling could provide an extrinsic timer for triggering termination of MB neurogenesis through regulation of E93 (Fig. 3.6A, schematic). To test this possibility, we used the GAL4 flip out cassette to generate MB neuroblast clones expressing *UAS-EcRRNAi* to knock down EcR, the ecdysone receptor. Unfortunately, significant animal lethality resulted, which precluded further analysis. Therefore, we knocked down EcR in a neuroblast specific manner using *worGAL4*. At 48 hours APF, EcR expression was not detected in *EcRRNAi* MB neuroblasts and E93 protein levels were reduced by half compared to controls (Fig. 3.6D,E, quantified in F and Figure S4A-C. Related to Figure 3.6). Consistent with moderate E93 reduction, we found some persisting *EcRRNAi* MB neuroblasts in brains of adult animals (Figure S4E,F. Related to Figure 3.6). We conclude that E93 is regulated by ecdysone signaling in MB neuroblasts, however other factors are likely to contribute.

Because E93 is expressed in MB neuroblasts during late stages only, we asked whether the cell intrinsic temporal factors, Imp and Syp, regulate E93 expression in MB neuroblasts. Imp and Syp are RNA binding proteins that mutually repress each other and distinguish “young” (Imp positive, Syp negative) larval MB neuroblasts from “older” (Imp negative, Syp positive) pupal

MB neuroblasts (Fig. 3.6C, schematic)(Liu et al. 2015). We used the GAL4 flip out cassette and heat shocked animals at 0 hours ALH to generate MB neuroblast clones expressing either *UAS-ImpRNAi* or *UAS-SypRNAi*. At 72 hours ALH, control clones have no E93 as expected, however, E93 was present in *ImpRNAi* MB neuroblast clones (Fig. 3.6J,K, quantified in L). This suggests that Imp inhibits premature E93 expression. Conversely, at 48 hours APF, in *SypRNAi* MB neuroblast clones, E93 was not detected (Fig. 3.6G,H, quantified in I). Consistent with strong E93 reduction, we found *SypRNAi* MB neuroblasts in brains of adult animals (Figure S4D,F. Related to Figure 3.6)(Yang et al., 2017). We conclude that Imp/Syp temporal factors regulate E93 expression in MB neuroblasts: Imp inhibits premature E93, while Syp promotes late E93 expression.

Next, we asked whether premature E93 expression in *ImpRNAi* MB neuroblasts is EcR dependent. Ecdysone triggers the Imp to Syp temporal transition in Type II neuroblasts and *ImpRNAi* MB neuroblasts express Syp prematurely (Liu et al. 2015; Syed et al. 2017b). We heat shocked animals at 0 hours ALH to generate MB neuroblast clones expressing both *UAS- ImpRNAi* and *UAS-EcRRNAi*. At 72 hours ALH, control clones had no E93 as expected, however E93 was still present in *ImpRNAi, EcRRNAi* MB neuroblast clones (Fig. 3.6M,N, quantified in O). This suggests that Imp functions independent of EcR to inhibit E93 expression.

Next, we asked whether premature E93 in *ImpRNAi* MB neuroblasts is Syp dependent. We heat shocked animals at 0 hours ALH to generate MB

neuroblast clones expressing both *UAS- ImpRNAi* and *UAS-SypRNAi*. At 72 ALH, E93 was not detected in control or *ImpRNAi,SypRNAi* MB neuroblast clones (Fig. 3.6P,Q, quantified R). We conclude that Imp/Syp regulate E93 independent of EcR during larval stages.

E93 is a late-acting temporal factor that subdivides the Syp temporal window into Imp/Syp and Syp/E93

Next, we asked whether E93 functionally interacts with Imp/Syp to control timing of neurogenesis during development. To determine whether premature termination of MB neurogenesis in the absence of Imp is due to premature E93 activity, we knocked down both Imp and E93 in MB neuroblasts using *worGAL4*. At 48 hours APF, all four MB neuroblasts were present in each brain hemisphere in control and *E93RNAi* animals, whereas no MB neuroblasts were observed in *ImpRNAi* or *ImpRNAi, E93RNAi* double knock down animals (Fig. 3.7A). Therefore, although E93 is expressed prematurely in the absence of Imp, and is necessary and sufficient to eliminate MB neuroblasts, E93 is not required for the premature elimination of *ImpRNAi* MB neuroblasts. Next, we knocked down both Imp and Syp to determine whether premature termination of MB neurogenesis in the absence of Imp is due to premature Syp activity. MB neuroblasts were observed in *ImpRNAi, SypRNAi* double knock-down animals at 48 hours APF and in adults, consistent with previous reports (Fig. 3.7A and data not shown)(Liu et al., 2015; Yang et al., 2017). Therefore, unlike E93, Syp is required for premature elimination of *ImpRNAi* MB neuroblasts. We conclude

that Syp, but not E93, inhibits Imp function. This suggests that Syp could have two roles: an early function to inhibit Imp-dependent developmental neurogenesis and a late function to positively regulate E93 for termination of MB neurogenesis.

To determine whether Syp has a late function independent of Imp, we used the heat shock GAL4 flip out cassette to control timing of Syp inactivation. Animals were heat shocked at either 0 hours ALH, 0 hours APF, or at 48 hours APF (Fig. 3.7B). Following all heat shock regimes, all *SypRNAi* MB neuroblast clones had one Dpn-positive neuroblast in adult animals (Fig. 3.7B,E). This suggests that Syp is required late and because Imp is not present in MB neuroblasts at 48 hours APF, Syp acts independently of Imp to regulate termination of neurogenesis. Because E93 is also required late and absent in *SypRNAi* MB neuroblasts, we next asked whether ectopic E93 expression could rescue *SypRNAi* MB neuroblasts for termination of neurogenesis. We co-expressed a wild type version of E93 in *SypRNAi* clones and heat shocked animals at 48 hours APF to generate MB neuroblasts clones expressing both *UAS-E93 WT* and *UAS-SypRNAi*. In *SypRNAi* MB neuroblast clones heat shocked at 48 hours APF, all RFP-expressing MB neuroblast clones had one Dpn-positive cell in adult animals (n=62 clones), compared to 37% in the *SypRNAi* MB neuroblasts clones with ectopic E93 (n=43 clones)(Fig. 3.7B,D,E). This suggests that E93 is sufficient to terminate prolonged *SypRNAi* MB neuroblast cell divisions. *SypRNAi* MB neuroblasts with ectopic E93 were also significantly smaller than *SypRNAi* MB neuroblasts, consistent with the notion

that E93 downregulates PI3- kinase and MB neuroblast growth for termination (Fig. 7C-E). We conclude that Imp, Syp, and E93 function together as part of a temporal cassette that determines the timeframe of when neurogenesis occurs during development. Imp promotes neurogenesis, Syp represses Imp and promotes E93, and E93 terminates neurogenesis, thus, linking early developmental neurogenesis with termination.

DISCUSSION

Lineage-specific intrinsic and extrinsic factors both determine timing of neurogenesis and the mechanism by which neurogenesis starts and stops during development (reviewed in Okano and Temple, 2009; Speder et al., 2011; Syed et al., 2017a). In Drosophila, non-MB neuroblasts exit quiescence and enter/exit cell cycle in a nutrient-dependent and PI3-kinase-dependent manner during early larval stages (Chell and Brand, 2010; Sousa-Nunes et al., 2011; Sipe and Siegrist, 2017). In contrast, MB neuroblasts divide continuously, even in the absence of dietary amino acids, which requires expression of the lineage-specific Ey transcription factor, a Pax-6 orthologue (Britton and Edgar, 1998; Lin et al., 2013; Sipe and Siegrist, 2017). Non-MB neuroblast divisions stop during early pupal stages due to changes in metabolic enzymes linked to levels of systemic 20-hydroxyecdysone (Homem et al., 2014), while MB neuroblast divisions continue several days longer. In MB neuroblasts, low levels of PI3-kinase pathway activity trigger MB neuroblasts to stop dividing, while non-MB neuroblasts are reported to stop independent of PI3-kinase (Siegrist et al., 2010;

Homem et al., 2014). Here, we report that E93, which we identified from a RNAi screen, functions in a cell-intrinsic manner to control timing of MB neurogenesis termination. When E93 is knocked down, MB neurogenesis prolongs into adulthood, and when E93 is expressed constitutively, MB neurogenesis terminates prematurely.

The Imp/Syp/E93 intrinsic temporal cassette

We found that Imp/Syp temporal factors regulate E93 expression in MB neuroblasts (see model Fig. 3.7F). Imp and Syp inhibit each other, and Syp positively regulates to control timing of MB neurogenesis termination (Liu et al., 2015; Yang et al., 2017). In the absence of Imp, E93 is expressed prematurely and in the absence of Syp, E93 is not expressed late. Premature expression of E93 in the absence of Imp is Syp dependent, but only knock down of Syp prevent the premature elimination of MB neuroblasts in the absence of Imp. This suggests that although Syp and E93 are both expressed late, they are functionally distinct. Only Syp inhibits Imp to repress neurogenesis. This is also evident when comparing prolonged neurogenesis phenotypes observed in Syp versus E93 knock down adult animals. In the absence of Syp, MB neuroblasts remain large in size and divide continuously, even in two-week-old adults (Pahl et. al, data not shown).

We also found that Syp promotes E93 for termination. In the absence of Syp, MB neurogenesis prolongs into adulthood and we showed here that ectopic E93 is sufficient to terminate MB neurogenesis when Syp is knocked down

(Yang et al. 2017). Importantly, ectopic E93 also reduces MB neuroblast size in the absence of Syp, consistent with the notion that E93 downregulates PI3-kinase levels to activate autophagy for MB neuroblast elimination. Syp is an RNA binding protein and may regulate E93 transcript stability. In fact, two of the three E93 transcripts annotated in Flybase (Figure S1. Related to Figure 3.1) and identified on Northern blot contain long 3'UTRs with predicted secondary structure (Baehrecke & Thummel 1995). Determining which E93 transcripts are expressed in MB neuroblasts and whether Syp directly regulates E93 at a post-transcriptional level will be important future work. In summary, Imp, Syp, and E93 form a temporal cassette that links early neurogenesis with termination: Imp inhibits Syp to promote neurogenesis, Syp represses Imp and promotes E93, and E93 terminates neurogenesis.

The Imp/Syp/E93 temporal cassette is also present in non-MB neuroblasts (Liu et al. 2015; Ren et al. 2017; Syed et al. 2017b; Yang et al. 2017). However, E93 is not required for termination of non-MB neurogenesis (Pahl. et al, unpublished). This suggests that E93 could be a lineage-specific termination factor. How could E93 function in a lineage-specific manner to terminate neurogenesis, if all neuroblasts express E93? One possibility could be the lineage- specific expression of other factors, which control timing of neurogenesis termination. For reasons not yet known, Imp expression is protracted in MB neuroblasts, compared to non-MB neuroblasts, which extends MB neurogenesis into late pupal stages (Liu et al. 2015). Protracted Imp results in delayed expression of Syp and E93 in MB neuroblasts, compared to non-MB neuroblasts.

This means that MB neuroblasts express E93 during later pupal stages, when systemic nutrients may be limited and hormone conditions different, compared to non-MB neuroblasts, which express E93 earlier. Declining systemic nutrients or hormones could provide a co-factor that enables E93 to induce autophagy for neuroblast elimination. In fact, when E93 is overexpressed, we failed to detect increased autophagosomes in MB neuroblasts when divisions terminate prematurely, suggesting that E93 could be a context-dependent termination factor (Pahl. et al, unpublished).

Alternatively, lineage-specific expression of other factors could control mechanism of neurogenesis termination. Non-MB neuroblasts are reported to terminally differentiate, triggered by a burst of nuclear Prospero received by neuroblasts after a final symmetric cell division (Maurange, Cheng & Alex P Gould 2008). In this case, E93 is not required for termination because non-MB neuroblasts differentiate. In contrast MB neuroblasts undergo apoptosis, coincident with increased autophagy due to reductions in levels of PI3-kinase activity (Siegrist et al. 2010). Increased autophagy could sensitize neuroblasts to apoptosis, by degrading some factor that promotes survival. This is the case in Drosophila nurse cells, in which dBruce, an inhibitor of apoptosis, becomes localized with Atg8 positive puncta and is degraded in the lysosome during autophagy (Nezis et al. 2010).

Steroid hormone receptor activation and E93-dependent regulation of PI3-kinase

Both autophagy and apoptosis together are required for MB neuroblast elimination, and we found that E93 downregulates PI3-kinase activity to activate autophagy in MB neuroblasts (see model Fig. 3.7F). Other tissues, including the salivary gland and midgut, also require E93 for autophagy, and similar to MB neuroblasts, levels of PI3-kinase activity are reduced (Lee et al., 2000; Lee and Baehrecke, 2001; Lee et al., 2002; Berry and Baehrecke, 2007). In the salivary gland and midgut, levels of the steroid hormone ecdysone regulate E93 expression (Lee et al., 2000; Lee and Baehrecke, 2001; Lee et al., 2002). This is likely the case for MB neuroblasts as well, since E93 levels are reduced in the absence of EcR. It is intriguing to note that 20-hydroxyecdysone levels spike midway through pupal development and correlate with timing of E93 expression in MB neuroblasts (see model Fig. 3.7F). In the future, it will be important to determine whether MB neuroblasts respond to this or to a different ecdysone pulse.

While E93 is required for MB neuroblast autophagy, it is expressed well before the time when MB neuroblasts are eliminated. This could suggest that E93 requires a co-factor for termination whose expression is dependent on extrinsic factors, as discussed above. Alternatively, E93 could induce autophagy in a cell autonomous manner. E93 is a transcription factor that regulates expression of thousands of genes, including some required for autophagy and PI3-kinase pathway activity (Lee et al., 2003; Uyehara et al.,

2017). Identifying E93 target genes required for MB neurogenesis termination will be important future work.

In Type II neuroblasts, the Imp to Syp temporal switch is regulated by ecdysone (Syed et al., 2017b). However, this is likely not the case for MB neuroblasts since premature E93 expression in the absence of Imp requires Syp, but not EcR. However, whether ecydsone and EcR are required to enforce changes in gene expression after MB neuroblasts switch from Imp to Syp, or whether EcR represses Imp directly, allowing Syp to function late independent of Imp, are two possibilities worth investigating. In summary, E93 integrates intrinsic temporal factors with extrinsic developmental hormone cues to activate autophagy for MB neuroblast elimination (see model Fig. 3.7F). In the absence of E93, MB neurogenesis continues, but only transiently due to compensation by apoptotic cell death. When E93 and apoptosis are both inhibited, MB neuroblasts persist long term. However, E93 and apoptosis-inhibited MB neuroblasts are small and produce few new neurons, likely due to Imp inhibition by Syp. In the future, it will be important to understand how apoptosis is regulated in MB neuroblasts and devise methods to re-initiate early neurogenesis in adult animals for tissue repair.

Terminating neurogenesis in mammals

Determining how neurogenesis terminates in mammals is significantly more difficult than Drosophila due to increased neural complexity, neural stem cell heterogeneity, and lack of identified molecular markers. In rodents, neural stem cells begin "disappearing" during late development, continuing into early

postnatal stages, where neural stem cell loss correlates with increased numbers of astrocytes and ependymal cells (Barry and McDermott, 2005; Spassky et al., 2005). This is consistent with neural stem cells being eliminated by terminal differentiation, however, some could also undergo apoptosis/autophagy and significant caspase-dependent cell death is observed in regions where neural stem cells normally reside (Ferrer et al., 1992; Blaschke et al., 1998; Kuan et al., 2000). It has also been reported that cultured hippocampal neural stem cells undergo autophagy and then death when insulin is withdrawn, and that neural stem cells loss can be reduced when Atg7 is knocked down (Ha et al. 2015; Baek et al. 2009). Imp, Syp, and E93 are all evolutionarily conserved, suggesting that the mechanism regulating neurogenesis termination could also be conserved. In fact, neural stem cells are also prematurely depleted in IMP1 knockdown mice (Nishino et al. 2013). However, at the moment, roles for Syp and E93 in mammalian neural stem cell biology have not yet been explored. Future work will be needed to determine the mechanism regulating termination of neurogenesis in mammals.

AUTHOR CONTRIBUTIONS

M.C.P., S.E.D., and S.E.S. designed and conducted the experiments. M.C.P. and S.E.S. wrote the paper.

DECLARATION OF INTERESTS

The authors declare no competing interests.

Materials and Methods

Fly husbandry and genetics: Animals were maintained on a standard Bloomington fly food diet, at 25°C on a 12 hour light/dark cycle. For all experiments, embryos were collected for 0-4 or 0-6 hours intervals and aged for 18-22 hours. Sixty freshly hatched larvae were then picked and transferred to a new vial containing Bloomington fly food. For larval staging, animals were aged from larval hatching. For pupal staging, animals were aged from white prepupae. For adults, animals were aged from the time of eclosion. Genotypes used are provided in supplementary table.

Heat Shock experiments: Animals were shifted to 37˚C for 20-30 minutes at the indicated times to generate GAL4 flip out clones. Following heat shock, animals were returned to 25˚C until the desired time.

Immunofluorescence and confocal imaging: Brains were dissected, fixed, and stained as described previously (Siegrist et al., 2010; Doyle et al., 2017; Sipe and Siegrist, 2017). Images were acquired using an upright Leica SP8 confocal microscope with a 63x 1.4NA oil immersion objective and analyzed using Imaris and ImageJ software. Figures were assembled using Adobe Photoshop and Illustrator software. The primary and secondary antibodies used are provided in a supplementary table. MB neuroblasts were positively identified based on a number of criteria, including location, axon projections from progeny, and expression of transcription factors including Dpn, Ey, and Tll. For MB neuroblast size measurements, average neuroblast diameter was calculated by measuring the length of two perpendicular diameters taken at the cell's widest point.

Quantification of fluorescence intensities and statistical analysis: Cytoplasmic and nuclear Foxo and E93 levels were quantified as described previously (Siegrist et al., 2010; Doyle et al., 2017; Sipe and Siegrist, 2017). In brief, NB membranes labeled with Scrib and nuclei labeled with Dpn were manually traced and the average Foxo (or E93) fluorescence intensity measured in either the whole cell or nucleus alone using Image J software. Background measurements were acquired from regions devoid of Foxo (or E93) expressing cells. In Figure 6, we report normalized average fluorescence intensity across genotypes. For box plots, the boundary of the box closest to zero indicates the 25th percentile, a line within the box marks the median, and the boundary of the box farthest from zero indicates the 75th percentile. Whiskers (error bars) above and below the box indicate the 90th and 10th percentiles, respectively. Data is presented in the text as ± standard error of the mean, unless noted and experimental data sets were tested for statistical significance using two-tailed Student's t-tests and one-way anova.

Acknowledgements

We thank Claude Desplan, Chris Q. Doe, Robert Tjian, Uwe Walldorf, and the Developmental Studies Hybridoma Bank for providing antibodies used in this study. We thank the Bloomington Stock Center, Harvard TRiP, Vienna Stock center, and Zurich FlyORF projects for providing transgenic flies. We especially thank Chris Doe, Karsten Siller, and Conor Sipe for providing comments on the manuscript.

STAR METHODS

Fly husbandry and genetics: Animals were maintained on a standard Bloomington fly food diet, at 25°C on a 12 hour light/dark cycle. For all experiments, embryos were collected for 0-4 or 0-6 hours intervals and aged for 18-22 hours. Sixty freshly hatched larvae were then picked and transferred to a new vial containing Bloomington fly food. For larval staging, animals were aged from larval hatching. For pupal staging, animals were aged from white prepupae. For adults, animals were aged from the time of eclosion. Genotypes used are provided in table below.

Heat Shock experiments: Animals were shifted to 37˚C for 20-30 minutes at the indicated times to generate GAL4 flip out clones. Following heat shock, animals were returned to 25˚C until the desired time.

Immunofluorescence and confocal imaging: Brains were dissected, fixed, and stained as described previously (Siegrist et al., 2010; Doyle et al., 2017; Sipe and Siegrist, 2017). Images were acquired using an upright Leica SP8 confocal microscope with a 63x 1.4NA oil immersion objective and analyzed using Imaris and ImageJ software. Figures were assembled using Adobe Photoshop and Illustrator software. The primary and secondary antibodies used are provided in table below. MB neuroblasts were positively identified based on a number of criteria, including location, axon projections from progeny, and expression of transcription factors including Dpn, Ey, and Tll. For MB neuroblast size measurements, average neuroblast diameter was

calculated by measuring the length of two perpendicular diameters taken at the cell's widest point.

Quantification of fluorescence intensities and statistical analysis: Cytoplasmic and nuclear Foxo and E93 levels were quantified as described previously (Siegrist et al., 2010; Doyle et al., 2017; Sipe and Siegrist, 2017). In brief, MB neuroblasts membranes labeled with Scrib and nuclei labeled with Dpn were manually traced and the average Foxo (or E93) fluorescence intensity measured in either the whole cell or nucleus alone using Image J software. Background measurements were acquired from regions devoid of Foxo (or E93) expressing cells in same focal plane. In Figure 6, we report normalized average fluorescence intensity across genotypes. For box plots, the boundary of the box closest to zero indicates the 25th percentile, a line within the box marks the median, and the boundary of the box farthest from zero indicates the 75th percentile. Whiskers (error bars) above and below the box indicate the 90th and 10th percentiles, respectively. Data is presented in the text as ± standard error of the mean, unless noted and experimental data sets were tested for statistical significance using two-tailed

Figures:

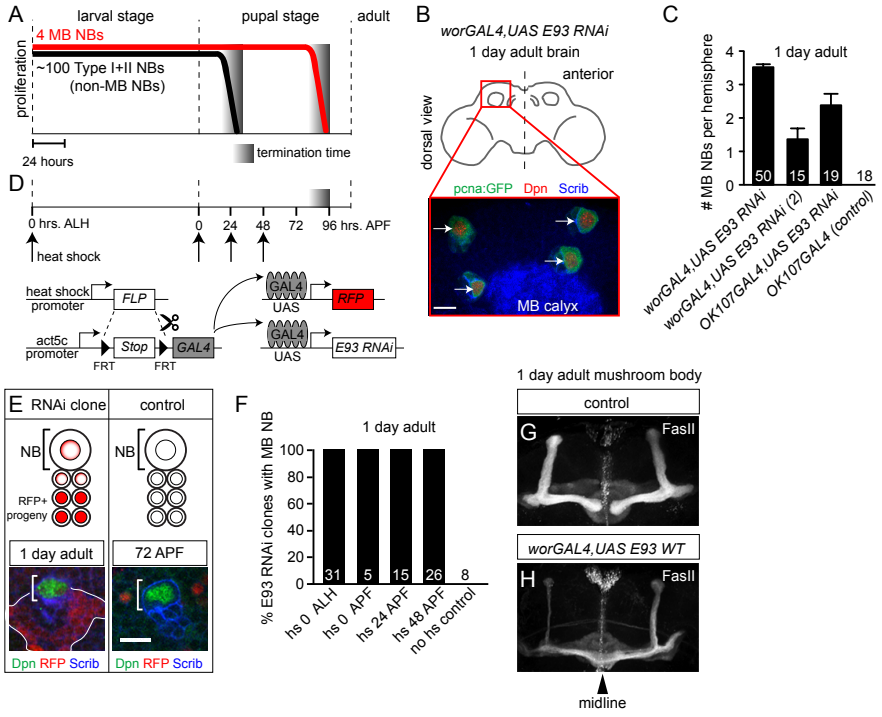

Figure 3.1: E93 is necessary and sufficient to eliminate MB neuroblasts and terminate MB neurogenesis.

(A) Schematic, timing of MB versus non-MB neuroblast (NB) elimination during development. (B) Top schematic, dorsal view of a one-day old adult brain, highlighting the position of the MB calyx, used as a landmark in locating MB neuroblasts, which are superficial and produce neurons with axons that project through the calyx into the mushroom body peduncle. Below, a maximum intensity projection of the region outlined above, from a *worGal4,UASE93RNAi, pcna:GFP* adult animal. Arrows indicate MB neuroblasts, labeled with antibodies against Dpn (red), GFP (green), and the membrane marker Scribble (Blue). (C) Average number of MB neuroblasts per brain hemisphere in 1-day-old adults. Numbers on bars indicate number of hemispheres scored for each of the

indicated genotypes listed below. Error bars s.e.m. (D) Schematic, times of heat-shock treatments (arrow) for GAL4 flip out experiments with GAL4 flip out cassette below (see text). (E) Left, a MB neuroblast *E93 RNAi* clone in a 1-day-old adult after heat shock at 0 hrs. APF. Right, a control MB neuroblast, heat shocked at 0 hours APF, fails to express *E93RNAi* (see text). Controls imaged at an earlier time to identify a Dpn positive MB neuroblast, that is normally absent in adulthood, but present when *E93* is knocked down. White brackets mark neuroblasts in this and all subsequent figures. (F) Percentage of MB neuroblast *E93 RNAi* clones with a Dpn positive neuroblast in one-day-old animals. Time of heat shock treatments indicated below and number of clones scored in columns. (G,H) Maximum intensity projections of adult MB neuropil. Scale bar (A) equals 20 μm and (E) 10 μm.

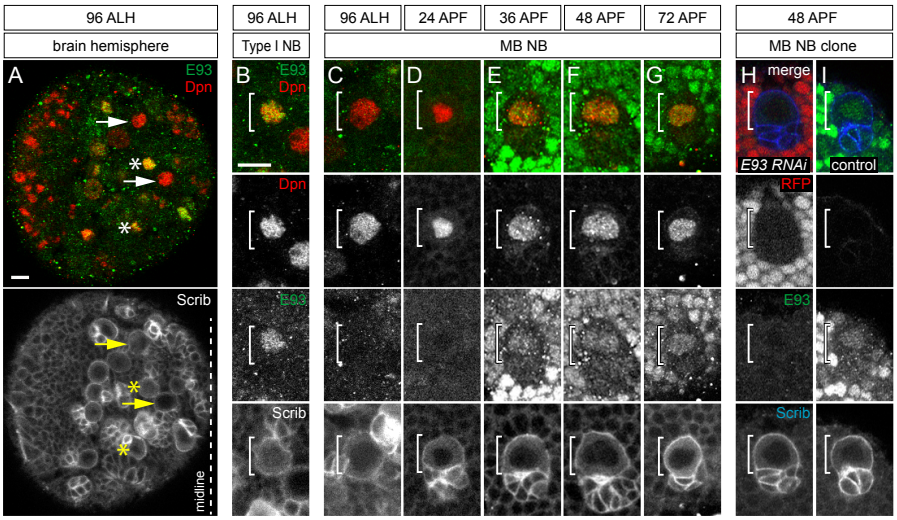

Figure 3.2: MB neuroblasts express E93 after non-MB neuroblasts, during later stages of pupal development.

(A) Dorsal view of a wild type larval brain hemisphere, midline is right, anterior up. Below, greyscale image of same brain hemisphere, labeled with Scrib which outlines neuroblasts (Dpn positive) that express E93 (yellow) or not (red). Arrows indicate MB neuroblasts, asterisks indicate non-MB neuroblasts. (B-G) Wild type neuroblasts from the indicated time points (above) stained with markers listed within panel B. (H-I) E93 is reduced in MB neuroblast *E93RNAi* clones (H) compared to control MB neuroblasts (I). Clones are positively marked with RFP.

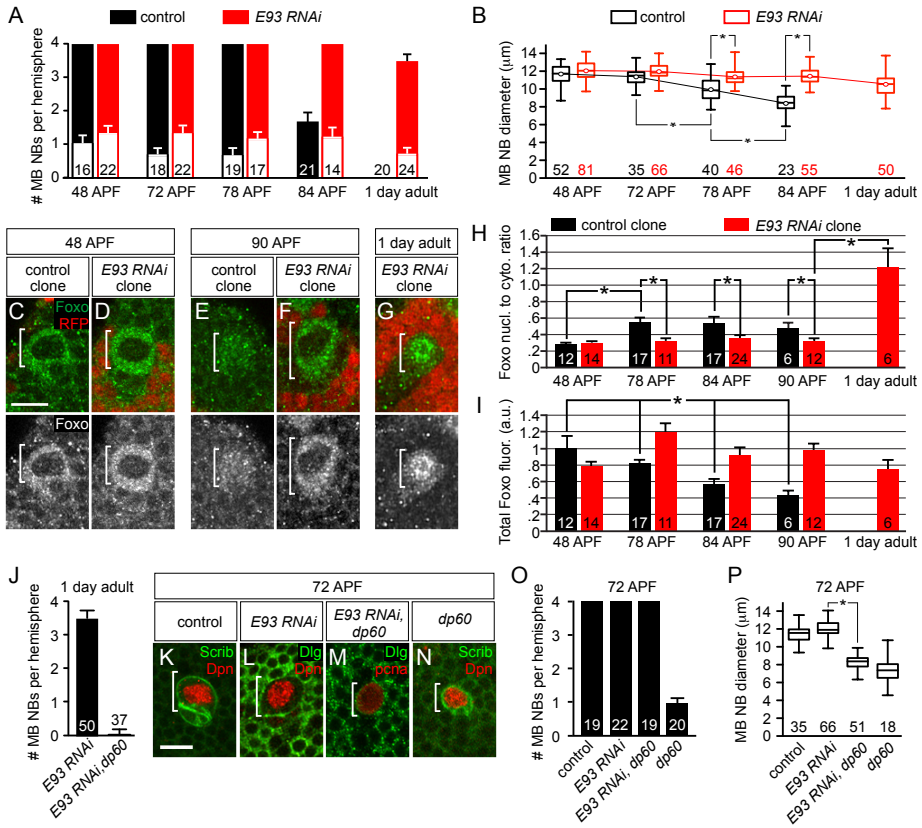

Figure 3.3: Failure to downregulate PI3-kinase activity on time allows *E93RNAi* MB neuroblasts to persist into adulthood.

(A,J,O) Average number of MB neuroblasts per brain hemisphere over time. Column numbers indicate number of hemispheres scored. Error bars indicate standard deviation. White columns (A) within colored columns indicate average number of mitotic MB neuroblasts. (B,P) Box plots of MB neuroblast diameters for indicated genotypes and times. Numbers at bottom indicate number MB neuroblasts analyzed. *p values<.001, two-tailed Student's t-tests. (C-G) Top, colored overlay with single channel greyscale image below of MB neuroblasts (white brackets). Markers listed within panels, genotypes and time above. (H,I) Quantification of MB neuroblast Foxo fluorescence intensities. Refer to methods. Column numbers equal

number of MB neuroblasts assayed. (H) *p values<.001, two-tailed Student's t-tests. (I) *p value=.0003, one- way ANOVA. (K-N) Colored overlay of MB neuroblasts (white brackets), markers listed within panels. Scale bar (C,K) Scale bar = 10 μm.

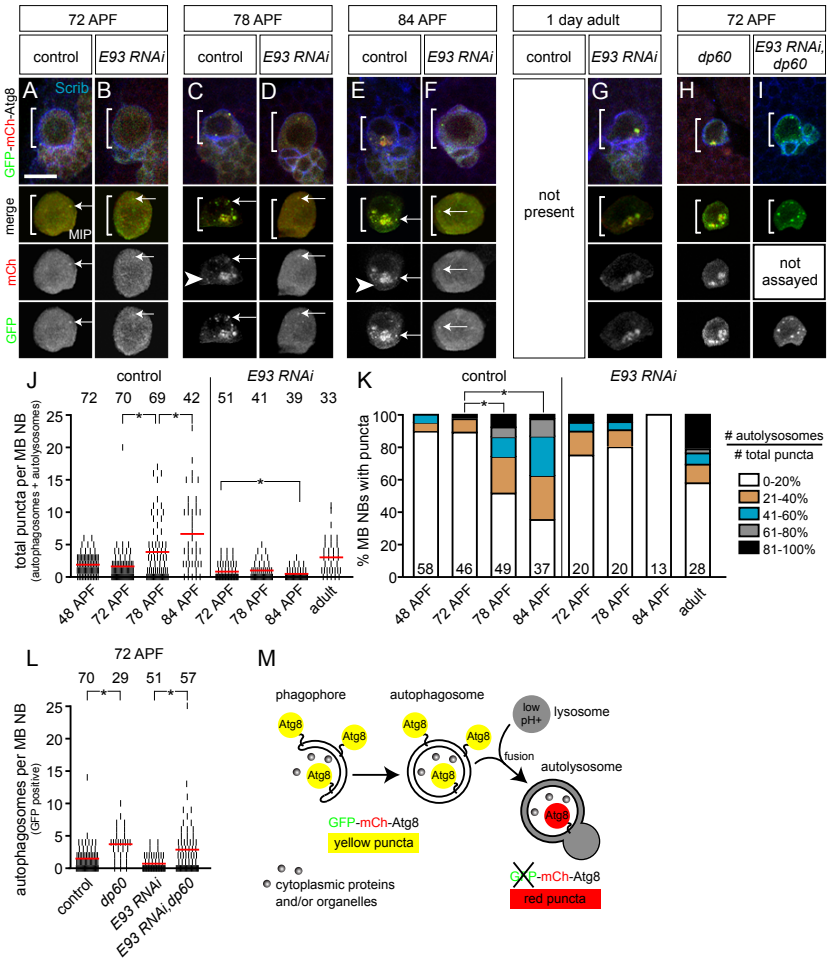

Figure 3.4: E93 regulates autophagy in MB neuroblasts.
(A-I) Top, colored overlay of MB neuroblasts (white brackets) at indicated times and genotypes. Below, colored overlay of cropped, maximum intensity projection of MB neuroblast above, single channel greyscale images below. White arrows indicate autophagomes (mCh,GFP double positive) and arrowheads indicate autolysosomes (mCh only). (A-H) Co-express *UAS-GFP-mCh-Atg8*, (I) *UAS-GFP-Atg8*. (J) Quantification of autophagosomes and autolysosomes or autophagosomes only (L) over time. Black tics represent individual MB neuroblasts. Total number of MB neuroblasts assayed at top of column, red lines denote mean. (K) Distribution of percentages of autolysosomes relative to total

puncta in MB neuroblasts over time (M) Schematic summary of autophagy flux reporter, *UAS-GFP-mCh-Atg8*. *p values<.001, two- tailed Student's t-tests. Scale bar (A) 10 μm.

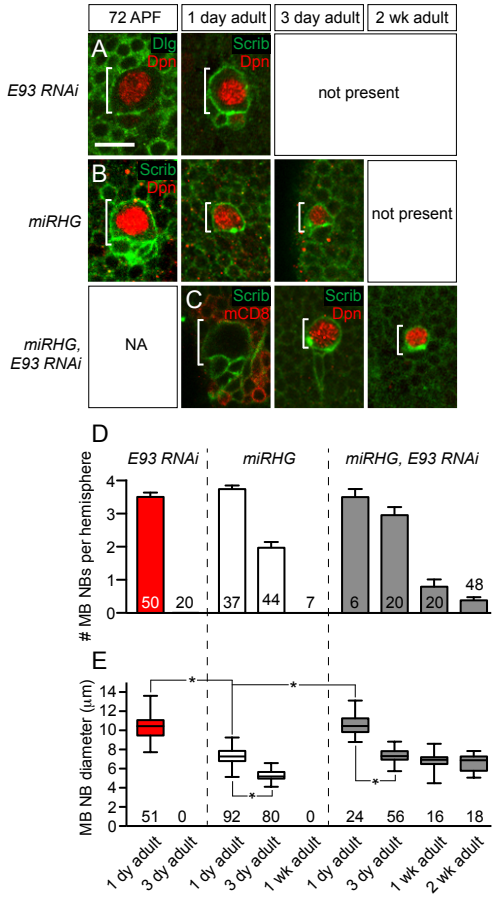

Figure 3.5: MB neuroblasts persist long-term in the absence of E93 and inhibition of apoptosis.

(A-C) Colored overlay of MB neuroblasts (white brackets) at indicated times and genotypes, markers listed within panels. (D) Average number of MB neuroblasts per brain hemisphere. Column numbers indicate number of hemispheres scored. Error bars indicate s.e.m. Scale bar 10 µm. (E) Boxplot of MB neuroblast diameters.

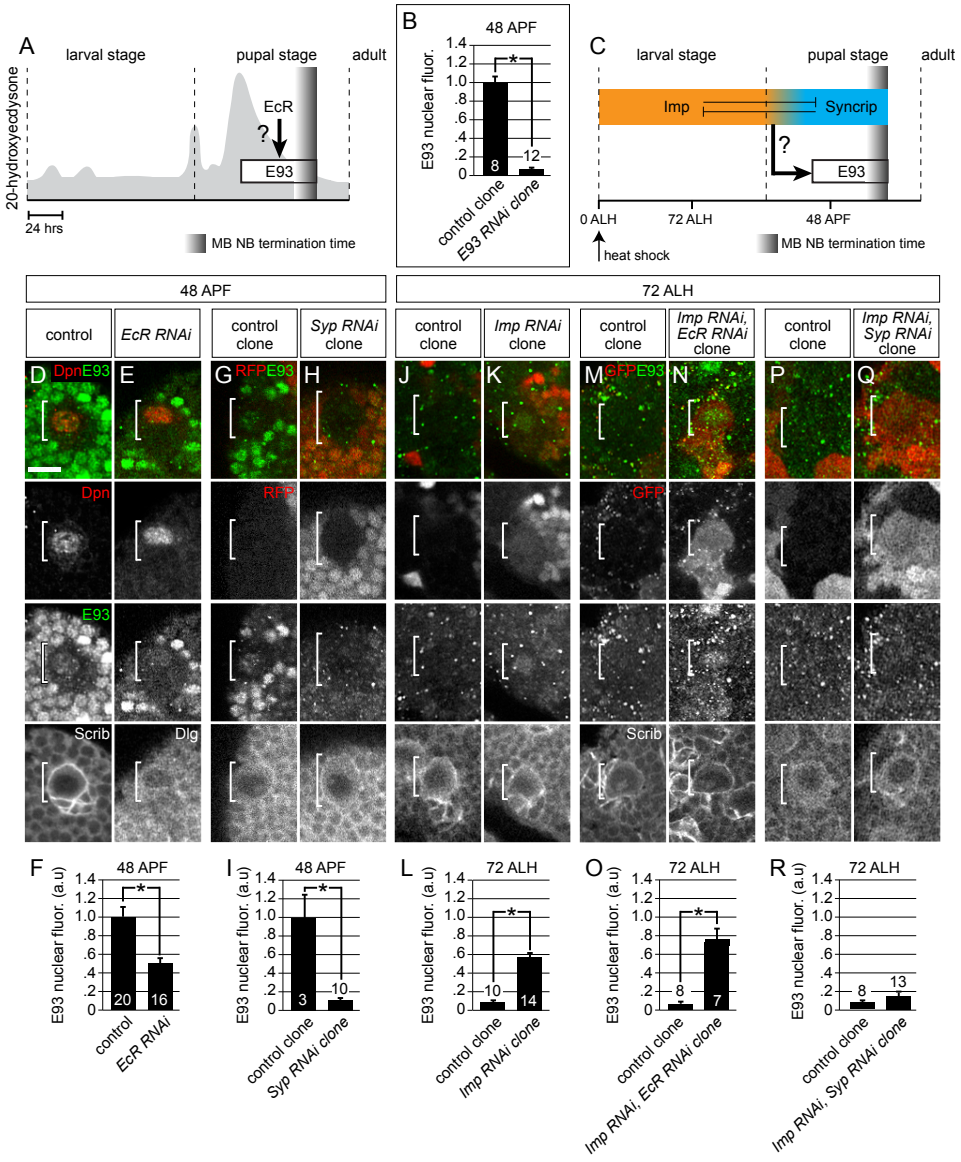

Figure 3.6: Imp, Syp, and EcR regulate E93 expression in MB neuroblasts. (A,C) Schematic summarizing changing 20-hydroxyecdysone levels (A) and timing of Imp and Syp expression in relation to E93 (C). (B) Quantification of E93 nuclear fluorescence intensities. Numbers in columns indicate number of clones scored. (D,E,G,H,J,K,M,N,P,Q) Top, colored overlay with single channel greyscale images below of MB neuroblasts (white brackets). Markers listed within panels and time points and genotypes above. (F,I,L,O,R) Quantification of

E93 nuclear fluorescence intensities. See methods. Column numbers refer to number of MB neuroblasts assayed or number of clones. (L,O,R) E93 nuclear fluorescence intensities normalized to control E93 nuclear fluorescence intensities at 48 APF (B). Error bars equal S.E.M. *p values<.001, two-tailed Student's t-tests. Scale bar (B,M) Scale bar = 10 μm

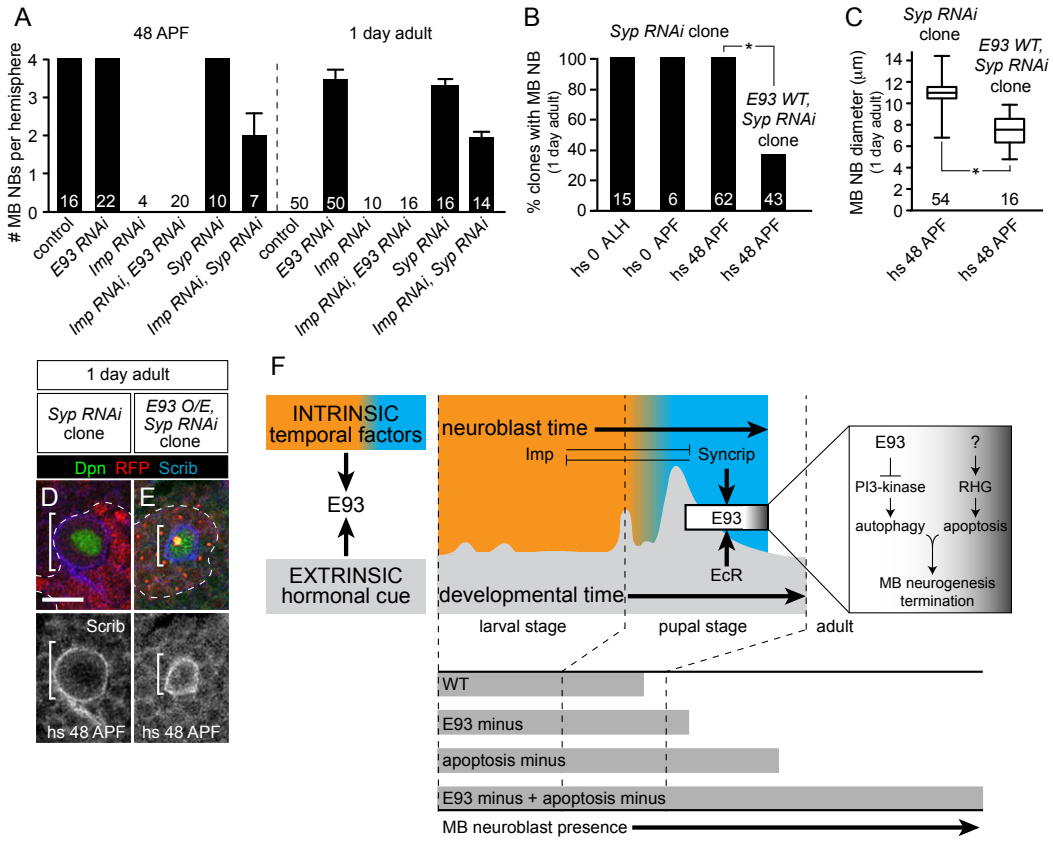

Figure 3.7: E93 terminates growth of *SypRNAi* MB neuroblasts.
(A) Average number of MB neuroblasts per brain hemisphere at indicated times and genotypes. Column numbers equal number of brain hemispheres scored. (B) Percentage of MB neuroblast clones with a MB neuroblast. Column numbers indicate number of clones scored and times below indicate time of heat shock treatment. (C) Box plots of MB neuroblast diameters for indicated genotype and time. Numbers at bottom indicate number MB neuroblasts analyzed. (D,E) Colored overlay of MB neuroblast (white bracket) with greyscale image below. (F) Model summary, see text for details. *p values<.001, two-tailed Student's t-tests.

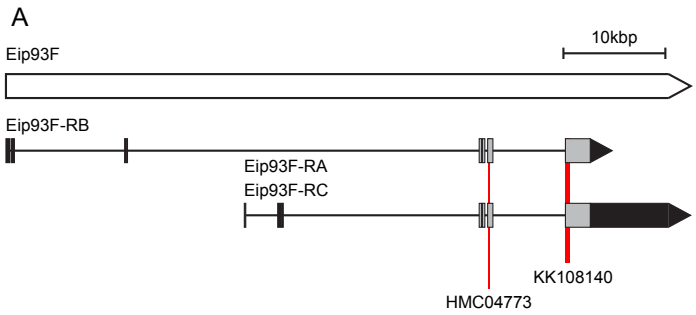

Figure S1. Related to Figure 3.1: E93 is necessary and sufficient to eliminate MB neuroblasts and terminate MB neurogenesis.

(A) Organization of E93 locus with 3 transcripts shown and locations of RNAi target regions (red). Grey regions are protein coding exons and black regions contains 5' and 3' UTRs.

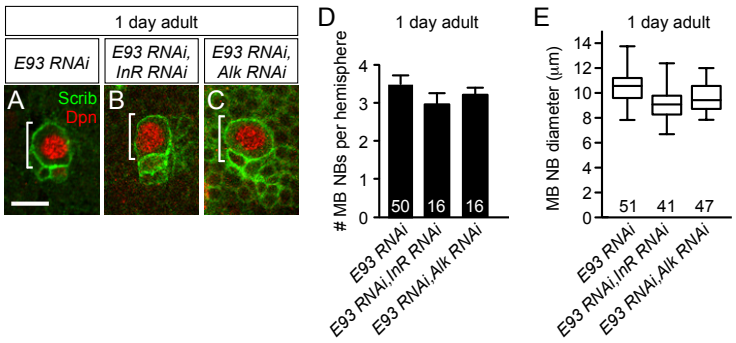

Figure S2. Related to Figure 3.3: Failure to downregulate PI3-kinase activity on time allows E93RNAi MB neuroblasts to persist into adulthood.

(A-C) Colored overlay of MB neuroblasts (white brackets) in one-day old adults, genotypes listed above. Error bars, s.e.m. (D) Average number of MB neuroblasts per brain hemisphere. Column numbers indicate number of brain hemispheres assayed. (E) Box plots of MBneuroblast diameters for indicated genotype and time. Numbers at bottom indicate number MB neuroblasts analyzed. Scale = 10 µm

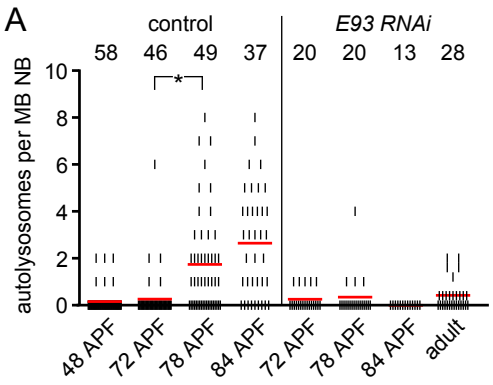

Figure S3. Related to Figure 3.4: E93 regulates autophagy in MB neuroblasts. (A) Quantification of autolysosomes alone, extracted from Fig. 4J. Number of MB neuroblasts with puncta at top of column, with black tics below representing individual MB neuroblasts. Red lines denote average. *p values<.001, two-tailed Student's t-tests.

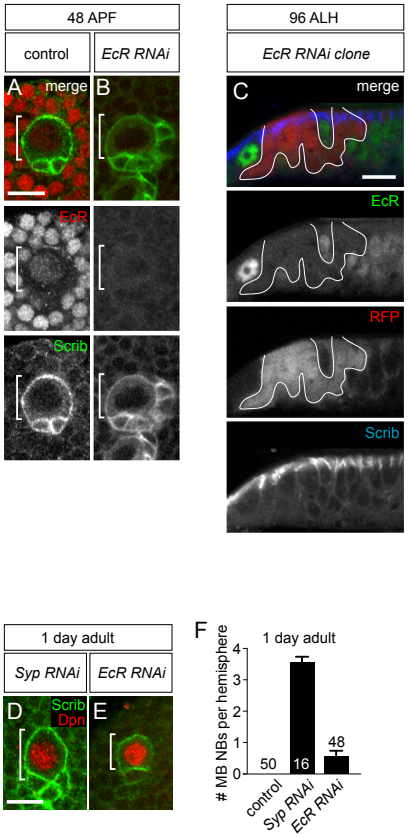

Figure S4. Related to Figure 3.6: Imp, Syp, and EcR regulate E93 expression in MB neuroblasts

(A-C) Colored overlay with greyscale images below of (A) MB neuroblasts (white brackets) and (C) an imaginal disk, showing loss of EcR expression in an RFP expressing *EcRRNAi* clone. (D,E) Colored overlay of MB neuroblasts with average number of MB neuroblasts per brain hemisphere (F). Column numbers equal number of brain hemispheres assayed. Error bars equal S.E.M. Scale bar (A,C,D) Scale bar = 10 μm.

Chapter 4
General discussion and Future Directions

Proper development of the adult brain requires that growth terminates as development reaches completion. In this dissertation, we have characterized the molecular mechanisms that regulate the elimination of Drosophila MB neuroblasts as a model to better understand how neurogenesis becomes restricted during development. Through an RNAi screen, we have uncovered several transcriptional regulators that are required for timing MB neuroblast elimination. We have begun to characterize two of these genes, Ey and E93, to better understand how they are involved in this process.

Chapter 2 described our directed RNAi screen for genes that influence when MB neuroblasts and non-MB neuroblasts are eliminated during development. From this work, we identified 151 canidate genes from a combination of bioinformatic prediction and from the literature. We screened 69 RNAi lines targeting some of these genes and found 14 genes that affect when neuroblasts terminate (Table. 2.2). Our lab has begun to characterize the role of several of these genes. We identified genes that may act as lineage specific factors, signaling pathways, or temporal factors (Table 2.2).. For example Ey, Rx, and Oc, all expressed in MB neuroblasts throughout development, they may act as lineage specific factors that prime MB neuroblasts to respond to termination signals (Kunz et al. 2012; Kraft et al. 2016; Urbach & Technau 2004). Moreover, we found that Ey has a function in MB neuroblasts late in development to eliminate MB neuroblast elimination via autophagy. One possibility is that these genes cooperate during MB neuroblast elimination.

In chapter 3, we have shown that E93, a temporal factor that we found during our screen, is both necessary and sufficient to eliminate MB neuroblasts by influencing the timing of down regulation of PI3-kinase signaling and promoting autophagy late in development. E93 is expressed during a late temporal window, which is coordinated by Imp/Syp temporal factors and ecdysone signaling, thereby linking progression through the neuroblast temporal program with neuroblast elimination.

Timing termination of MB neurogenesis.

We found that E93 acts downstream of the Imp/Syp temporal program to promote termination of MB neurogenesis. The early factor Imp inhibits E93 during larval stages, while the late factor Syp is necessary for its expression in pupal stages. While all neuroblasts express E93 late in development, it is not required in all cells for elimination, suggesting that it promotes termination in a lineage-specific manner. Conversely, Syp is required for termination in all neuroblasts (Yang et al. 2017). Thus, a possible mechanism of E93 function is through interactions with lineage-specific factors to terminate MB neuroblasts. This may function similar to the function of temporal factor Grainyhead (Grh) in embryonic neuroblasts, where Grh can either promote quiescence or apoptosis of neuroblasts in the ventral nerve cord, depending on which homeotic genes they express (Khandelwal et al. 2017; Cenci & Gould 2005). E93 may cooperate with the MB neuroblast specific genes including, Ey, Rx, and Oc to regulate MB elimination.

The timing of the Imp to Syp switch in MB neuroblasts correlates with the overall duration of neurogenesis in different lineages (Liu et al. 2015; Yang et al. 2017). How might lineage-specific factors delay the Imp to Syp transition in MB neuroblasts? One possibility is that they keep MB neuroblasts in an early temporal window by promoting Imp or repressing Syp expression. One gene that may regulate this is the orphan nuclear receptor Tailless (Tll). Tll is expressed in MB neuroblasts and is necessary and sufficient for their extended neurogenesis (Kurusu et al. 2009). The mechanism that Tll extends MB neurogenesis is currently unknown. Tll may promote expression of Imp or inhibit expression of Syp.

Although we showed that Imp/Syp regulate expression of E93, how E93 is transcriptionally regulated is not fully resolved. Knockdown of EcR, the canonical regulator of E93, resulted in a relatively weak persistence phenotype (Fig 3.5). Additionally, when we inhibited ecdysone signaling in neuroblasts by expressing a dominant negative mutant of the ecdysone receptor, we found that MB neuroblasts were eliminated early (Appendix). Inconsistent results have been reported when EcR is inhibited by RNAi or via mis-expression of dominant negative transgenes in other tissues. This is likely due to EcR being involved in both activation and repression of its targets depending on specific contexts (Mirth et al. 2009). Both knockdown approaches come with caveats: depletion of EcR by RNAi may allow target genes normally repressed by EcR to be permissively expressed, while dominant negatives may lead to transcriptional repression at sites not normally repressed by endogenous EcR levels. One candidate that may

regulate E93 transcriptionally is the orphan nuclear receptor βFtz-f1, which is known to provide competence for E93 expression during early pupal stages (Broadus et al. 1999).

While characterizing the timing of E93 expression, we identified a possible regulatory element located within its large intron that is contained on the Janelia fragment R84C02 (appendix). This element replicated the expression pattern of E93 in MB and non-MB neuroblasts, suggesting that this region is critical for transcription of E93. Further work to characterize this region will lead to a better understanding of how E93 transcription is regulated. As a first step, generating a collection of deletions spanning the region using Crispr/Cas9, would be valuable for both validating the region's role in regulating E93 expression. One could test functionally if the region is required for E93 expression in MB neuroblasts. Generating a collection of regulatory element deletions would also assist in narrowing down the region of interest to attempt to identify transcription factor binding sites, to find candidate genes that may regulate E93 transcriptionally.

Autophagy as a mechanism to restrict growth in MB neuroblasts

Autophagy is associated with both cell survival and cell death in different cellular contexts. In MB neuroblasts, inhibition of autophagy causes a delay of their elimination while also acting as a secondary death mechanism when apoptosis is blocked (Siegrist et al. 2010). Using a reporter of autophagic flux, we found that MB neuroblasts begin to undergo autophagy shortly before their elimination. Moreover, we found that knockdown of E93 or Ey suppresses

autophagy in MB neuroblasts. How autophagy promotes elimination in MB neuroblasts remains unclear. One way that autophagy may promote cell death is by degrading proteins required for cell survival, which occurs in Drosophila nurse cells, where autophagy degrades the inhibitor of apoptosis protein dBruce (Nezis et al. 2010). Another possibility is that autophagosomes could act as a platform to regulate the initiation of apoptosis, as has been shown in cell culture models where autophagosomes recruit activated caspase 8 to initiate the caspase cascade (Young et al. 2012). Careful characterization of components of the apoptotic machinery in neuroblasts where autophagy is blocked may shed light on this process. This could be done by immunostaining of several prosurvival or proapoptotic proteins to see if any are specifically disrupted when autophagy is blocked. Initial characterization of the subcellular localization of Grim and Skl would be a good starting point as both are required for MB neuroblast apoptosis (Siegrist et al. 2010; Appendix). The both Grim and Skl are required for MB elimination. One possibility is that the two form a heterodimer to promote cell death as has been reported for Rpr and Hid (Sandu et al. 2010).

How does Ey regulate autophagy? One possibility is that Ey directly regulates the transcription of the Atg genes. To test this it will be important to determine if Ey binds near any autophagy genes. Alternatively Ey may regulate autophagy indirectly by through modulating activity of signaling pathways. Insulin, TOR, and AMPK all regulate autophagy and may be good candidates to test for interactions with Ey during MB neuroblast elimination (Jimenez-Sanchez et al. 2012).

E93 is a transcription factor that regulates the expression of thousands of genes, including some required for autophagy and PI3-kinase pathway activity (Lee et al., 2003; Uyehara et al., 2017). We have shown that E93 may function reduce levels of PI3-Kinase activity. However, how E93 might regulate levels of PI3-kinase signaling remains unclear. Identifying the target genes of the transcription factors that we identified to regulate neuroblast termination will be important future work. Identifying these genes may require both chromatin immunoprecipation and RNA sequencing to identify to form a comprehensive picture of E93 target genes in MB neuroblasts.

Termination of neurogenesis in mammals

The molecular mechanisms that restrict neurogenesis during development in mammals remain largely unexplored. In mice, the number of neural stem cells begins to reduced in late embryonic stages corresponding to an increase in the number of astrocytes and ependymal cells (Barry & McDermott 2005; Spassky et al. 2005). Significant caspase-dependent cell death is observed in neurogenic regions, suggesting that some neural stem cells may undergo apoptosis (Blaschke et al. 1998; Yeo & Gautier 2004). The development of new technologies like single-cell sequencing to identify molecular markers will facilitate the characterization the molecular diversity of neural stem cells, making investigations into the mechanisms that restrict neurogenesis mammals tractable.

In the future it will be important to determine if the Imp/Syp/E93 cassette also regulate the termination of neurogenesis in mammals. Decreasing

gradients of Imp are observed in multiple stem cell types, including those in the developing cortex, and may represent a common stem cell aging mechanism (Nishino et al. 2013; Toledano et al. 2012). While both the Syp and E93 genes are highly conserved, the roles for Syp and E93 in mammalian neurogenesis have not yet been explored.

In summary, this dissertation work expands our knowledge of the regulatory mechanisms that restrict growth and proliferation in the brain. We identified several genes that are involved in this process. In particular, we characterized the role of a temporal gene in promoting elimination of a specific neural stem cell lineage. Identifying the mechanisms in model organisms such as *Drosophila* will provide an important conceptual basis for understanding how the completion of neurogenesis is controlled in more complex organisms.

References

Albertson, R., 2004. Scribble protein domain mapping reveals a multistep localization mechanism and domains necessary for establishing cortical polarity. *Journal of Cell Science*, 117(25), pp.6061–6070. Available at: http://jcs.biologists.org/cgi/doi/10.1242/jcs.01525.

Albertson, R. & Doe, C.Q., 2003. Dlg, Scrib and Lgl regulate neuroblast cell size and mitotic spindle asymmetry. *Nature Cell Biology*, 5(2), pp.166–170.

Alsiö, J.M. et al., 2015. Ikaros promotes early-born neuronal fates in the cerebral cortex: Fig. 6. *Proceedings of the National Academy of Sciences*, 112(23), pp.E3088–E3088. Available at: http://www.pnas.org/lookup/doi/10.1073/pnas.1508413112.

Amamoto, R. et al., 2016. Adult axolotls can regenerate original neuronal diversity in response to brain injury. *eLife*, 5(MAY2016), pp.1–22.

Arya, R. et al., 2015. Neural stem cell progeny regulate stem cell death in a Notch and Hox dependent manner. *Cell Death and Differentiation*, 22(8), pp.1378–1387. Available at: http://dx.doi.org/10.1038/cdd.2014.235.

Atwood, S.X. & Prehoda, K.E., 2009. aPKC Phosphorylates Miranda to Polarize Fate Determinants during Neuroblast Asymmetric Cell Division. *Current Biology*, 19(9), pp.723–729. Available at: http://dx.doi.org/10.1016/j.cub.2009.03.056.

Baehrecke, E.H. & Thummel, C.S., 1995. The Drosophila E93 Gene from the 93F Early Puff Displays Stage- and Tissue-Specific Regulation by 20-Hydroxyecdysone. *Developmental Biology*, 171(1), pp.85–97.

Baek, S.H. et al., 2009. Insulin withdrawal-induced cell death in adult hippocampal neural stem cells as a model of autophagic cell death. *Autophagy*, 5(2), pp.277–279.

Barry, D. & McDermott, H., 2005. Differentiation of radial glia from radial precursor cells and transformation into astrocytes in the developing rat spinal cord. *Glia*, 50(3), pp.187–197.

Baumgardt, M. et al., 2009. Neuronal Subtype Specification within a Lineage by Opposing Temporal Feed-Forward Loops. *Cell*, 139(5), pp.969–982.

Bayraktar, O.A. & Doe, C.Q., 2013. Combinatorial temporal patterning in progenitors expands neural diversity. *Nature*, 498(7455), pp.449–455. Available at: http://dx.doi.org/10.1038/nature12266.

Bello, B., 2006. The brain tumor gene negatively regulates neural progenitor cell proliferation in the larval central brain of Drosophila. *Development*, 133(14), pp.2639–2648. Available at: http://dev.biologists.org/cgi/doi/10.1242/dev.02429.

Bello, B.C., Hirth, F. & Gould, A.P., 2003. A pulse of the Drosophila Hox protein Abdominal-A schedules the end of neural proliferation via neuroblast apoptosis. *Neuron*, 37(2), pp.209–19. Available at: http://www.ncbi.nlm.nih.gov/pubmed/12546817.

Benito-Sipos, J. et al., 2010. A genetic cascade involving klumpfuss, nab and castor specifies the abdominal leucokinergic neurons in the Drosophila CNS.

Development, 137(19), pp.3327–3336. Available at: http://dev.biologists.org/cgi/doi/10.1242/dev.052233.

Berdnik, D. & Knoblich, J.A., 2002. Drosophila Aurora-A is required for centrosome maturation and actin-dependent asymmetric protein localization during mitosis. *Current Biology*, 12(8), pp.640–647.

Berry, D.L. & Baehrecke, E.H., 2007. Growth Arrest and Autophagy Are Required for Salivary Gland Cell Degradation in Drosophila. *Cell*, 131(6), pp.1137–1148.

Betschinger, J., Mechtler, K. & Knoblich, J.A., 2006. Asymmetric Segregation of the Tumor Suppressor Brat Regulates Self-Renewal in Drosophila Neural Stem Cells. *Cell*, 124(6), pp.1241–1253.

Bhardwaj, R.D. et al., 2006. Neocortical neurogenesis in humans is restricted to development. *Proceedings of the National Academy of Sciences*, 103(33), pp.12564–12568. Available at: http://www.pnas.org/cgi/doi/10.1073/pnas.0605177103.

Bier, E. et al., 1992. deadpan, an essential pan-neural gene in Drosophila, encodes a helix-loop- helix protein similar to the hairy gene product. *Genes and Development*, 6(11), pp.2137–2151.

Blaschke, A.J., Weiner, J.A. & Chun, J., 1998. Programmed cell death is a universal feature of embryonic and postnatal neuroproliferative regions throughout the central nervous system. *Journal of Comparative Neurology*, 396(1), pp.39–50.

Boldrini, M. et al., 2018. Short Article Human Hippocampal Neurogenesis Persists throughout Aging Short Article Human Hippocampal Neurogenesis Persists throughout Aging. , pp.589–599.

Bowman, S.K. et al., 2006. The Drosophila NuMA Homolog Mud Regulates Spindle Orientation in Asymmetric Cell Division. *Developmental Cell*, 10(6), pp.731–742.

Bowman, S.K. et al., 2008. The Tumor Suppressors Brat and Numb Regulate Transit-Amplifying Neuroblast Lineages in Drosophila. *Developmental Cell*, 14(4), pp.535–546.

Brand, A.H. & Livesey, F.J., 2011. Neural Stem Cell Biology in Vertebrates and Invertebrates: More Alike than Different? *Neuron*, 70(4), pp.719–729. Available at: http://dx.doi.org/10.1016/j.neuron.2011.05.016.

Brand, A.H. & Perrimon, N., 1993. Targeted gene expression as a means of altering cell fates and generating dominant phenotypes. *Development (Cambridge, England)*, 118(2), pp.401–15. Available at: http://www.ncbi.nlm.nih.gov/pubmed/8223268.

Britton, J.S. et al., 2002. Drosophila's insulin/PI3-kinase pathway coordinates cellular metabolism with nutritional conditions. *Developmental Cell*, 2(2), pp.239–249.

Britton, J.S. & Edgar, B. a, 1998. Environmental control of the cell cycle in Drosophila: nutrition activates mitotic and endoreplicative cells by distinct mechanisms. *Development (Cambridge, England)*, 125(11), pp.2149–2158. Available at: http://dev.biologists.org/content/develop/125/11/2149.full.pdf.

Broadus, J. et al., 1999. The Drosophila βFTZ-F1 orphan nuclear receptor

provides competence for stage-specific responses to the steroid hormone ecdysone. *Molecular Cell*, 3(2), pp.143–149.
Broadus, J., Fuerstenberg, S. & Doe, C.Q., 1998. Staufen-dependent localization of prospero mRNA contributes to neuroblast daughter-cell fate. *Nature*, 391(6669), pp.792–795.
Brody, T. & Odenwald, W.F., 2000. Programmed transformations in neuroblast gene expression during Drosophila CNS lineage development. *Developmental Biology*, 226(1), pp.34–44.
Brogiolo, W. et al., 2001. An evolutionarily conserved function of the Drosophila insulin receptor and insulin-like peptides in growth control. *Current Biology*, 11, pp.213–221.
Butt, S.J.B. et al., 2008. The Requirement of Nkx2-1 in the Temporal Specification of Cortical Interneuron Subtypes. *Neuron*, 59(5), pp.722–732.
Butt, S.J.B. et al., 2005. The temporal and spatial origins of cortical interneurons predict their physiological subtype. *Neuron*, 48(4), pp.591–604.
Callaerts, P. et al., 2001. Drosophila Pax-6 / eyeless is Essential for Normal Adult Brain Structure and Function. *Journal of neurobiology*, 46(2), pp.73–88.
Cayre, M. et al., 2002. The common properties of neurogenesis in the adult brain: From invertebrates to vertebrates. *Comparative Biochemistry and Physiology - B Biochemistry and Molecular Biology*, 132(1), pp.1–15.
Cenci, C. & Gould, A.P., 2005. Drosophila Grainyhead specifies late programmes of neural proliferation by regulating the mitotic activity and Hox-dependent apoptosis of neuroblasts. *Development (Cambridge, England)*, 132(17), pp.3835–45. Available at: http://www.ncbi.nlm.nih.gov/pubmed/16049114 [Accessed March 14, 2014].
Chabu, C. & Doe, C.Q., 2009. Twins/PP2A regulates aPKC to control neuroblast cell polarity and self-renewal. *Developmental Biology*, 330(2), pp.399–405. Available at: http://dx.doi.org/10.1016/j.ydbio.2009.04.014.
Chai, J. et al., 2003. Molecular mechanism of Reaper-Grim-Hid-mediated suppression of DIAP1-dependent Dronc ubiquitination. *Nature structural biology*, 10(11), pp.892–8. Available at: http://www.ncbi.nlm.nih.gov/pubmed/14517550 [Accessed February 28, 2014].
Chai, P.C. et al., 2013. Hedgehog Signaling Acts with the Temporal Cascade to Promote Neuroblast Cell Cycle Exit. *PLoS Biology*, 11(2).
Chang, K.C. et al., 2010. Interplay between the Transcription Factor Zif and aPKC Regulates Neuroblast Polarity and Self-Renewal. *Developmental Cell*, 19(5), pp.778–785. Available at: http://dx.doi.org/10.1016/j.devcel.2010.10.007.
Chell, J.M. & Brand, A.H., 2010. Nutrition-responsive glia control exit of neural stem cells from quiescence. *Cell*, 143(7), pp.1161–1173. Available at: http://dx.doi.org/10.1016/j.cell.2010.12.007.
Cheng, L.Y. et al., 2011. Anaplastic lymphoma kinase spares organ growth during nutrient restriction in drosophila. *Cell*, 146(3), pp.435–447. Available at: http://dx.doi.org/10.1016/j.cell.2011.06.040.
Chenn, A. & Walsh, C.A., 2011. Neural Precursors Regulation of Cerebral

Cortical Size by Control of Cell Cycle Exit in Neural Precursors. , 365(2002), pp.365–370.

Chesler, D.A., 2012. The potential origin of glioblastoma initiating cells. *Frontiers in Bioscience*, S4(1), p.190. Available at: https://www.ncbi.nlm.nih.gov/pmc/articles/PMC3635065/pdf/nihms448270.pdf%0Ahttp://www.ncbi.nlm.nih.gov/pubmed/22202053%0Ahttp://www.pubmedcentral.nih.gov/articlerender.fcgi?artid=PMC3635065%0Ahttp://www.bioscience.org/2012/v4s/af/261/list.htm.

Cheung, T.H. & Rando, T.A., 2013. Molecular regulation of stem cell quiescence. *Nature Reviews Molecular Cell Biology*, 14(6), pp.329–340. Available at: http://dx.doi.org/10.1038/nrm3591.

Chia, W., Somers, W.G. & Wang, H., 2008. Drosophila neuroblast asymmetric divisions: Cell cycle regulators, asymmetric protein localization, and tumorigenesis. *Journal of Cell Biology*, 180(2), pp.267–272.

Choksi, S.P. et al., 2006. Prospero Acts as a Binary Switch between Self-Renewal and Differentiation in Drosophila Neural Stem Cells. , pp.775–789.

Christensen, R.G. et al., 2012. Recognition models to predict DNA-binding specificities of homeodomain proteins. *Bioinformatics*, 28(12), pp.84–89.

Christich, A. et al., 2002. The damage-responsive Drosophila gene sickle encodes a novel IAP binding protein similar to but distinct from reaper, grim, and hid. *Current biology : CB*, 12(2), pp.137–40. Available at: http://www.ncbi.nlm.nih.gov/pubmed/11818065.

Cleary, M.D. et al., 2006. Michael D. Cleary and Chris Q. Doe 1. *Genes & Development*, pp.429–434.

Cleary, M.D. & Doe, C.Q., 2006. Regulation of neuroblast competence: multiple temporal identity factors specify distinct neuronal fates within a single early competence window. *Genes & development*, 20(4), pp.429–34. Available at: http://www.pubmedcentral.nih.gov/articlerender.fcgi?artid=1369045&tool=pmcentrez&rendertype=abstract [Accessed February 20, 2014].

Colombani, J. & Le, P., 2010. Antagonistic Actions of Ecdysone and Insulins Determine Final Size in Drosophila. , 667(2005), pp.667–671.

Doe, C.Q., 1992. Molecular markers for identified neuroblasts and ganglion mother cells in the Drosophila central nervous system. *Development (Cambridge, England)*, 116(4), pp.855–63. Available at: http://www.ncbi.nlm.nih.gov/pubmed/1295739.

Doe, C.Q., 2008. Neural stem cells: balancing self-renewal with differentiation. *Development (Cambridge, England)*, 135(9), pp.1575–87. Available at: http://www.ncbi.nlm.nih.gov/pubmed/18356248 [Accessed January 31, 2014].

Doe, C.Q., 2017. Temporal Patterning in the Drosophila CNS. *Annual Review of Cell and Developmental Biology Annu. Rev. Cell Dev. Biol*, 33, pp.219–40. Available at: https://doi.org/10.1146/annurev-cellbio-111315-125210.

Doyle, S.E. et al., 2017. Neuroblast niche position is controlled by Phosphoinositide 3-kinase-dependent DE-Cadherin adhesion. *Development*, 144(5), pp.820–829. Available at: http://dev.biologists.org/lookup/doi/10.1242/dev.136713.

Dwyer, N.D. et al., 2016. Neural Stem Cells to Cerebral Cortex: Emerging Mechanisms Regulating Progenitor Behavior and Productivity. *The Journal of Neuroscience*, 36(45), pp.11394–11401. Available at: http://www.jneurosci.org/lookup/doi/10.1523/JNEUROSCI.2359-16.2016.

Dyer, M.A. et al., 2003. Prox1 function controls progenitor cell proliferation and horizontal cell genesis in the mammalian retina. *Nature Genetics*, 34(1), pp.53–58.

Eriksson, P.S. et al., 1998. Neurogenesis in the adult human hippocampus. *Nature medicine*, 4(11), pp.1313–7. Available at: http://www.ncbi.nlm.nih.gov/pubmed/19714567.

Farkas, L.M. et al., 2008. Insulinoma-Associated 1 Has a Panneurogenic Role and Promotes the Generation and Expansion of Basal Progenitors in the Developing Mouse Neocortex. *Neuron*, 60(1), pp.40–55.

Florio, M. & Huttner, W.B., 2014. Neural progenitors , neurogenesis and the evolution of the neocortex. *Development*, pp.2182–2194.

Frantz, G.D. et al., 1994. Otx1 and Otx2 define layers and regions in developing cerebral cortex and cerebellum. *The Journal of neuroscience : the official journal of the Society for Neuroscience*, 14(10), pp.5725–5740.

Frantz, G.D. & McConnell, S.K., 1996. Restriction of late cerebral cortical progenitors to an upper-layer fate. *Neuron*, 17(1), pp.55–61. Available at: http://www.ncbi.nlm.nih.gov/pubmed/8755478.

Froldi, F. et al., 2015. The transcription factor Nerfin-1 prevents reversion of neurons into neural stem cells. *Genes and Development*, 29(2), pp.129–143.

Fuchs, Y. & Steller, H., 2011. Programmed cell death in animal development and disease. *Cell*, 147(4), pp.742–58. Available at: http://www.ncbi.nlm.nih.gov/pubmed/22078876 [Accessed February 2, 2014].

Gao, P. et al., 2014. Deterministic progenitor behavior and unitary production of neurons in the neocortex. *Cell*, 159(4), pp.775–788. Available at: http://dx.doi.org/10.1016/j.cell.2014.10.027.

Gauhar, Z. et al., 2009. Genomic mapping of binding regions for the Ecdysone receptor protein complex. *Genome Research*, 19(6), pp.1006–1013.

Goffart, N., Kroonen, J. & Rogister, B., 2013. Glioblastoma-initiating cells: Relationship with neural stem cells and the micro-environment. *Cancers*, 5(3), pp.1049–1071.

Gonçalves, J.T., Schafer, S.T. & Gage, F.H., 2016. Adult Neurogenesis in the Hippocampus: From Stem Cells to Behavior. *Cell*, 167(4), pp.897–914.

Gotz, M., Stoykova, A. & Gruss, P., 1998. Pax6 Controls Radial Glia Differentiation. *Neuron*, 21, pp.1031–1044.

Grether, M.E. et al., 1995. The head involution defective gene of Drosophila melanogaster functions in programmed cell death. *Genes & development*, 9, pp.1694–1708.

Grosskortenhaus, R. et al., 2005. Regulation of temporal identity transitions in drosophila neuroblasts. *Developmental Cell*, 8(2), pp.193–202.

Grosskortenhaus, R., Robinson, K.J. & Doe, C.Q., 2006. Pdm and Castor specify late-born motor neuron identity in the NB7-1 lineage. *Genes and*

Development, 20(18), pp.2618–2627.
Ha, S. et al., 2015. Regulation of autophagic cell death by glycogen synthase kinase-3β in adult hippocampal neural stem cells following insulin withdrawal. *Molecular Brain*, 8(1), p.30. Available at: http://www.molecularbrain.com/content/8/1/30.
Haga-yamanaka, S. et al., 2018. A Membrane Transporter Is Required for Steroid Hormone Uptake in Drosophila A Membrane Transporter Is Required for Steroid Hormone Uptake in Drosophila. *Developmental Cell*, pp.1–12. Available at: https://doi.org/10.1016/j.devcel.2018.09.012.
Hartenstein, V. & Campos-Ortega, J.A., 1984. Early neurogenesis in wild-type Drosophila melanogaster. *Wilhelm Roux's Archives of Developmental Biology*, 193(5), pp.308–325.
Hartenstein, V. & Wodarz, A., 2013. Initial neurogenesis in *Drosophila*. *Wiley Interdisciplinary Reviews: Developmental Biology*, 2(5), pp.701–721. Available at: http://doi.wiley.com/10.1002/wdev.111.
Hazlett, H. & Poe, M., 2011. Early Brain Overgrowth in Autism associated with an increase in cortical surface area before age 2. *Archives of …*, 68(5), pp.467–476. Available at: http://archpsyc.jamanetwork.com/article.aspx?articleid=211294 [Accessed March 13, 2014].
Heisenberg, M., 1998. What Do the Mushroom Bodies Do for the Insect Brain ? An Introduction. *Learning & Memory*, 5, pp.1–10.
Hirono, K. et al., 2012. Identification of hunchback cis-regulatory DNA conferring temporal expression in neuroblasts and neurons. *Gene Expression Patterns*, 12(1–2), pp.11–17. Available at: http://dx.doi.org/10.1016/j.gep.2011.10.001.
Homem, C.C.F. et al., 2014. Ecdysone and mediator change energy metabolism to terminate proliferation in drosophila neural stem cells. *Cell*, 158(4), pp.874–888. Available at: http://dx.doi.org/10.1016/j.cell.2014.06.024.
Homem, C.C.F., Repic, M. & Knoblich, J.A., 2015. Proliferation control in neural stem and progenitor cells. *Nature Reviews Neuroscience*, 16(11), pp.647–659. Available at: http://www.nature.com/doifinder/10.1038/nrn4021.
Ikeshima-Kataoka, H. et al., 1997. Miranda directs Prospero to a daughter cell during Drosophila asymmetric divisions. *Nature*, 390(6660), pp.625–629.
Isshiki, T. et al., 2001. Drosophila neuroblasts sequentially express transcription factors which specify the temporal identity of their neuronal progeny. *Cell*, 106(4), pp.511–521.
Ito, K. et al., 1997. The Drosophila mushroom body is a quadruple structure of clonal units each of which contains a virtually identical set of neurones and glial cells. *Development (Cambridge, England)*, 124(4), pp.761–771. Available at: papers://5b5dd7df-cb43-4c9c-aba9-19017de79ffc/Paper/p7433.
Ito, K. & Hotta, Y., 1992. Proliferation pattern of postembryonic neuroblasts in the brain of Drosophila melanogaster. *Developmental biology*, pp.134–148. Available at: http://www.sciencedirect.com/science/article/pii/001216069290270Q [Accessed March 14, 2014].
Izumi, Y. et al., 2006. Drosophila Pins-binding protein Mud regulates spindle-

polarity coupling and centrosome organization. *Nature Cell Biology*, 8(6), pp.586–593.

Jayaram, N., Usvyat, D. & R. Martin, A.C., 2016. Evaluating tools for transcription factor binding site prediction. *BMC Bioinformatics*, (i), pp.1–12. Available at: http://bmcbioinformatics.biomedcentral.com/articles/10.1186/s12859-016-1298-9.

Jiang, C. et al., 2000. A steroid-triggered transcriptional hierarchy controls salivary gland cell death during Drosophila metamorphosis. *Molecular cell*, 5(3), pp.445–55. Available at: http://www.ncbi.nlm.nih.gov/pubmed/10882130.

Jiang, D.P. et al., 2011. [Effects of secretary leukocyte protease inhibitor-transfected bone marrow mesenchymal stem cells on airway inflammation and mucus secretion in chronic obstructive pulmonary disease]. *Zhonghua Yi Xue Za Zhi*, 91(48), pp.3438–3441. Available at: http://www.ncbi.nlm.nih.gov/pubmed/22333260.

Jimenez-Sanchez, M. et al., 2012. The Hedgehog signalling pathway regulates autophagy. *Nature Communications*, 3, pp.1200–1211. Available at: http://dx.doi.org/10.1038/ncomms2212.

Jin, H. et al., 2013. Genome-Wide Screens for In Vivo Tinman Binding Sites Identify Cardiac Enhancers with Diverse Functional Architectures. *PLoS Genetics*, 9(1).

Junger, M.A. et al., 2003. The Drosophila forkhead transcription factor FOXO mediates the reduction in cell number associated with reduced insulin signaling. *J Biol*, 2(3), p.20. Available at: http://www.pubmedcentral.nih.gov/articlerender.fcgi?artid=333403&tool=pmcentrez&rendertype=abstract%5Cnhttp://www.ncbi.nlm.nih.gov/entrez/query.fcgi?cmd=Retrieve&db=PubMed&dopt=Citation&list_uids=12908874.

Jussen, D., von Hilchen, J. & Urbach, R., 2016. Genetic regulation and function of epidermal growth factor receptor signalling in patterning of the embryonic *Drosophila* brain. *Open Biology*, 6(12), p.160202. Available at: http://rsob.royalsocietypublishing.org/lookup/doi/10.1098/rsob.160202.

Kambadur, R. et al., 1998. Regulation of POU genes by *castor* and *hunchback* establishes layered compartments in the *Drosophila* CNS. *Genes & Development*, 12(2), pp.246–260.

Kang, K.H. & Reichert, H., 2015. Control of neural stem cell self-renewal and differentiation in Drosophila. *Cell and Tissue Research*, 359(1), pp.33–45.

Kao, C.F. et al., 2012. Hierarchical Deployment of Factors Regulating Temporal Fate in a Diverse Neuronal Lineage of the Drosophila Central Brain. *Neuron*, 73(4), pp.677–684. Available at: http://dx.doi.org/10.1016/j.neuron.2011.12.018.

Kato, K., Awasaki, T. & Ito, K., 2009. Neuronal programmed cell death induces glial cell division in the adult Drosophila brain. , 59, pp.51–59.

Kelsom, C. & Lu, W., 2012. Uncovering the link between malfunctions in Drosophila neuroblast asymmetric cell division and tumorigenesis. *Cell and Bioscience*, 2(1), pp.1–12.

Kessaris, N., Pringle, N. & Richardson, W.D., 2001. and the Neuron-Glial Switch.

, 31, pp.677–680.
Khandelwal, R. et al., 2017. *Combinatorial action of Grainyhead, Extradenticle and Notch in regulating Hox mediated apoptosis in Drosophila larval CNS*,
Kimura, S., Noda, T. & Yoshimori, T., 2007. Dissection of the autophagosome maturation process by a novel reporter protein, tandem fluorescent-tagged LC3. *Autophagy*, 3(5), pp.452–460.
King-Jones, K. & Thummel, C.S., 2005. Nuclear receptors - A perspective from Drosophila. *Nature Reviews Genetics*, 6(4), pp.311–323.
Knoblich, J.A., 2008. Mechanisms of Asymmetric Stem Cell Division. *Cell*, 132(4), pp.583–597.
Kohwi, M. et al., 2013. Developmentally regulated subnuclear genome reorganization restricts neural progenitor competence in Drosophila. *Cell*, 152(1–2), pp.97–108. Available at: http://dx.doi.org/10.1016/j.cell.2012.11.049.
Kraft, K.F. et al., 2016. Retinal homeobox promotes cell growth, proliferation and survival of mushroom body neuroblasts in the Drosophila brain. *Mechanisms of Development*, 142, pp.50–61. Available at: http://dx.doi.org/10.1016/j.mod.2016.07.003.
Kraut, R. et al., 1996. Role of inscuteable in orienting asymmetric cell divisions in Drosophila. *Nature*, 383(6595), pp.50–55.
Kucherenko, M.M., Barth, J. & Shcherbata, H.R., 2012. Steroid-induced microRNA let-7 acts as a spatio-temporal code for neuronal cell fate in the developing Drosophila brain. , 31(24), pp.4511–4523.
Kuert, Philipp A et al., 2014. Neuroblast lineage identification and lineage-specific Hox gene action during postembryonic development of the subesophageal ganglion in the Drosophila central brain. *Developmental biology*, 390, pp.102–115. Available at: http://dx.doi.org/10.1016/j.ydbio.2014.03.021.
Kuert, P. a, Bello, B.C. & Reichert, H., 2012. The labial gene is required to terminate proliferation of identified neuroblasts in postembryonic development of the Drosophila brain. *Biology open*, 1(10), pp.1006–15. Available at: http://www.pubmedcentral.nih.gov/articlerender.fcgi?artid=3507175&tool=pmcentrez&rendertype=abstract [Accessed March 13, 2014].
Kunz, T. et al., 2012. Origin of Drosophila mushroom body neuroblasts and generation of divergent embryonic lineages. *Development*, 139(14), pp.2510–2522. Available at: http://dev.biologists.org/cgi/doi/10.1242/dev.077883.
Kurusu, M. et al., 2009. A conserved nuclear receptor, Tailless, is required for efficient proliferation and prolonged maintenance of mushroom body progenitors in the Drosophila brain. *Developmental Biology*, 326(1), pp.224–236. Available at: http://dx.doi.org/10.1016/j.ydbio.2008.11.013.
Kurusu, M. et al., 2000. Genetic control of development of the mushroom bodies, the associative learning centers in the Drosophila brain, by the eyeless, twin of eyeless, and dachshund genes. *Proceedings of the National Academy of Sciences*, 97(5), pp.2140–2144. Available at: http://www.pnas.org/cgi/doi/10.1073/pnas.040564497.

Kuzin, A. et al., 2018. Structure and *cis* -regulatory analysis of a *Drosophila grainyhead* neuroblast enhancer. *Genesis*, 56(3), p.e23094. Available at: http://doi.wiley.com/10.1002/dvg.23094.

Kuzin, A. et al., 2012. The cis-regulatory dynamics of the Drosophila CNS determinant castor are controlled by multiple sub-pattern enhancers. *Gene Expression Patterns*, 12(7–8), pp.261–272. Available at: http://dx.doi.org/10.1016/j.gep.2012.05.004.

Lai, S.L. & Doe, C.Q., 2014. Transient nuclear Prospero induces neural progenitor quiescence. *eLife*, 3(October2014), pp.1–12.

Lanet, E., Gould, A.P. & Maurange, C., 2013. Protection of Neuronal Diversity at the Expense of Neuronal Numbers during Nutrient Restriction in the Drosophila Visual System. *Cell Reports*, 3(3), pp.587–594.

Lee, C.-Y. & Baehrecke, E.H., 2001. Steroid regulation of autophagic programmed cell death during development. *Development*, 128, pp.1443–1455. Available at: http://dx.doi.org/10.1038/sj.cdd.4400753.

Lee, C., Robinson, K.J. & Doe, C.Q., 2006. Lgl , Pins and aPKC regulate neuroblast self-renewal versus differentiation. , 439(February).

Lee, C.Y., Wilkinson, B.D., et al., 2006. Brat is a Miranda cargo protein that promotes neuronal differentiation and inhibits neuroblast self-renewal. *Developmental Cell*, 10(4), pp.441–449.

Lee, C.Y., Andersen, R.O., et al., 2006. Drosophila Aurora-A kinase inhibits neuroblast self-renewal by regulating aPKC/Numb cortical polarity and spindle orientation. *Genes and Development*, 20(24), pp.3464–3474.

Lee, C.Y. et al., 2000. E93 directs steroid-triggered programmed cell death in Drosophila. *Molecular Cell*, 6(2), pp.433–443.

Lee, C.Y., Robinson, K.J. & Doe, C.Q., 2006. Lgl, Pins and aPKC regulate neuroblast self-renewal versus differentiation. *Nature*, 439(7076), pp.594–598.

Lee, G. et al., 2013. Essential role of grim-led programmed cell death for the establishment of corazonin-producing peptidergic nervous system during embryogenesis and metamorphosis in Drosophila melanogaster. *Biology open*, 2(3), pp.283–94. Available at: http://www.pubmedcentral.nih.gov/articlerender.fcgi?artid=3603410&tool=pmcentrez&rendertype=abstract [Accessed March 13, 2014].

Lee, T. & Luo, L., 1999. Mosaic analysis with a repressible neurotechnique cell marker for studies of gene function in neuronal morphogenesis. *Neuron*, 22(3), pp.451–461.

Lehtinen, M.K. et al., 2011. The Cerebrospinal Fluid Provides a Proliferative Niche for Neural Progenitor Cells. *Neuron*, 69(5), pp.893–905. Available at: http://dx.doi.org/10.1016/j.neuron.2011.01.023.

Li, P. et al., 1997. Inscuteable and staufen mediate asymmetric localization and segregation of prospero RNA during drosophila neuroblast cell divisions. *Cell*, 90(3), pp.437–447.

Li, S. et al., 2017. An intrinsic mechanism controls reactivation of neural stem cells by spindle matrix proteins. *Nature Communications*, 8(1), pp.1–11. Available at: http://dx.doi.org/10.1038/s41467-017-00172-9.

Li, X. et al., 2013. Temporal patterning of Drosophila medulla neuroblasts controls neural fates. *Nature*, 498(7455), pp.456–462. Available at: http://dx.doi.org/10.1038/nature12319.

Lim, D.A. & Alvarez-buylla, A., 2016. The Adult Ventricular – Subventricular Zone. *Cold Spring Harbor Perspectives in Biology*.

Liu, N. et al., 2011. Mice lacking microRNA 133a develop dynamin 2-dependent centronuclear myopathy. *J Clin Invest*, 121(8), pp.3258–3268. Available at: http://www.ncbi.nlm.nih.gov/entrez/query.fcgi?cmd=Retrieve&db=PubMed&dopt=Citation&list_uids=21737882.

Liu, Z. et al., 2015. Opposing intrinsic temporal gradients guide neural stem cell production of varied neuronal fates. *Science*, 350(6258).

Livesey, F.J., Cepko, C.L. & Medical, H.H., 2001. VERTEBRATE NEURAL CELL-FATE DETERMINATION : LESSONS FROM THE RETINA. *Nature Neuroscience*, 2(February).

Llamazares, S. et al., 1991. Polo encodes a protein kinase homolog required for mitosis in Drosophila. *Genes and Development*, 5(12), pp.2153–2165.

Marchetto, M.C. et al., 2017. Altered proliferation and networks in neural cells derived from idiopathic autistic individuals. *Molecular Psychiatry*, 22(6), pp.820–835.

Mattar, P. et al., 2015. A Conserved Regulatory Logic Controls. *Neuron*, 85(3), pp.497–504. Available at: http://dx.doi.org/10.1016/j.neuron.2014.12.052.

Maurange, C., Cheng, L. & Gould, A.P., 2008. Temporal transcription factors and their targets schedule the end of neural proliferation in Drosophila. *Cell*, 133(5), pp.891–902. Available at: http://www.ncbi.nlm.nih.gov/pubmed/18510932 [Accessed January 27, 2014].

Maurange, C., Cheng, L. & Gould, A.P., 2008. Temporal Transcription Factors and Their Targets Schedule the End of Neural Proliferation in Drosophila. *Cell*, 133(5), pp.891–902.

Maurange, C. & Gould, A.P., 2005. Brainy but not too brainy: Starting and stopping neuroblast divisions in Drosophila. *Trends in Neurosciences*, 28(1), pp.30–36.

McGuire, S.E. et al., 2003. Spatiotemporal rescue of memory dysfunction in Drosophila. *Science (New York, N.Y.)*, 302(5651), pp.1765–8. Available at: http://www.ncbi.nlm.nih.gov/pubmed/14657498 [Accessed January 27, 2014].

McGuire, S.E., Mao, Z. & Davis, R.L., 2004. Spatiotemporal Gene Expression Targeting with the TARGET and Gene-Switch Systems in Drosophila. *Science Signaling*, 2004(220), pp.pl6-pl6. Available at: http://stke.sciencemag.org/cgi/doi/10.1126/stke.2202004pl6.

Mettler, U., Vogler, G. & Joachim, U., 2006. Timing of identity: spatiotemporal regulation of hunchback in neuroblast lineages of Drosophila by Seven-up and Prospero. *Development*, 133(3), pp.429–437. Available at: http://dev.biologists.org/cgi/doi/10.1242/dev.02229.

Mirth, C.K., Truman, J.W. & Riddiford, L.M., 2009. The Ecdysone receptor controls the post-critical weight switch to nutrition-independent differentiation

in Drosophila wing imaginal discs. , 2353, pp.2345–2353.
Moon, N.-S. et al., 2008. E2F and p53 induce apoptosis independently during Drosophila development but intersect in the context of DNA damage. *PLoS genetics*, 4(8), p.e1000153. Available at: http://www.pubmedcentral.nih.gov/articlerender.fcgi?artid=2491587&tool=pmcentrez&rendertype=abstract [Accessed February 2, 2014].
Moorman, C. et al., 2006. Hotspots of transcription factor colocalization in the genome of Drosophila melanogaster. *Proceedings of the National Academy of Sciences*, 103(32), pp.12027–12032. Available at: http://www.pnas.org/cgi/doi/10.1073/pnas.0605003103.
Mou, X. et al., 2012. Control of target gene specificity during metamorphosis by the steroid response gene E93. *Proceedings of the National Academy of Sciences*, 109(8), pp.2949–2954. Available at: http://www.pnas.org/cgi/doi/10.1073/pnas.1117559109.
Narbonne-Reveau, K. et al., 2016. Neural stem cell-encoded temporal patterning delineates an early window of malignant susceptibility in Drosophila. *eLife*, 5(JUN2016), pp.1–29.
Négre, N. et al., 2011. A cis-regulatory map of the Drosophila genome. *Nature*, 471(7339), pp.527–531.
Nezis, I.P. et al., 2010. Autophagic degradation of dBruce controls DNA fragmentation in nurse cells during late Drosophila melanogaster oogenesis. *Journal of Cell Biology*, 190(4), pp.523–531.
Nipper, R.W. et al., 2007. G i generates multiple Pins activation states to link cortical polarity and spindle orientation in Drosophila neuroblasts. *Proceedings of the National Academy of Sciences*, 104(36), pp.14306–14311. Available at: http://www.pnas.org/cgi/doi/10.1073/pnas.0701812104.
Nishino, J. et al., 2013. A network of heterochronic genes including Imp1 regulates temporal changes in stem cell properties. *eLife*, 2013(2), pp.1–30.
Nóbrega-Pereira, S. et al., 2008. Postmitotic Nkx2-1 Controls the Migration of Telencephalic Interneurons by Direct Repression of Guidance Receptors. *Neuron*, 59(5), pp.733–745.
Noctor, S.C. et al., 2002. Dividing Precursor Cells of the Embryonic Cortical Ventricular Zone Have Morphological and Molecular Characteristics of Radial Glia. *The Journal of Neuroscience*, 22(8), pp.3161–3173. Available at: http://www.jneurosci.org/lookup/doi/10.1523/JNEUROSCI.22-08-03161.2002.
Noveen, a, Daniel, a & Hartenstein, V., 2000a. Early development of the Drosophila mushroom body: the roles of eyeless and dachshund. *Development (Cambridge, England)*, 127, pp.3475–3488.
Noveen, a, Daniel, a & Hartenstein, V., 2000b. Early development of the Drosophila mushroom body: the roles of eyeless and dachshund. *Development (Cambridge, England)*, 127, pp.3475–3488.
Odenwald, W.F. et al., 2005. EVOPRINTER, a multigenomic comparative tool for rapid identification of functionally important DNA. *Proceedings of the National Academy of Sciences of the United States of America*, 102(41), pp.14700–5. Available at:

http://www.pubmedcentral.nih.gov/articlerender.fcgi?artid=1239946&tool=pmcentrez&rendertype=abstract.

Otsuki, L. & Brand, A.H., 2018. Cell cycle heterogeneity directs the timing of neural stem cell activation from quiescence-supplementary materials. *Science*, pp.1–5. Available at: www.sciencemag.org/content/360/6384/99/suppl/DC1.

Pavlopoulos, A. & Akam, M., 2011. Hox gene Ultrabithorax regulates distinct sets of target genes at successive stages of Drosophila haltere morphogenesis. *Proceedings of the National Academy of Sciences*, 108(7), pp.2855–2860. Available at: http://www.pnas.org/cgi/doi/10.1073/pnas.1015077108.

Perkins, L.A. et al., 2015. The transgenic RNAi project at Harvard medical school: Resources and validation. *Genetics*, 201(3), pp.843–852.

Peterson, C. et al., 2002. reaper is required for neuroblast apoptosis during Drosophila development. *Development (Cambridge, England)*, 129(6), pp.1467–76. Available at: http://www.ncbi.nlm.nih.gov/pubmed/11880355.

Petryk, A. et al., 2003. Shade is the Drosophila P450 enzyme that mediates the hydroxylation of ecdysone to the steroid insect molting hormone 20-hydroxyecdysone. *Proceedings of the National Academy of Sciences*, 100(24), pp.13773–13778. Available at: http://www.pnas.org/cgi/doi/10.1073/pnas.2336088100.

Pinto-Teixeira, F., Konstantinides, N. & Desplan, C., 2016. Programmed cell death acts at different stages of Drosophila neurodevelopment to shape the central nervous system. *FEBS Letters*, 590, pp.2435–2453.

Popken, G.J. et al., 2004. In vivo effects of insulin-like growth factor-I (IGF-I) on prenatal and early postnatal development of the central nervous system. , 19, pp.2056–2068.

Prokop, a et al., 1998. Homeotic regulation of segment-specific differences in neuroblast numbers and proliferation in the Drosophila central nervous system. *Mechanisms of development*, 74(1–2), pp.99–110. Available at: http://www.ncbi.nlm.nih.gov/pubmed/9651493.

Puig, O. & Tjian, R., 2006. Nutrient Availability and Growth. *Cell Cycle*, (March), pp.503–505.

Puig, O. & Tjian, R., 2005. Transcriptional feedback control of insulin receptor by dFOXO/FOXO1. *Genes and Development*, 19(20), pp.2435–2446.

Quiring, R. et al., 1994. Homology of the eyeless Gene of Drosophila to the Small eye Gene in Mice and Aniridia in Humans Author (s): Rebecca Quiring , Uwe Walldorf , Urs Kloter and Walter J . Gehring Published by : American Association for the Advancement of Science Stable URL. *Science1*, 265(5173), pp.785–789.

Rebollo, E. et al., 2007. Functionally Unequal Centrosomes Drive Spindle Orientation in Asymmetrically Dividing Drosophila Neural Stem Cells. *Developmental Cell*, 12(3), pp.467–474.

Reif, A. et al., 2007. Neurogenesis and schizophrenia: Dividing neurons in a divided mind? *European Archives of Psychiatry and Clinical Neuroscience*, 257(5), pp.290–299.

Ren, Q. et al., 2017. Stem Cell-Intrinsic, Seven-up-Triggered Temporal Factor

Gradients Diversify Intermediate Neural Progenitors. *Current Biology*, 27(9), pp.1303–1313. Available at: http://dx.doi.org/10.1016/j.cub.2017.03.047.

Rhee, D.Y. et al., 2014. Transcription factor networks in Drosophila melanogaster. *Cell Reports*, 8(6), pp.2031–2043. Available at: http://dx.doi.org/10.1016/j.celrep.2014.08.038.

Rolls, M.M. et al., 2003. Drosophila aPKC regulates cell polarity and cell proliferation in neuroblasts and epithelia. *Journal of Cell Biology*, 163(5), pp.1089–1098.

Ross, J. et al., 2015. cis-regulatory analysis of the Drosophila pdm locus reveals a diversity of neural enhancers. *BMC Genomics*, 16(1), pp.1–20. Available at: http://dx.doi.org/10.1186/s12864-015-1897-2.

Rusten, T.E. et al., 2004. Autophagy Fatbody Ecdysone Pi3K Pathway.Pdf. , 7, pp.179–192.

Sandu, C., Ryoo, H.D. & Steller, H., 2010. Drosophila IAP antagonists form multimeric complexes to promote cell death. *Journal of Cell Biology*, 190(6), pp.1039–1052.

Sansom, S.N. et al., 2009. The level of the transcription factor Pax6 is essential for controlling the balance between neural stem cell self-renewal and neurogenesis. *PLoS Genetics*, 5(6), pp.20–23.

Schaefer, M. et al., 2000. A protein complex containing Inscuteable and the Galpha-binding protein Pins orients asymmetric cell divisions in Drosophila. *Current biology : CB*, 10(7), pp.353–362.

Schoenfeld, T.J. & Cameron, H.A., 2015. Adult neurogenesis and mental illness. *Neuropsychopharmacology*, 40(1), pp.113–128. Available at: http://dx.doi.org/10.1038/npp.2014.230.

Scott, R.C., Juhász, G. & Neufeld, T.P., 2007. Direct Induction of Autophagy by Atg1 Inhibits Cell Growth and Induces Apoptotic Cell Death. *Current Biology*, 17(1), pp.1–11.

Scuderi, A. et al., 2006. scylla and charybde, homologues of the human apoptotic gene RTP801, are required for head involution in Drosophila. *Developmental Biology*, 291(1), pp.110–122.

Shaw, R.E. et al., 2018. *In vivo* expansion of functionally integrated GABAergic interneurons by targeted increase in neural progenitors. *The EMBO Journal*, 37(13), p.e98163. Available at: http://emboj.embopress.org/lookup/doi/10.15252/embj.201798163.

Shen, C.P. et al., 1998. Miranda as a multidomain adapter linking apically localized Inscuteable and basally localized Staufen and Prospero during asymmetric cell division in Drosophila. *Genes and Development*, 12(12), pp.1837–1846.

Shen, C.P., Jan, L.Y. & Jan, Y.N., 1997. Miranda is required for the asymmetric localization of prospero during mitosis in Drosophila. *Cell*, 90(3), pp.449–458.

Shitamukai, A., Konno, D. & Matsuzaki, F., 2011. Oblique Radial Glial Divisions in the Developing Mouse Neocortex Induce Self-Renewing Progenitors outside the Germinal Zone That Resemble Primate Outer Subventricular Zone Progenitors. , 31(10), pp.3683–3695.

Siegrist, S.E. et al., 2010. Inactivation of both Foxo and reaper promotes long-term adult neurogenesis in Drosophila. *Current biology : CB*, 20(7), pp.643–8. Available at: http://www.pubmedcentral.nih.gov/articlerender.fcgi?artid=2862284&tool=pmcentrez&rendertype=abstract [Accessed March 3, 2014].

Siegrist, S.E. & Doe, C.Q., 2005. Microtubule-induced pins/Gαi cortical polarity in Drosophila neuroblasts. *Cell*, 123(7), pp.1323–1335.

Siller, K.H., Cabernard, C. & Doe, C.Q., 2006. The NuMA-related Mud protein binds Pins and regulates spindle orientation in Drosophila neuroblasts. *Nature Cell Biology*, 8(6), pp.594–600.

Siller, K.H. & Doe, C.Q., 2009. Spindle orientation during asymmetric cell division. *Nature cell biology*, 11(4), pp.365–74. Available at: http://www.ncbi.nlm.nih.gov/pubmed/19337318.

Simpson, J.H., 2009. *Chapter 3 Mapping and Manipulating Neural Circuits in the Fly Brain* 1st ed., Elsevier Inc. Available at: http://dx.doi.org/10.1016/S0065-2660(09)65003-3.

Sipe, C.W. & Siegrist, S.E., 2017. Eyeless uncouples mushroom body neuroblast proliferation from dietary amino acids in drosophila. *eLife*, 6, pp.1–26.

Skeath, J.B., 1998. The Drosophila EGF receptor controls the formation and specification of neuroblasts along the dorsal-ventral axis of the Drosophila embryo. *Development*, 125(17), pp.3301–3312.

Smith, C.A. et al., 2007. aPKC-mediated phosphorylation regulates asymmetric membrane localization of the cell fate determinant Numb. *EMBO Journal*, 26(2), pp.468–480.

Sorrells, S.F. et al., 2018. Human hippocampal neurogenesis drops sharply in children to undetectable levels in adults. *Nature*, 555(7696), pp.377–381. Available at: http://dx.doi.org/10.1038/nature25975.

Soula, C. et al., 2001. Distinct sites of origin of oligodendrocytes and somatic motoneurons in the chick spinal cord : oligodendrocytes arise from Nkx2 . 2-expressing progenitors by a Shh-dependent mechanism. , 1379, pp.1369–1379.

Sousa-Nunes, R., Yee, L.L. & Gould, A.P., 2011. Fat cells reactivate quiescent neuroblasts via TOR and glial insulin relays in Drosophila. *Nature*, 471(7339), pp.508–513.

Spana, E.P. & Doe, C.Q., 1995. The prospero transcription factor is asymmetrically localized to the cell cortex during neuroblast mitosis in Drosophila. *Development (Cambridge, England)*, 121, pp.3187–3195.

Spassky, N. et al., 2005. Adult Ependymal cells are postmitotic and are derived from Radial Glial cells during embryogenesis. *Journal of Neuroscience*, 10(1), pp.10–18.

Spéder, P. & Brand, A.H., 2018. Systemic and local cues drive neural stem cell niche remodelling during neurogenesis in drosophila. *eLife*, 7.

Srinivasula, S.M. et al., 2002. Sickle, a novel Drosophila death gene in the reaper/hid/grim region, encodes an IAP-inhibitory protein. *Current Biology*, 12, pp.125–130.

Stratmann, J. & Thor, S., 2017. Neuronal cell fate specification by the molecular

convergence of different spatio-temporal cues on a common initiator terminal selector gene. *PLoS Genetics*, 13(4). Available at: http://dx.doi.org/10.1371/journal.pgen.1006729.

Sussel, L. et al., 1999. Loss of Nkx2 . 1 homeobox gene function results in a ventral to dorsal molecular respecification within the basal telencephalon : evidence for a transformation of the pallidum into the striatum. *Development*, 126, pp.3359–3370.

Syed, M.H., Mark, B. & Doe, C.Q., 2017a. Playing Well with Others: Extrinsic Cues Regulate Neural Progenitor Temporal Identity to Generate Neuronal Diversity. *Trends in Genetics*, 33(12).

Syed, M.H., Mark, B. & Doe, C.Q., 2017b. Steroid hormone induction of temporal gene expression in drosophila brain neuroblasts generates neuronal and glial diversity. *eLife*, 6, pp.1–23.

Tan, Y. et al., 2011. Coordinated expression of cell death genes regulates neuroblast apoptosis. *Development (Cambridge, England)*, 138(11), pp.2197–206. Available at: http://www.pubmedcentral.nih.gov/articlerender.fcgi?artid=3091491&tool=pmcentrez&rendertype=abstract [Accessed February 24, 2014].

Tan, Y. et al., 2011. Coordinated expression of cell death genes regulates neuroblast apoptosis. *Development*, 138(11), pp.2197–2206. Available at: http://dev.biologists.org/cgi/doi/10.1242/dev.058826.

Tazaki, A., Tanaka, E.M. & Fei, J.F., 2017. Salamander spinal cord regeneration: The ultimate positive control in vertebrate spinal cord regeneration. *Developmental Biology*, 432(1), pp.63–71. Available at: https://doi.org/10.1016/j.ydbio.2017.09.034.

Thummel, C.S., 2001. Steroid-triggered death by autophagy. , (1), pp.677–682.

Toledano, H. et al., 2012. The let-7-Imp axis regulates ageing of the Drosophila testis stem-cell niche. *Nature*, 485(7400), pp.605–610. Available at: http://dx.doi.org/10.1038/nature11061.

Touma, J.J., Weckerle, F.F. & Cleary, M.D., 2012. Drosophila Polycomb complexes restrict neuroblast competence to generate motoneurons. *Development*, 139(4), pp.657–666. Available at: http://dev.biologists.org/cgi/doi/10.1242/dev.071589.

Tran, K.D. & Doe, C.Q., 2008. Pdm and Castor close successive temporal identity windows in the NB3-1 lineage. *Development*, 135(21), pp.3491–3499. Available at: http://dev.biologists.org/cgi/doi/10.1242/dev.024349.

Von Trotha, J.W., Egger, B. & Brand, A.H., 2009. Cell proliferation in the Drosophila adult brain revealed by clonal analysis and bromodeoxyuridine labelling. , 8, pp.1–8.

Truman, J.W. et al., 1994. Ecdysone receptor expression in the CNS correlates with stage-specific responses to ecdysteroids during Drosophila and Manduca development. *Development (Cambridge, England)*, 120, pp.219–234.

Truman, J.W. & Bate M, 1988. Spatial and Temporal Patterns of Neurogenesis in the Central Nervous System of Drosophila melanogaster. *Developmental biology*, 125, pp.145–157.

Tsuji, T., Hasegawa, E. & Isshiki, T., 2008. Neuroblast entry into quiescence is regulated intrinsically by the combined action of spatial Hox proteins and temporal identity factors. *Development*, 135(23), pp.3859–3869. Available at: http://dev.biologists.org/cgi/doi/10.1242/dev.025189.

Urbach, R., 2003. Molecular markers for identified neuroblasts in the developing brain of Drosophila. *Development*, 130(16), pp.3621–3637. Available at: http://dev.biologists.org/cgi/doi/10.1242/dev.00533.

Urbach, R., Jussen, D. & Technau, G.M., 2012. Gene expression profiles uncover individual identities of gnathal neuroblasts and serial homologies in the embryonic CNS of Drosophila. *Development*, pp.1290–1301.

Urbach, R. & Technau, G.M., 2004. Neuroblast formation and patterning during early brain development in Drosophila. *BioEssays*, 26(7), pp.739–751.

Urbach, R. & Technau, G.M., 2003. Segment polarity and DV patterning gene expression reveals segmental organization of the Drosophila brain. , pp.3607–3620.

Uyehara, C.M. et al., 2017. Hormone-dependent control of developmental timing through regulation of chromatin accessibility. *Genes and Development*, 31(9), pp.862–875.

Del Valle Rodríguez, A., Didiano, D. & Desplan, C., 2012. Power tools for gene expression and clonal analysis in Drosophila. *Nature Methods*, 9(1), pp.47–55.

Valvo, G. et al., 2013. Somatic overgrowth predisposes to seizures in autism spectrum disorders. *PloS one*, 8(9), p.e75015. Available at: http://www.pubmedcentral.nih.gov/articlerender.fcgi?artid=3781047&tool=pmcentrez&rendertype=abstract [Accessed March 13, 2014].

Venken, K., Schulze, K. & Haelterman, N., 2011. MiMIC: a highly versatile transposon insertion resource for engineering Drosophila melanogaster genes. *Nature …*, 8(9), pp.737–743. Available at: http://www.nature.com/nmeth/journal/v8/n9/abs/nmeth.1662.html [Accessed March 14, 2014].

Visel, A., Bristow, J. & Pennacchio, L.A., 2007. Enhancer identification through comparative genomics. *Seminars in Cell and Developmental Biology*, 18(1), pp.140–152.

Wang, C. et al., 2009. Protein phosphatase 2A regulates self-renewal of Drosophila neural stem cells. *Development*, 136(17), pp.3031–3031. Available at: http://dev.biologists.org/cgi/doi/10.1242/dev.042432.

Wang, H. et al., 2006. Aurora-A acts as a tumor suppressor and regulates self-renewal of Drosophila neuroblasts. *Genes and Development*, 20(24), pp.3453–3463.

Wang, H. et al., 2007. Polo inhibits progenitor self-renewal and regulates Numb asymmetry by phosphorylating Pon. *Nature*, 449(7158), pp.96–100.

Weinkove, D. et al., 1999. Regulation of imaginal disc cell size, cell number and organ size by Drosophila class I(A) phosphoinositide 3-kinase and its adaptor. *Current Biology*, 9(18), pp.1019–1029.

White, K. et al., 1994. Genetic Control of Programmed Cell Death in Drosophila. *Science*, 264, pp.677–683. Available at: http://www.jstor.org/stable/2883512.

Wing, J.P. et al., 1998. Distinct cell killing properties of the Drosophila reaper, head involution defective, and grim genes. *Cell death and differentiation*, 5(11), pp.930–9. Available at: http://www.ncbi.nlm.nih.gov/pubmed/9846179.

Wing, J.P. et al., 2002. Drosophila sickle is a novel grim-reaper cell death activator. *Current biology : CB*, 12(2), pp.131–5. Available at: http://www.ncbi.nlm.nih.gov/pubmed/11818064.

Wing, J.P., Schwartz, L.M. & Nambu, J.R., 2001. The RHG motifs of Drosophila Reaper and Grim are important for their distinct cell death-inducing abilities. *Mechanisms of Development*, 102(1–2), pp.193–203.

Winner, B. & Winkler, J., 2007. Adult neurogenesis in neurodegenerative diseases. *Cold Spring Harbor Perspectives in Biology*, pp.445–460.

Wu, J.N. et al., 2010. grim promotes programmed cell death of Drosophila microchaete glial cells. *Mechanisms of development*, 127(9–12), pp.407–17. Available at: http://www.pubmedcentral.nih.gov/articlerender.fcgi?artid=2956798&tool=pmcentrez&rendertype=abstract [Accessed February 2, 2014].

Wu, Y. et al., 2012. Let-7-Complex MicroRNAs Regulate the Temporal Identity of Drosophila Mushroom Body Neurons via chinmo. *Developmental Cell*, pp.202–209.

Yamanaka, N., Marque, G. & Connor, M.B.O., 2015. Vesicle-Mediated Steroid Hormone Secretion in Drosophila melanogaster Article Vesicle-Mediated Steroid Hormone Secretion in Drosophila melanogaster. , pp.907–919.

Yamanaka, N., Rewitz, K.F. & Connor, M.B.O., 2013. Ecdysone Control of Developmental Transitions : Lessons from Drosophila Research.

Yang, C.-P. et al., 2017. Imp and Syp RNA-binding proteins govern decommissioning of *Drosophila* neural stem cells. *Development*, 144(19), pp.3454–3464. Available at: http://dev.biologists.org/lookup/doi/10.1242/dev.149500.

Yeo, W. & Gautier, J., 2004. Early neural cell death: Dying to become neurons. *Developmental Biology*, 274(2), pp.233–244.

Young, M.M. et al., 2012. Autophagosomal membrane serves as platform for intracellular death-inducing signaling complex (iDISC)-mediated caspase-8 activation and apoptosis. *Journal of Biological Chemistry*, 287(15), pp.12455–12468.

Yu, F. et al., 2000. Analysis of partner of inscuteable, a novel player of Drosophila asymmetric divisions, reveals two distinct steps in inscuteable apical localization. *Cell*, 100(4), pp.399–409.

Yu, S.-W. et al., 2008. Autophagic Death of Adult Hippocampal Neural Stem Cells Following Insulin Withdrawal. *Stem Cells*, 26(10), pp.2602–2610. Available at: http://doi.wiley.com/10.1634/stemcells.2008-0153.

Zaffran, S., Das, G. & Frasch, M., 2000. The NK-2 homeobox gene scarecrow (scro) is expressed in pharynx, ventral nerve cord and brain of Drosophila embryos. *Mechanisms of Development*, 94(1–2), pp.237–241.

Zhang, C. et al., 2014. An intergenic regulatory region mediates Drosophila Myc-induced apoptosis and blocks tissue hyperplasia. *Oncogene*, (April), pp.1–13. Available at: http://www.ncbi.nlm.nih.gov/pubmed/24931167.

Zhang, T. et al., 2009. Zinc finger transcription factor INSM1 interrupts cyclin D1 and CDK4 binding and induces cell cycle arrest. *Journal of Biological Chemistry*, 284(9), pp.5574–5581.

Zhang, Y., Lin, N., Carroll, P., et al., 2008. Epigenetic blocking of an enhancer region controls irradiation-induced proapoptotic gene expression in Drosophila embryoes. *Developmental cell*, 14(4), pp.481–493. Available at: http://www.sciencedirect.com/science/article/pii/S1534580708000464 [Accessed March 14, 2014].

Zhang, Y., Lin, N., Carroll, P.M., et al., 2008. Epigenetic Blocking of an Enhancer Region Controls Irradiation-Induced Proapoptotic Gene Expression in Drosophila Embryos. *Developmental Cell*, 14(4), pp.481–493.

Zhu, S. et al., 2006. Gradients of the Drosophila Chinmo BTB-Zinc Finger Protein Govern Neuronal Temporal Identity. *Cell*, 127(2), pp.409–422.

Zhu, S. et al., 2012. The bHLH Repressor Deadpan Regulates the Self-renewal and Specification of Drosophila Larval Neural Stem Cells Independently of Notch. *PLoS ONE*, 7(10).

Appendix:

Grim and sickle regulate MB neuroblast apoptosis

Abstract:

The mushroom body neuroblasts (MB neuroblasts) undergo programmed cell death before the adult ecloses from its pupal case. This cell death requires four proapoptotic genes, *reaper, grim, hid, and sickle*, located in a gene poor 300kb genomic region. Originally, large deletions and transgenes that targeted multiple regulators were used to target this region, leading to uncertainty of which of the proapoptotic genes are required for MB neuroblast cell death. Here we identified *grim* and *skl* as the critical regulators of MB neuroblast termination.

Introduction:

We use *Drosophila* to understand how neurogenesis becomes restricted during development. The eight (four per brain hemisphere) mushroom body neuroblasts (MB neuroblasts) proliferate continuously during development until undergoing programmed cell death in late pupal stages approximately ten hours before eclosion (Siegrist et al. 2010).

In *Drosphila,* four proapoptotic genes: *grim*, *reaper (rpr)*, *head involution defective (hid)*, and *sickle (skl)* are located in a shared 300kb genomic region were shown to be necessary for MB neuroblast apoptosis (Siegrist et al. 2010). The proapoptotic proteins act as antagonists of inhibitors of apoptosis proteins (IAPs), a class of proteins that regulate cell death by binding to caspases and

promoting their ubiquitination (Fuchs & Steller 2011). This results in degradation of caspases within in the proteasome, ensuring cell survival.

The IAP antagonists are critical regulators of developmental programmed cell death in Drosophila (Fuchs & Steller 2011). IAP antagonists act through a shared six-amino acid long N-terminal motif known as the IAP Binding motif (IBM). The IAP antagonists bind to IAPs competitively and promote their autoubiquitination, which leads to its degradation by the proteasome (Chai et al. 2003). Although IAP antagonists promote cell death through similar mechanisms, functional differences exist between them. For example Hid contains a mitochondrial localization domain, which is necessary for its antagonist activity (Zhang, Lin, P. M. Carroll, et al. 2008), reaper activity requires localization to the mitochondria, through heterodimerizing with hid (Sandu et al. 2010).

Transcription of the four IAP antagonists in the reaper locus is coordinately regulated by shared long-range enhancers that promotes expression of combinations of proapoptotic genes during development (Zhang et al. 2014; Zhang, Lin, P. M. Carroll, et al. 2008; Ying Tan et al. 2011). These enhancers coordinate expression of the proapoptotic genes. One of these regions coordinates expression of grim and reaper during programmed cell death in embryonic neuroblasts (Ying Tan et al. 2011; Khandelwal et al. 2017).

Flies in trans for two overlapping deletions H99 and XR38 allow MB neuroblasts to persist into adult stages (Appendix Fig 1a) (Siegrist et al. 2010). H99 spans rpr, grim, and hid, while XR38 spans rpr and skl. In trans XR38/H99 animals are homozygous null for reaper and heterozygous for grim, hid, and skl

(Peterson et al. 2002; Siegrist et al. 2010). From this combination, it was concluded that the persisting MB neuroblast phenotype observed in XR38/H99 animals was likely caused by deletion of rpr because it was the only null gene in this combination (Siegrist et al. 2010).

However, these large deletions also span several previously described long-distance enhancers located in this locus and careful characterization of these deletions found that the XR38 chromosome carried additional point mutations in grim such that it also likely acts as a loss of function allele (Y. Tan et al. 2011; Khandelwal et al. 2017; Zhang, Lin, P. Carroll, et al. 2008). (Lee et al. 2013). Taken together this suggests that rather than being specific to reaper, MB neuroblast apoptosis may be regulated by one or more IAP antagonist.

In this chapter, I describe the identification of grim and skl as the genes that regulate apoptosis of MB neuroblasts.

Results:

Grim and sickle are necessary for MB neuroblast termination

Previously four proapoptotic genes: *reaper, grim, hid,* and *sickle* located in a 300kb region of the left arm of the third chromosome were implicated in the regulation of apoptosis in MB neuroblasts (White et al. 1994; Grether et al. 1995). Due to a lack of single mutant alleles, previous work used large deletions, which span multiple genes. One method was to put XR38 and H99 in trans (Appendix Fig 1). The XR38 deletion spans *rpr* and *skl*, while H99 spans *reaper, grim*, and *hid* (White et al. 1994; Siegrist et al. 2010).

To better characterize which of the four proapoptotic genes eliminate MB neuroblasts, we assayed for the presence MB neuroblast in 1-day-old adults that carry small deletions specifically deleting either *grim, reaper,* or *sickle* (Appendix Fig 1A). We identified MB neuroblasts based their position on the dorsal surface of central brain and expression of the neuroblast marker Deadpan (Siegrist et al. 2010). In control animals all the neuroblasts have been eliminated and no neuroblasts are found in adult animals (Siegrist et al. 2010). We found that MB neuroblasts were present in grim null and skl null, but not rpr null mutants (Quantified in appendix Fig 1F). Hid mutants were lethal early in development preventing them from being assayed. This suggests that grim and skl are required for MB neuroblast elimination.

To confirm our results with the null alleles, we used the GAL4/UAS system to express artificial microRNAs that target *grim, reaper, hid,* and *sickle* individually. We expressed each *UAS-microRNA* line in neuroblasts using *worGAL4* (Appendix Fig. 1B,C, quantified in F) (Lee et al. 2013). We found that MB neuroblasts persist in 1 day old adults when either grim or skl is knocked down, but not with knockdown of rpr or hid. This confirms our observation with the null mutants that Grim and Skl are the proapoptotic genes required for MB neuroblast elimination.

We also asked whether misexpression of proapoptotic genes is sufficient to eliminate MB neuroblasts early. The proapoptotic genes are reported to have different specificities for promoting cell death (Wing et al. 1998; Wing et al. 2002). We wondered if MB neuroblasts had different effects in non-MB neuroblasts. To

avoid early lethality, we restricted misexpression of each to pupal phases using a temperature sensitive *GAL80* transgene, which allows for temporal control of gene expression (McGuire et al. 2004). GAL80ts inhibits GAL4-UAS at 18°C, at higher temperature GAL80ts is destabilized, relieving repression of GAL4-UAS. Animals were shifted to 29°C as white prepupae (P0) and dissected 48 hours later. Misexpression of grim, but not rpr, hid, or skl is sufficient to eliminate neuroblasts under this paradigm (Appendix Fig. 2A).

We also wanted to characterize when the proapoptotic genes began to express Grim and Sickle. Unfortunately we were unable to find an Skl antibody that could detect endogenous levels. We assayed Grim in control animals and found that grim is enriched in MB neuroblasts by 72 hours APF (Appendix Fig 3A). In later stages, we observed that grim staining becomes punctate by 84 hours after pupal formation (Appendix Fig 3B).

Discussion:

From our initial characterization of this locus we found that *grim* and *skl* are necessary for promoting MB neuroblast apoptosis. Sickle is the least well characterized of the proapoptotic genes, and is mainly thought to enhance sensitivity to undergo apoptosis, rather than drive apoptosis itself (Wing et al. 2002; Christich et al. 2002; Srinivasula et al. 2002). Grim, however, is thought to act as the primary proapoptotic gene in the central nervous system (Wing et al. 2001; Lee et al. 2013).

We found that multiple proapoptotic genes are necessary for programmed cell death in MB neuroblasts. This suggests that the proapoptotic genes

cooperate in eliminating MB neuroblasts. One way this could be achieved is through hetero-dimerization regulating their protein stability as has been reported to occur with rpr and hid (Sandu et al. 2010).

The subcellular localization of Grim showed a striking pattern shortly before termination, which may suggest that it may associate with an organelle, possibly by its interaction with Skl. Unfortunately we were unable to obtain a useable antibody against Skl to test this hypothesis.

Materials and Methods:

Fly stocks: *OregonR, grim*^{A6C} (Wu et al. 2010), *hid*^{05014} (Scuderi et al. 2006), *rpr*^{87} (Moon et al. 2008), *skl*^{e3} (Lee et al. 2013), *worGAL4; pcnaGFP* (Siegrist et al. 2010), *UASmigrim* (Lee et al. 2013), *UASmirpr* (Lee et al. 2013), *UASmihid* (Lee et al. 2013), *UASmiskl* (Lee et al. 2013).

Temperature shift: For the temperature shift experiment, embryos were collected and kept at 18°C. White pupae then shifted 29°C to for 48 hours at (P0).

Immunofluorescence and confocal microscopy: Brains were dissected, fixed, and stained as described previously (Siegrist et al., 2010; Doyle et al., 2017; Sipe and Siegrist, 2017). Images were acquired using an upright Leica SP8 confocal microscope with a 63x 1.4NA oil immersion objective and analyzed using Imaris and ImageJ software. Figures were assembled using Adobe Photoshop and Illustrator software. Primary antibodies used were rat anti-Dpn (1:5; gift from C. Doe), mouse or chicken anti-GFP (1:500, 1:1000 respectively), rabbit anti-grim

(gift from C. Clavería; 1:1000), mouse anti-Dlg (DSHB, 1:40), and rabbit anti-Scrib (a gift from C. Doe; 1:1000).

Quantification: For box plots, the boundary of the box closest to zero indicates the 25th percentile, a line within the box marks the median, and the boundary of the box farthest from zero indicates the 75th percentile. Whiskers (error bars) above and below the box indicate the 90th and 10th percentiles, respectively.

Acknowledgements: We acknowledge Kristin White for sharing the grim and reaper mutant lines; we thank Miki Fujioka and Chun-Hong Chen for and transgenic flies. We thank Cristina Clavería for sharing the grim antibody.

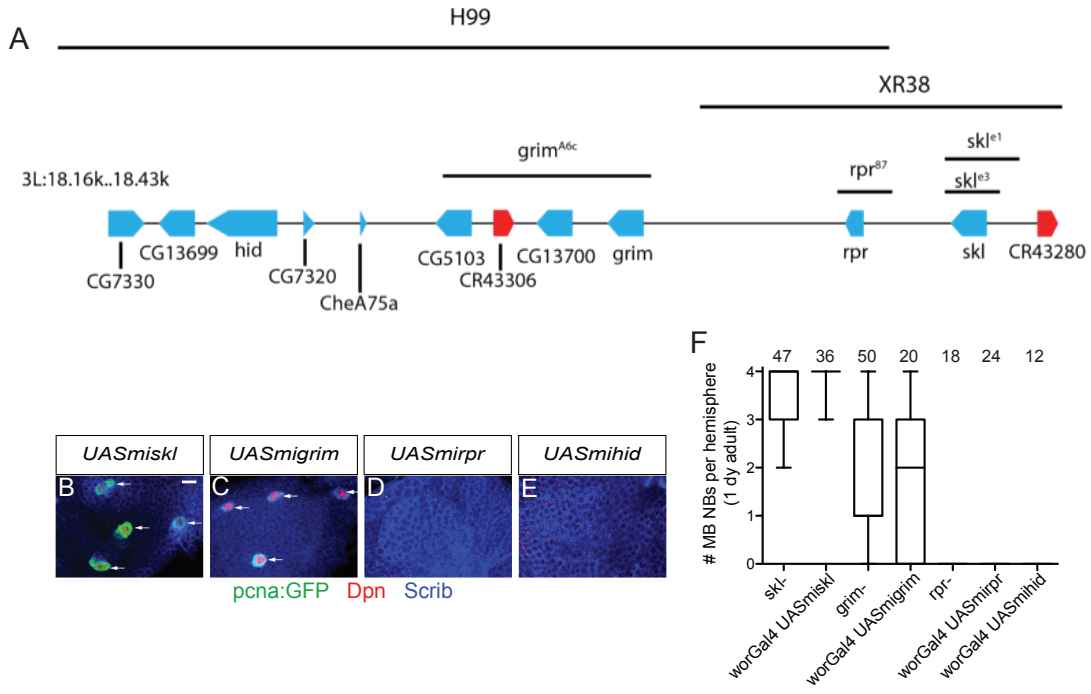

Appendix Figure 1 Sickle and grim are required for MB neuroblast apoptosis: (A) Diagram of the "reaper" locus, which spans approximately 300 kb. Lines above indicate the area different deletions span (Siegrist et al. 2010). Small deletions for the proapoptotic proteins are indicated below. Blue arrows indicate protein-coding genes, while red arrows indicate non-coding RNA. (B-E) Maximum intensity projection of the dorsal surface of the brains 1-day-old adult flies, expressing artificial microRNA against each of the four-proapoptotic genes. Arrows indicate MB neuroblasts, labeled with antibodies against Dpn (red), GFP (green), and the membrane marker Scribble (Blue). (F) Quantification the number of MB neuroblasts persisting in 1 day old adult brains in indicated genotypes. Numbers at the top indicate the number of brain hemispheres assayed. Scale bar = 10 μm.

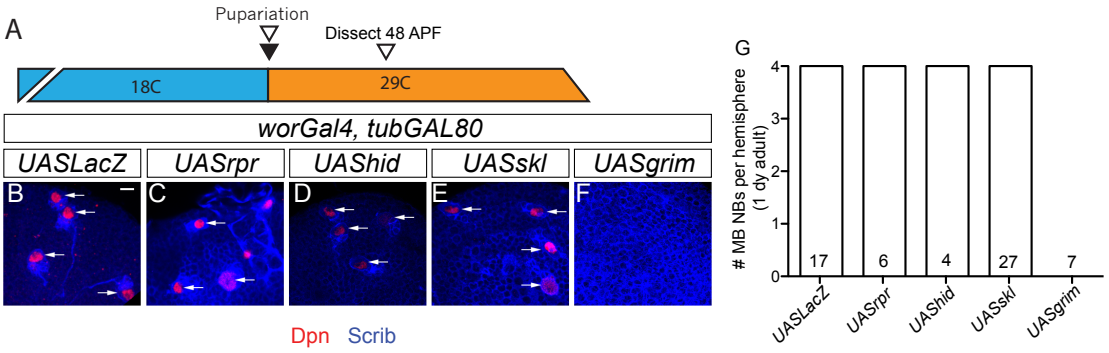

Appendix Figure 2: Over-expression of Grim is sufficient to eliminate MB neuroblasts early. (A) We used *worniuGAL4, tubGal80ts* to drive expression of the each apoptotic protein. We raised animals at 18°C, where GAL80 inhibits GAL4 activity. We shifted white prepupae to 29°C and assayed 48hr later. (B-F) Maximum intensity projections showing the dorsal surface of the brain in 48 APF animals. Scale bar = 10 μm. (G) The number of persisting MB neuroblasts in each of the indicated genotypes. The number on the bottom indicates the number of brain hemispheres assayed.

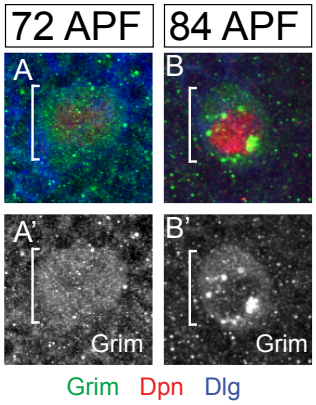

Appendix Figure 3. Grim localization in MB neuroblasts. Color overlays MB neuroblasts labeled with Grim (green), Dpn (red), and Dlg (blue) at 72 APF (A) and 84 APF (B). Single channel of grim (A',B'). The genotype is OregonR.

Related to Chapter 2

Appendix Table 1: List of transcription factors with putative binding sites in conserved regions located near grim and sickle.

Gene ID	FlybaseID	Gene Name
al	FBgn0000061	aristaless [Source:FlyBase;Acc:FBgn0000061]
ap	FBgn0267978	apterous [Source:FlyBase;Acc:FBgn0267978]
ase	FBgn0000137	asense [Source:FlyBase;Acc:FBgn0000137]
ato	FBgn0010433	atonal [Source:FlyBase;Acc:FBgn0010433]
bap	FBgn0004862	bagpipe [Source:FlyBase;Acc:FBgn0004862]
bcd	FBgn0000166	bicoid [Source:FlyBase;Acc:FBgn0000166]
bigmax	FBgn0039509	
bowl	FBgn0004893	brother of odd with entrails limited [Source:FlyBase;Acc:FBgn0004893]
br	FBgn0283451	broad [Source:FlyBase;Acc:FBgn0283451]
btn	FBgn0014949	buttonless [Source:FlyBase;Acc:FBgn0014949]
cad	FBgn0000251	caudal [Source:FlyBase;Acc:FBgn0000251]
caup	FBgn0015919	caupolican [Source:FlyBase;Acc:FBgn0015919]
CG12605	FBgn0035481	
CG15601	FBgn0030673	
CG33557	FBgn0053557	
CG34031	FBgn0054031	
CG4238	FBgn0031384	
CG4404	FBgn0030432	
CG5953	FBgn0032587	
CG7386	FBgn0035691	
CG8281	FBgn0035824	
Clk	FBgn0023076	Clock [Source:FlyBase;Acc:FBgn0023076]
CrebA	FBgn0004396	Cyclic-AMP response element binding protein A [Source:FlyBase;Acc:FBgn0004396]
cwo	FBgn0259938	clockwork orange [Source:FlyBase;Acc:FBgn0259938]
cyc	FBgn0023094	cycle [Source:FlyBase;Acc:FBgn0023094]
D19A	FBgn0022935	
da	FBgn0267821	daughterless [Source:FlyBase;Acc:FBgn0267821]
Doc2	FBgn0035956	Dorsocross2 [Source:FlyBase;Acc:FBgn0035956]
dpn	FBgn0010109	deadpan [Source:FlyBase;Acc:FBgn0010109]
dsf	FBgn0015381	dissatisfaction [Source:FlyBase;Acc:FBgn0015381]
E(spl)m3-HLH	FBgn0002609	Enhancer of split m3, helix-loop-helix [Source:FlyBase;Acc:FBgn0002609]
E(spl)mbeta-HLH	FBgn0002733	Enhancer of split mbeta, helix-loop-helix [Source:FlyBase;Acc:FBgn0002733]
E(spl)mdelta-HLH	FBgn0002734	Enhancer of split mdelta, helix-loop-helix [Source:FlyBase;Acc:FBgn0002734]
E(spl)mgamma-HLH	FBgn0002735	Enhancer of split mgamma, helix-loop-helix [Source:FlyBase;Acc:FBgn0002735]

Eip93F	FBgn0264490	Ecdysone-induced protein 93F [Source:FlyBase;Acc:FBgn0264490]
en	FBgn0000577	engrailed [Source:FlyBase;Acc:FBgn0000577]
erm	FBgn0031375	earmuff [Source:FlyBase;Acc:FBgn0031375]
esg	FBgn0001981	escargot [Source:FlyBase;Acc:FBgn0001981]
Fer1	FBgn0037475	48 related 1 [Source:FlyBase;Acc:FBgn0037475]
Fer2	FBgn0038402	48 related 2 [Source:FlyBase;Acc:FBgn0038402]
Fer3	FBgn0037937	48 related 3 [Source:FlyBase;Acc:FBgn0037937]
GATAd	FBgn0032223	
GATAe	FBgn0038391	
gce	FBgn0261703	germ cell-expressed bHLH-PAS [Source:FlyBase;Acc:FBgn0261703]
Gsc	FBgn0010323	Goosecoid [Source:FlyBase;Acc:FBgn0010323]
gt	FBgn0001150	giant [Source:FlyBase;Acc:FBgn0001150]
H	FBgn0001169	hairy [Source:FlyBase;Acc:FBgn0001169]
her	FBgn0001185	hermaphrodite [Source:FlyBase;Acc:FBgn0001185]
Hey	FBgn0027788	Hairy/E(spl)-related with YRPW motif [Source:FlyBase;Acc:FBgn0027788]
hkb	FBgn0261434	huckebein [Source:FlyBase;Acc:FBgn0261434]
HLH4C	FBgn0011277	Helix loop helix protein 4C [Source:FlyBase;Acc:FBgn0011277]
ind	FBgn0025776	intermediate neuroblasts defective [Source:FlyBase;Acc:FBgn0025776]
Jra	FBgn0001291	Jun-related antigen [Source:FlyBase;Acc:FBgn0001291]
kay	FBgn0001297	kayak [Source:FlyBase;Acc:FBgn0001297]
ken	FBgn0011236	ken and barbie [Source:FlyBase;Acc:FBgn0011236]
Kr	FBgn0001325	Kruppel [Source:FlyBase;Acc:FBgn0001325]
lola	FBgn0283521	longitudinals lacking [Source:FlyBase;Acc:FBgn0283521]
Met	FBgn0002723	Methoprene-tolerant [Source:FlyBase;Acc:FBgn0002723]
mio	FBgn0031399	missing oocyte [Source:FlyBase;Acc:FBgn0031399]
Mitf	FBgn0263112	
nau	FBgn0002922	nautilus [Source:FlyBase;Acc:FBgn0002922]
net	FBgn0002931	
nub	FBgn0085424	nubbin [Source:FlyBase;Acc:FBgn0085424]
oc	FBgn0004102	ocelliless [Source:FlyBase;Acc:FBgn0004102]
Oli	FBgn0032651	Olig family [Source:FlyBase;Acc:FBgn0032651]
onecut	FBgn0028996	
pdm2	FBgn0004394	POU domain protein 2 [Source:FlyBase;Acc:FBgn0004394]
Poxn	FBgn0003130	Pox neuro [Source:FlyBase;Acc:FBgn0003130]
prd	FBgn0003145	paired [Source:FlyBase;Acc:FBgn0003145]
Ptx1	FBgn0020912	
rib	FBgn0003254	ribbon [Source:FlyBase;Acc:FBgn0003254]
ro	FBgn0003267	rough [Source:FlyBase;Acc:FBgn0003267]
Rx	FBgn0020617	Retinal Homeobox [Source:FlyBase;Acc:FBgn0020617]
Scr	FBgn0003339	Sex combs reduced [Source:FlyBase;Acc:FBgn0003339]

sima	FBgn0266411	similar [Source:FlyBase;Acc:FBgn0266411]
sna	FBgn0003448	snail [Source:FlyBase;Acc:FBgn0003448]
srp	FBgn0003507	serpent [Source:FlyBase;Acc:FBgn0003507]
ss	FBgn0003513	spineless [Source:FlyBase;Acc:FBgn0003513]
Su(H)	FBgn0004837	Suppressor of Hairless [Source:FlyBase;Acc:FBgn0004837]
tai	FBgn0041092	taiman [Source:FlyBase;Acc:FBgn0041092]
tap	FBgn0015550	target of Poxn [Source:FlyBase;Acc:FBgn0015550]
tgo	FBgn0264075	tango [Source:FlyBase;Acc:FBgn0264075]
tin	FBgn0004110	tinman [Source:FlyBase;Acc:FBgn0004110]
tll	FBgn0003720	tailless [Source:FlyBase;Acc:FBgn0003720]
Trh	FBgn0035187	trachealess [Source:FlyBase;Acc:FBgn0035187]
ttk	FBgn0003870	tramtrack [Source:FlyBase;Acc:FBgn0003870]
twi	FBgn0003900	twist [Source:FlyBase;Acc:FBgn0003900]
Usf	FBgn0029711	
vnd	FBgn0261930	ventral nervous system defective [Source:FlyBase;Acc:FBgn0261930]
Vsx2	FBgn0263512	Visual system homeobox 2 [Source:FlyBase;Acc:FBgn0263512]
zen	FBgn0004053	zerknullt [Source:FlyBase;Acc:FBgn0004053]
Zif	FBgn0037446	Zinc-finger protein [Source:FlyBase;Acc:FBgn0037446]

Related to Chapter 2:
Appendix Table 2: Screen candidate regulators from literature

Gene name	Symbol	CG number	Class	Prediction
abdominal a	abd-A	CG11648	TF	lit(Hox)/modEncode
abdominal b	abd-B	CG11648	TF	lit(Hox)/modEncode
antennapedia	Antp	CG1028	TF	lit(Hox)
Broad	br	CG11491	TF	lit(apoptosis)
C-terminal Binding Protein	CtBP	CG7583	Chromatin modifer	Binds to modify chromatin with other targets
castor	cas	CG2102	TF	Temporal cascade
Cut	cut	CG11387	TF	lit(apoptosis)
Dacshund	dac	CG4952	TF	Lit(retinal determination)
daughterless	da	CG5102	TF	modEncode
Deformed	Dfd	CG2189	TF	lit(homeobox)
Dichete	D	CG5893	TF	Lit (apoptosis(
Distalless	Dll	CG3629	TF	lit(apoptosis)
dorsal	dl	CG6667	TF	modEncode
Ecdysone Receptor	EcR	CG1765	TF	lit(apoptosis)
Ecdysone Responsive Protein 74 EF	Eip74EF	CG32180	TF	lit(apoptosis)
Ecdysone Responsive protein 93F	E93	CG18389	TF	lit(apoptosis)
Empty Spiracles	ems	CG2988	TF	Expressed
Enhancer of zeste	E(z)	CG6502	Chromatin modfier	Chromatin modifier
Eyeless	ey	CG1464	TF	lit(retinal determination, Mushroom body expression, apoptosis)
forkhead	fkh	CG10002	TF	lit(apoptosis)
Grainyhead	grh	CG42311	TF	Temporal cascade
groucho	gro	CG8384	TF	Binds to modify chromatin with other targets
hairy	h	CG6494	Chromatin modifer, NB survival	modEncode
Hunchback	hb	CG9786	TF	Temporal cascade
Kruppel	Kr	CG3340	TF	Temporal cascade
labial	lab	CG1264	TF	lit(hox)
longitudinals lacking	lola	CG12052	TF	lit(apoptosis)
Medea	Med	CG1775	TF	modEncode
Methoprene tolerant	Met	CG1705	TF	lit(Ecdysone Signaling)
mod(mdg4)	mod(mdg4)	CG32491	Chromatin modifer	Lit (apoptosis)
nanos	nos	CG5637	RNA-binding Protein	lit(apoptosis)
nervous fingers	nerfin-1	CG13906	TF	Neuroblast elimination

Notch	N	CG3936	Receptor	lit(apoptosis)
Occeliless	oc	CG12154	TF	Lit(hox retinal determination)
Optix	Optix	CG18455	TF	Lit(retinal determination)
Gene name	Symbol	CG number	Class	Prediction
Polycomb	Pc	CG32443	Chromatin modifer	modEncode
abnormal chemosensory jump 6	acj6	CG9151	TF	lit(hox)
crocodile	croc	CG5069	TF	lit(head patterning)
Discs overgrown	Dco	CG2048	Kinase	lit(y2h)
Dorsal Related Immunity Factor	Dif	CG6794	TF	lit(NFKB)
Epidermal Growth factor receptor	EGFR	CG10079	Receptor	lit(survival)
eyes absent	eya	CG9554	TF/phosphatase	lit(retinal determination)
ftz transcription factor 1	ftz-f1	CG4059	TF	lit(ecdysone)
gooseberry-neuro	gsb-n	CG2692	TF	lit(apoptosis)
Hormone Receptor 39	HR39	CG8676	TF	lit(ecdysone)
Max	Max	CG9648	TF	lit(apoptosis)
Myc	dm	CG10798	TF	lit(apoptosis)
POU domain protein 2	Pdm2	CG12287	TF	Temporal cascade
probosopedia	pb	CG31481	TF	lit(hox)
Relish	Rel	CG11992	TF	lit(NKFB)
Retinal Homeobox	Rx	CG10052	TF	Lit(retinal determination)
Scarecrow	scro	CG17594	TF	Expression
senseless	sens	CG32120	TF	modEncode
Seven-up	svp	CG11502	TF	Temporal cascade
Sex Combs Reduced	Scr	CG1030	TF	lit(hox)
Sine Oculis	so	CG11121	TF	Lit(retinal determination)
Sloppy Paired 1	slp1	CG16738	TF	Temporal cascade
snail	sna	CG3956	Chromatin modifer	modEncode
Stat92E	Stat92E	CG4257	TF	lit(apoptosis)
Supressor Hairless	Su(H)	CG3497	TF	lit(apoptosis)
Tailless	tll	CG1378	TF	MB neuroblast/temp_cascade
Taiman	tai	CG13109	TF	lit(Ecdysone Signaling)
tao	tao	CG14217	Kinase	lit(apoptosis)
Torso	Tor	CG1389	Receptor	lit(apoptosis)
Transforming Growth Factor Beta activated Kinase 1	Tak1	CG18492	Kinase	Kinase putative interaction with skl
Trithoraxlike	Trl	CG33261	Chromatin modifer	modEncode/bioinfo
Twin of Eyeless	toy	CG11186	TF	MB neuroblast
twin of eyeless	toy	CG11186	TF	lit(apoptosis)
Ultrabithorax	Ubx	CG10388	TF	lit(hox)

Ultraspircle	usp	CG4380	TF	lit(ecdysone)
Ventral Veins Lacking	vvl	CG10037	TF	lit(apoptosis)
Visual System Homeobox 1	Vsx1	CG4136	TF	lit(hox/retinal determination)
Visual System Homeobox 2	Vsx2	CG33980	TF	lit(hox/retinal determination)
yorkie	yki	CG4005	TF	lit(apoptosis)
Zernkuilt	zen	CG1046	TF	lit(hox)

Appendix Table 3: Putative transcription factor binding sites near *grim* and *skl*

Transcription Factor	p.value	Seq.id	Location
E(spl)mbeta-HLH	5.44E-06	020158_002F	grim_3L:18,303,730..18304984
Rx	7.12E-05	020159_021F	grim_3L:18,306,586..18,307,282
ro	4.84E-05	020159_017F	grim_3L:18,306,586..18,307,282
bcd	5.95E-05	020124_001F	grim_3L:18,306,586..18,307,282
esg	4.10E-05	020121_011F	grim_3L:18,306,586..18,307,282
nau	4.03E-05	020121_011F	grim_3L:18,306,586..18,307,282
Clk	3.87E-06	020111_003F	grim_3L:18,306,586..18,307,282
Clk	1.55E-05	020111_003F	grim_3L:18,306,586..18,307,282
E(spl)mdelta-HLH	6.47E-06	020158_002F	grim_3L:18,307,081..18,308,509
gce	9.50E-06	020158_002F	grim_3L:18,307,081..18,308,509
CG8281	4.44E-05	020127_030F	grim_3L:18,316,084..18,316,386
CAD	6.78E-05	020127_026F	grim_3L:18,316,084..18,316,386
trh	8.10E-06	020111_003F	grim_3L:18,316,084..18,316,386
Usf	2.86E-05	020111_003F	grim_3L:18,316,084..18,316,386
CrebA	1.55E-06	020111_003F	grim_3L:18,318,121..18,319,283
Scr	8.48E-05	020110_011F	grim_3L:18,318,121..18,319,283
CG33980	4.53E-05	020110_008F	grim_3L:18,318,121..18,319,283
Clk	4.72E-05	020105_003F	grim_3L:18,318,121..18,319,283
Mio	2.26E-05	020105_003F	grim_3L:18,318,121..18,319,283
btn	5.76E-05	020101_013F	grim_3L:18,318,121..18,319,283
vnd	1.30E-05	020121_004F	grim_3L:18,320,479..18,321,497
vnd	1.30E-05	020121_004F	grim_3L:18,320,479..18,321,497
D19A	1.54E-05	020118_010F	grim_3L:18,320,479..18,321,497
vnd	5.39E-05	020121_004F	grim_3L:18,323,100..18,324,336
tin	3.75E-05	020121_001F	grim_3L:18,323,100..18,324,336
Doc2	7.54E-05	020118_010F	grim_3L:18,323,100..18,324,336
ap	7.13E-05	020159_017F	grim_3L:18,329,066..18,329,594
tai	9.89E-06	020158_001F	grim_3L:18,329,066..18,329,594
erm	3.83E-05	020156_007F	grim_3L:18,329,066..18,329,594
Su(H)	3.39E-05	020156_007F	grim_3L:18,329,066..18,329,594
lola	1.73E-05	020156_005F	grim_3L:18,329,066..18,329,594
Her	5.73E-05	020132_006F	grim_3L:18,329,066..18,329,594
CG16778	5.57E-05	020132_004F	grim_3L:18,329,066..18,329,594
CG33980	3.99E-05	020123_006F	grim_3L:18,329,066..18,329,594
ro	7.52E-05	020123_006F	grim_3L:18,329,066..18,329,594

Vsx2	3.99E-05	020123_006F	grim_3L:18,329,066..18,329,594
CG33557	3.40E-05	020122_016F	grim_3L:18,329,066..18,329,594
CG33557	1.76E-05	020122_014F	grim_3L:18,329,066..18,329,594
hkb	1.07E-06	020122_008F	grim_3L:18,329,066..18,329,594
Hey	8.10E-05	020114_007F	grim_3L:18,329,066..18,329,594
zen	9.06E-05	020114_006F	grim_3L:18,329,066..18,329,594
zen	1.17E-05	020114_006F	grim_3L:18,329,066..18,329,594
sna	9.20E-05	020114_005F	grim_3L:18,329,066..18,329,594
da	2.98E-05	020114_004F	grim_3L:18,329,066..18,329,594
tap	2.98E-05	020114_004F	grim_3L:18,329,066..18,329,594
E(spl)mgamma-HLH	8.07E-05	020114_002F	grim_3L:18,329,066..18,329,594
tin	4.72E-05	020114_002F	grim_3L:18,329,066..18,329,594
Mitf	3.00E-05	020111_003F	grim_3L:18,329,066..18,329,594
Clk	4.72E-05	020105_004F	grim_3L:18,329,066..18,329,594
cyc	1.55E-05	020111_003F	grim_3L:18,331,384..18,331,950
E(spl)m3-HLH	3.72E-05	020111_003F	grim_3L:18,331,384..18,331,950
dsf	3.38E-05	021030_03F	grim_3L:18,332,615..18,332,929
GATAe	8.37E-05	020160_005F	grim_3L:18,332,615..18,332,929
al	8.17E-05	020159_017F	grim_3L:18,332,615..18,332,929
Kr	3.50E-05	020159_013F	grim_3L:18,332,615..18,332,929
da	7.60E-05	020127_019F	grim_3L:18,332,615..18,332,929
Gsc	9.24E-05	020124_001F	grim_3L:18,332,615..18,332,929
CG34031	5.66E-05	020121_009F	grim_3L:18,332,615..18,332,929
tin	1.74E-05	020121_004F	grim_3L:18,332,615..18,332,929
CG4404	2.95E-05	020117_007F	grim_3L:18,332,615..18,332,929
Hey	8.10E-05	020115_007F	grim_3L:18,332,615..18,332,929
dei	7.45E-05	020101_001F	grim_3L:18,332,615..18,332,929
Oli	1.08E-05	020101_001F	grim_3L:18,334,148..18,334,448
bowl	3.91E-05	020100_004F	grim_3L:18,334,148..18,334,448
CG34031	8.43E-05	020126_017F	grim_3L:18,339,770..18,340,070
gt	1.46E-05	020118_008F	grim_3L:18,339,770..18,340,070
br	9.35E-05	020117_012F	grim_3L:18,339,770..18,340,070
ase	6.61E-05	020102_005F	grim_3L:18,339,770..18,340,070
net	2.06E-05	020126_014F	grim_3L:18,345,085..18,345,515
h	5.18E-05	020111_003F	grim_3L:18,345,085..18,345,515
srp	7.10E-05	020160_005F	grim_3L:18,346,827..18,347,425
onecut	7.95E-05	020159_007F	grim_3L:18,346,827..18,347,425
sna	2.48E-05	020159_003F	grim_3L:18,346,827..18,347,425

bap	3.86E-05	020132_001F	grim_3L:18,346,827..18,347,425
Fer1	7.60E-05	020127_019F	grim_3L:18,346,827..18,347,425
Eip93F	2.43E-05	020126_010F	grim_3L:18,346,827..18,347,425
da	6.61E-05	020122_004F	grim_3L:18,346,827..18,347,425
da	3.67E-05	020122_004F	grim_3L:18,346,827..18,347,425
twi	1.59E-06	020120_005F	grim_3L:18,346,827..18,347,425
da	4.92E-05	020113_004F	grim_3L:18,346,827..18,347,425
Fer3	4.92E-05	020113_004F	grim_3L:18,346,827..18,347,425
Scr	8.48E-05	020109_011F	grim_3L:18,346,827..18,347,425
CG33980	4.53E-05	020109_008F	grim_3L:18,346,827..18,347,425
Fer1	7.60E-05	020128_015F	grim_3L:18,348,503..18,349,787
CG17181	1.52E-06	020126_014F	grim_3L:18,348,503..18,349,787
oc	3.07E-05	020124_001F	grim_3L:18,348,503..18,349,787
twi	5.66E-05	020121_020F	grim_3L:18,348,503..18,349,787
CG12605	1.35E-06	020121_011F	grim_3L:18,348,503..18,349,787
da	4.03E-05	020121_011F	grim_3L:18,348,503..18,349,787
h	6.81E-05	020111_003F	grim_3L:18,348,503..18,349,787
HLH106	3.32E-05	020111_003F	grim_3L:18,348,503..18,349,787
tgo	2.42E-06	020111_003F	grim_3L:18,348,503..18,349,787
da	3.67E-05	020107_003F	grim_3L:18,348,503..18,349,787
HLH4C	3.67E-05	020107_003F	grim_3L:18,348,503..18,349,787
ss	4.49E-06	020126_019F	grim_3L:18,350,793..18,351,301
tgo	4.49E-06	020126_019F	grim_3L:18,350,793..18,351,301
Kr	1.29E-05	020120_004F	grim_3L:18,350,793..18,351,301
CG7386	9.04E-05	020118_010F	grim_3L:18,350,793..18,351,301
tll	2.91E-05	021030_03F	grim_3L:18,353,455..18,354,073
dpn	9.94E-05	020160_011F	grim_3L:18,353,455..18,354,073
Fer2	4.47E-05	020160_011F	grim_3L:18,353,455..18,354,073
ttk	6.81E-06	020160_006F	grim_3L:18,353,455..18,354,073
GATAd	3.27E-05	020160_005F	grim_3L:18,353,455..18,354,073
erm	7.19E-06	020159_014F	grim_3L:18,353,455..18,354,073
erm	7.79E-06	020159_014F	grim_3L:18,353,455..18,354,073
h	5.68E-05	020111_003F	grim_3L:18,354,811..18,355,837
al	8.96E-05	020114_001F	grim_3L:18,360,704..18,362,238
tgo	2.53E-05	020111_003F	grim_3L:18,360,704..18,362,238
zen	3.75E-05	020108_004F	grim_3L:18,360,704..18,362,238
rib	5.93E-05	020108_002F	grim_3L:18,360,704..18,362,238
ind	8.49E-05	020114_001F	grim_3L:18,361,247..18,362,615

tgo	8.10E-06	020111_003F	grim_3L:18,361,247..18,362,615
ato	7.95E-05	020107_003F	grim_3L:18,361,247..18,362,615
da	7.95E-05	020107_003F	grim_3L:18,361,247..18,362,615
ato	9.29E-05	020159_013F	grim_3L:18,364,229..18,364,569
caup	3.72E-05	020126_009F	grim_3L:18,364,229..18,364,569
hkb	1.07E-06	020122_008F	grim_3L:18,364,229..18,364,569
HLH106	5.33E-05	020111_003F	grim_3L:18,366,305..18,366,991
Met	3.87E-06	020111_003F	grim_3L:18,366,305..18,366,991
Mio	4.91E-05	020111_003F	grim_3L:18,366,305..18,366,991
Vsx2	4.53E-05	020109_008F	grim_3L:18,366,305..18,366,991
CG8281	4.44E-05	020128_026F	grim_3L:18,369,496..18,369,796
CG34031	4.35E-05	020160_003F	grim_3L:18,370,849..18,371,149
Mitf	9.83E-05	020158_028F	grim_3L:18,370,849..18,371,149
CG15601	5.97E-05	020131_006F	grim_3L:18,370,849..18,371,149
kay	6.92E-05	020121_020F	grim_3L:18,370,849..18,371,149
bcd	3.74E-05	020124_001F	grim_3L:18319715..18320097
ap	9.69E-05	020123_006F	grim_3L:18319715..18320097
bigmax	4.91E-05	020111_003F	grim_3L:18319715..18320097
nub	6.32E-06	020159_017F	grim_3L:18338020..18448662
bap	5.30E-05	020132_001F	grim_3L:18338020..18448662
tai	2.42E-06	020111_003F	grim_3L:18338020..18448662
D19A	7.04E-05	020101_002F	grim_3L:18338020..18448662
ind	6.05E-05	020159_017F	grim_3L:18355996..18357362
Rx	8.80E-05	020159_017F	grim_3L:18355996..18357362
Met	4.54E-05	020158_002F	grim_3L:18355996..18357362
Clk	3.75E-05	020158_001F	grim_3L:18355996..18357362
da	7.60E-05	020128_015F	grim_3L:18355996..18357362
tap	6.61E-05	020122_004F	grim_3L:18355996..18357362
tap	3.67E-05	020122_004F	grim_3L:18355996..18357362
Jra	6.92E-05	020121_020F	grim_3L:18355996..18357362
Gsc	6.89E-05	020102_005F	grim_3L:18355996..18357362
Ptx1	2.17E-05	020124_001F	skl_3L:18,439,003..18,440,463
sna	2.17E-05	020107_003F	skl_3L:18,439,003..18,440,463
da	1.08E-05	020101_001F	skl_3L:18,439,003..18,440,463
pdm2	4.13E-05	020159_017F	skl_3L:18,447,149..18,448,383
erm	2.18E-05	020158_026F	skl_3L:18,447,149..18,448,383
Kr	3.58E-06	020158_025F	skl_3L:18,447,149..18,448,383
Kr	8.86E-06	020158_025F	skl_3L:18,447,149..18,448,383

KR	1.55E-07	020158_025F	skl_3L:18,447,149..18,448,383
Gsc	8.98E-05	020158_024F	skl_3L:18,447,149..18,448,383
erm	6.13E-05	020130_003F	skl_3L:18,447,149..18,448,383
da	2.06E-05	020126_014F	skl_3L:18,447,149..18,448,383
esg	7.96E-05	020126_014F	skl_3L:18,447,149..18,448,383
Zif	7.91E-06	020125_003F	skl_3L:18,447,149..18,448,383
bcd	9.61E-05	020124_001F	skl_3L:18,447,149..18,448,383
br	9.91E-05	020117_012F	skl_3L:18,447,149..18,448,383
CG34031	5.67E-05	020117_010F	skl_3L:18,447,149..18,448,383
br	6.31E-06	020111_003F	skl_3L:18,447,149..18,448,383
E(spl)mdelta-HLH	5.76E-05	020111_003F	skl_3L:18,447,149..18,448,383
Vsx2	4.53E-05	020110_008F	skl_3L:18,447,149..18,448,383
sna	4.41E-05	020107_003F	skl_3L:18,447,149..18,448,383
bap	6.92E-05	020101_006F	skl_3L:18,447,149..18,448,383
tin	7.26E-05	021030_05F	skl_3L:18,451,217..18,451,959
CG5953	5.55E-05	020159_016F	skl_3L:18,451,217..18,451,959
nub	4.57E-05	020158_020F	skl_3L:18,451,217..18,451,959
Clk	9.50E-06	020158_002F	skl_3L:18,451,217..18,451,959
Clk	9.89E-06	020158_001F	skl_3L:18,451,217..18,451,959
bcd	5.82E-05	020129_006F	skl_3L:18,451,217..18,451,959
al	7.41E-05	020129_003F	skl_3L:18,451,217..18,451,959
cwo	4.85E-05	020129_002F	skl_3L:18,451,217..18,451,959
CAD	6.78E-05	020128_022F	skl_3L:18,451,217..18,451,959
lola	7.07E-05	020122_006F	skl_3L:18,451,217..18,451,959
Poxn	6.13E-05	020122_005F	skl_3L:18,451,217..18,451,959
Hey	8.10E-05	020115_007F	skl_3L:18,451,217..18,451,959
sima	2.53E-05	020111_003F	skl_3L:18,451,217..18,451,959
ken	2.40E-05	020108_010F	skl_3L:18,451,217..18,451,959
Mio	2.26E-05	020105_004F	skl_3L:18,451,217..18,451,959
da	7.45E-05	020101_001F	skl_3L:18,451,217..18,451,959
en	7.54E-05	020159_021F	skl_3L:18,452,060..18,453,586
Clk	4.54E-05	020158_002F	skl_3L:18,452,060..18,453,586
E(spl)m3-HLH	1.14E-05	020158_002F	skl_3L:18,452,060..18,453,586
Met	3.75E-05	020158_001F	skl_3L:18,452,060..18,453,586
Ptx1	4.14E-05	020124_001F	skl_3L:18,452,060..18,453,586
prd	4.33E-05	020122_005F	skl_3L:18,452,060..18,453,586
ro	8.78E-05	020114_001F	skl_3L:18,452,060..18,453,586

Related to Chapter 3

While characterizing the pattern of E93 expression during development, we observed a difference between two different tools. We used an E93 protein trap line (MI05200; E93GFP). The P element containing GFP was inserted into the large intron of E93 (Appendix 3A) (Venken et al. 2011). This line has been previously characterized as a functional allele as it complements a know null allele of E93 (Uyehara et al. 2017). With immunostaining of E93 on control animals we observed E93 absent in larval, stages when it is expressed by other neuroblast lineages (Syed et al. 2017b). E93GFP was expressed early in MB neuroblasts, but it expression was absent from MB neuroblasts at 48hr APF.

The differences in expression between endogenous E93 and the protein trap lead us wonder if the P element carrying E93GFP disrupted a cis-regulatory element located within the intron. To first characterize this, we assayed the pattern of GFP expression with driven by two 3.9kb fragments fused to Gal4 from Janelia, R84C02 and R84C12. R84C02 contains the loci with the insertion. R84C02 is expression is absent from MB neuroblasts in wL3 larvae, but it matches the pattern of E93 immunostaining. R84C12 downstream of the insertion and does not drive expression in MB neuroblasts in wL3 or pupal stages (Appendix Fig. 1 H,I).

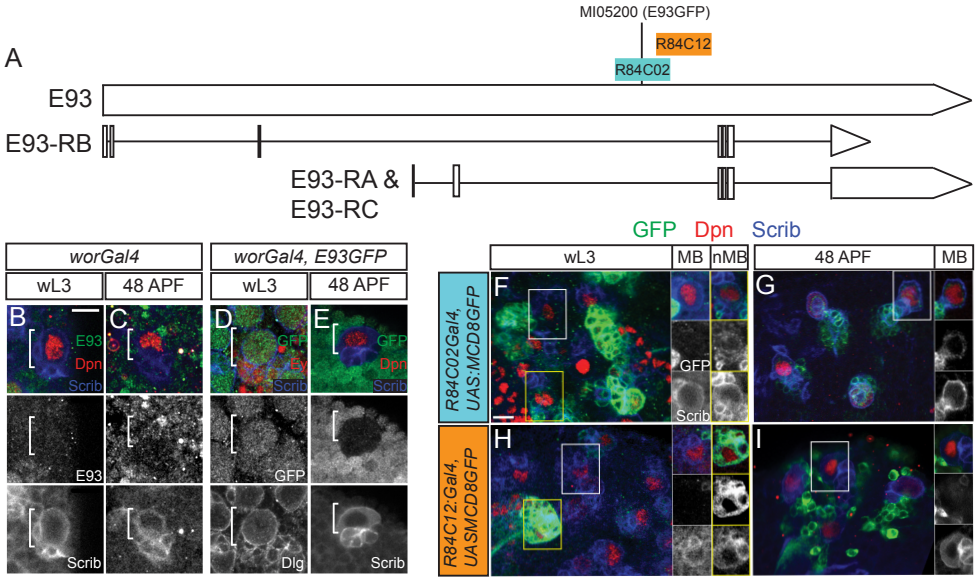

Appendix Fig. 1. Identification of a possible regulatory region located in a large E93 intron. (A) Diagram of the E93 locus, showing the structure of its three transcripts. The top indicates location of transgenes used in experiments below. MI05200 is a P-element insertion carrying GFP flanked by splice acceptor and donor sites used for protein trapping. R84C02 and R84C12 are fragments of E93 large intron fused to Gal4. (B-E) Covered overlay of MB neuroblasts showing gray scale images below. (B,C) Control animals labeled with anti-E93 at the indicated time points. (D,E) Small Z projections of the central brain GFP protein trap inserted into the endogenous E93 loci (diagramed above). Characterization of GFP expression pattern driven by one of two partially overlapping constructs containing ~3.9kb fused to GAL4 that were generated by the Janelia Flylight collection. Insets indicate show single planes MB neuroblasts (MB) or non-MB neuroblasts (nMB). Scale bar = 10 μm

Appendix Table 3: Predicted transcription factor motifs in R84C02.

Symbol	FlybaseID	Gene Name
Abd-B	FBgn0000015	Abdominal B [Source:FlyBase;Acc:FBgn0000015]
Aef1	FBgn0005694	Adult enhancer factor 1 [Source:FlyBase;Acc:FBgn0005694]
cad	FBgn0000251	caudal [Source:FlyBase;Acc:FBgn0000251]
CG11504	FBgn0039733	
CG3838	FBgn0032130	
CG5953	FBgn0032587	
cic	FBgn0262582	capicua [Source:FlyBase;Acc:FBgn0262582]
cyc	FBgn0023094	cycle [Source:FlyBase;Acc:FBgn0023094]
da	FBgn0267821	daughterless [Source:FlyBase;Acc:FBgn0267821]
Deaf1	FBgn0013799	Deformed epidermal autoregulatory factor-1 [Source:FlyBase;Acc:FBgn0013799]
fru	FBgn0004652	fruitless [Source:FlyBase;Acc:FBgn0004652]
hb	FBgn0001180	hunchback [Source:FlyBase;Acc:FBgn0001180]
kni	FBgn0001320	knirps [Source:FlyBase;Acc:FBgn0001320]
lola	FBgn0283521	longitudinals lacking [Source:FlyBase;Acc:FBgn0283521]
Max	FBgn0017578	
mio	FBgn0031399	missing oocyte [Source:FlyBase;Acc:FBgn0031399]
Mitf	FBgn0263112	
Mnt	FBgn0023215	
nau	FBgn0002922	nautilus [Source:FlyBase;Acc:FBgn0002922]
odd	FBgn0002985	odd skipped [Source:FlyBase;Acc:FBgn0002985]
Oli	FBgn0032651	Olig family [Source:FlyBase;Acc:FBgn0032651]
pad	FBgn0038418	poils au dos [Source:FlyBase;Acc:FBgn0038418]
slbo	FBgn0005638	slow border cells [Source:FlyBase;Acc:FBgn0005638]
su(Hw)	FBgn0003567	suppressor of Hairy wing [Source:FlyBase;Acc:FBgn0003567]
twi	FBgn0003900	twist [Source:FlyBase;Acc:FBgn0003900]
zen	FBgn0004053	zerknullt [Source:FlyBase;Acc:FBgn0004053]

E93 is expressed in late born MB neurons

Temporal patterning in the neuroblast affects the molecular identity of the neurons and glia that they generate (Doe 2017). While characterizing the role of E93 in terminating the MB neuroblast lineage, we found that expression of E93 is retained in a subset of late born MB neurons.

We labeled 1 dy old adult brains with Dacshund (Dac) marking MB neurons, E93, and either Imp or Syp. Imp is enriched in the early born neurons, while Syp is enriched in the later born neurons (Liu et al. 2015). We found that E93 was absent from Imp+ early born MB neurons and enriched in the late born Syp+ neurons. This suggests that neurons generated during the E93+ temporal window retain expression of E93.

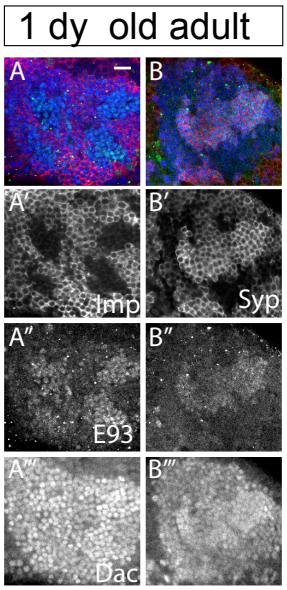

Appendix Figure 2. E93 expression is restricted to Imp-/Syp+ α/β MB neurons in adult animals.(A) Color overlays of the dorsal surface of control animals labeled with Imp (A) or Syp (B) (red), E93 (green), and a marker for MB neurons Dacshund (Dac) (blue). Below single channels of Imp (A') or Syp (B'), E93 (A'',B''), and Dac (A''',B'''). Scale bar = 10 μm.

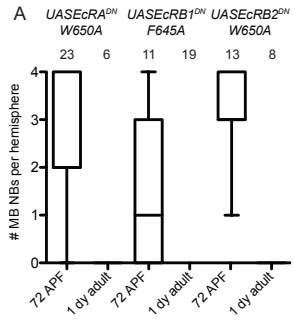

Appendix Figure 3. EcR dominant negative promotes early loss of MB neuroblasts. (A) Quantification of number of MB neuroblasts in the indicated genotypes and stages. Box and whisker plots indicate the number of persisting MB neuroblasts.

KEY RESOURCE TABLE

REAGENT OR	SOURCE	IDENTIFIER
ANTIBODIES		
Rabbit anti-Scribble Antibody (1:1000)	Gift from Chris Q. Doe	N/A
Rat anti-Dpn antibody (1:100)	Abcam	ab195173
Chicken anti-GFP Antibody (1:500)	Abcam	ab13970
Rabbit anti-phospho-S10-Histone (1:1000)	Abcam	ab5176
Guinea Pig anti-E93 Antibody (1:200)	Gift from Chris Q. Doe	N/A
Rabbit anti-Tll Antibody (1:200)	Gift from Claude Desplan	N/A
Rabbit anti-Foxo Antibody (1:500)	Gift from R. Tjian	N/A
Rabbit anti-Ey Antibody (1:2000)	Gift from Uwe Waldorf	N/A
Mouse anti-Dlg Antibody (1:40)	Developmental Studies Hybridoma Bank	4F3
Mouse anti-Fas2 Antibody (1:200)	Developmental Studies Hybridoma Bank	1D4

Rabbit anti-dsRed (1:1000)	Clontech	632496
Goat anti-mouse Alexa 488 secondary antibody (1:1000)	Thermo Fisher Scientific	Catalog # A-11001
Goat anti-mouse Alexa 555 secondary antibody (1:1000)	Thermo Fisher Scientific	Catalog # A-21422
Goat anti-mouse Alexa 633 secondary antibody (1:1000)	Thermo Fisher Scientific	Catalog # A-21052
Goat anti-guinea pig Alexa 488 secondary antibody (1:1000)	Thermo Fisher Scientific	Catalog # A-11073
Goat anti-rabbit Alexa 405 secondary antibody (1:1000)	Thermo Fisher Scientific	Catalog # A-31556
Goat anti-rabbit Alexa 488 secondary antibody (1:1000)	Thermo Fisher Scientific	Catalog # A-11034
Goat anti-rabbit Alexa 633 secondary antibody (1:1000)	Thermo Fisher Scientific	Catalog # A-21071
Goat anti-rat Alexa 488 secondary antibody (1:1000)	Thermo Fisher Scientific	Catalog # A-11006
Goat anti-rat Alexa 555 secondary antibody (1:1000)	Thermo Fisher Scientific	Catalog # A-21434

CHEMICALS		
SlowFade™ Diamond antifade reagent	Invitrogen	S36963
SlowFade™ Gold antifade reagent	Invitrogen	S36937
Normal Goat Serum	Thermo Fisher Scientific	31873
Paraformaldehyde 16% solution EM grade	Electron Microscopy Sciences	15710

SOFTWARE		
ImageJ/Fiji	Fiji	http://fiji.sc/
LAS AF	Leica Microsystems	https://www.leica-microsystems.com/products/microscope-software/details/product/leica-las-x-ls/
Imaris	Bitplane	http://www.bitplane.com/
Prism 5	Graphpad	https://www.graphpad.com/scientific-software/prism/
Photoshop CS6	Adobe	http://www.adobe.com/uk/products/photoshop.html
Illustrator CS6	Adobe	http://www.adobe.com/uk/products/illustrator.html

EXPERIMENTAL MODEL: ORGANISM STRAIN		
OregonR	Bloomington Drosophila Stock Center	
wor-Gal4	Chris Doe	N/A
OK107-Gal4	Bloomington Drosophila Stock Center	854
pcna:GFP	(Thacker et al., 2003)	
UAS-mCD8GFP	Bloomington Drosophila Stock Center	5137
UAS-Eip93F (HMC04773)	Bloomington Drosophila Stock Center	57868
UAS-Eip93F (KK108140)	Vienna Stock Center	V104390
UAS-Eip93F WT	Zurich FlyORF	F000587
Act5c-FRT-CD2-FRT-Gal4, UAS-RFP	Bloomington Drosophila Stock Center	30558
Act5c-FRT-CD2-FRT-Gal4, UAS-GFP	Iswar Hariharan	N/A
hsFlp (on X)	Iswar Hariharan	N/A
UAS-GFPmChAtg8	Bloomington Drosophila Stock Center	37749
UAS-GFPAtg8	Bloomington Drosophila Stock Center	51656
UAS-miRHG	Siegrist et al., 2010	NA
UAS-dp60	Weinkove et al., 1999	NA
UAS-InR RNAi (GL00139)	Bloomington Drosophila Stock Center	35251
UAS-Alk RNAi (JF02668)	Bloomington Drosophila Stock Center	27518
UAS-Imp RNAi (HMS01168)	Bloomington Drosophila Stock Center	34977
UAS-Syp RNAi (HMC04412)	Bloomington Drosophila Stock Center	56972
UAS-EcR RNAi (HMC03114)	Bloomington Drosophila Stock Center	50712

***Drosophila* genotypes per figure**	
Figure	**Genotype**
Figure 1B	*worGal4,UAS E93RNAi (*#HMC04773*); pcna:GFP*
Figure 1C	*worGal4,UAS E93RNAi (*#HMC04773*)* *worGal4,UAS E93RNAi 2 (*#KK108140*)* *UAS E93RNAi (*#HMC04773),*UAS mCD8GFP,OK107Gal4* *UAS mCD8GFP,OK107Gal4*
Figure 1E,F	*hsflp,act>CD2>Gal4,UASRFP,UAS E93RNAi (*#HMC04773)
Figure 1G,H	*worGal4/+ (OregonR)* *worGal4,UAS E93-WT*
Figure 2A-G	*worGal4/+ (OregonR)*
Figure 2H,I	*hsflp,act>CD2>Gal4,UASRFP,UAS E93RNAi (*#HMC04773)
Figure 3A,B	*worGal4/+ (OregonR)* *worGal4,UAS E93RNAi (*#HMC04773)
Figure 3C-I	*hsflp; act>CD2>Gal4,UASRFP,UAS E93RNAi (*#HMC04773)
Figure 3J	*worGal4,UAS E93RNAi (*#HMC04773) *worGal4,UAS dp60, UAS E93RNAi (*#HMC04773)
Figure 3K,O,P	*worGal4/+ (OregonR)*
Figure 3L,O,P	*worGal4,UAS E93RNAi (*#HMC04773)
Figure 3M,O,P	*worGal4,UAS dp60,UAS E93RNAi (*#HMC04773)

Figure 3N,O,P	*worGal4,UAS dp60*
Figure 4A,C,E,J,K	*worGal4,UAS GFP-mCh-Atg8*
Figure 4B,D,F,G,J,K	*worGal4,UAS GFP-mCh-Atg8,UAS E93RNAi (*#HMC04773)
Figure 4H,L	*worGal4,UAS GFP-mCh-Atg8,UAS dp60*
Figure 4I,L	*worGal4,UAS GFP-Atg8,UAS dp60,UAS E93RNAi (*#HMC04773)
Figure 5A,D	*worGal4,UAS E93RNAi (*#HMC04773)
Figure 5B,D	*worGal4,UAS miRHG*
Figure 5C,D	*worGal4,UAS miRHG,UAS E93RNAi (*#HMC04773)
Figure 6B	*hsflp,act>CD2>Gal4,UASRFP,UAS E93RNAi (*#HMC04773)
Figure 6D,F	*worGal4/+ (OregonR)*
Figure 6E,F	*worGal4,UAS EcRRNAi*
Figure 6G,H,I	*hsflp,act>CD2>Gal4,UASRFP,UAS SypRNAi*
Figure 6J,K,L	*hsflp,act>CD2>Gal4,UASRFP,UAS ImpRNAi*
Figure 6M,N,O	*hsflp,act>CD2>Gal4,UAS GFP,UAS ImpRNAi,UAS EcRRNAi*
Figure 6P,Q,R	*hsflp,act>CD2>Gal4,UAS GFP,UAS ImpRNAi,UAS SypRNAi*
Figure 7A	*worGal4/+ (OregonR)* *worGal4,UAS E93RNAi (*#HMC04773) *worGal4,UAS ImpRNAi* *worGal4,UAS ImpRNAi,UAS E93RNAi (*#HMC04773) *worGal4,UAS SypRNAi* *worGal4,UAS ImpRNAi,UAS SypRNAi*

Figure 7B,C,D,E	*hsflp,act>CD2>Gal4,UASRFP,UAS SypRNAi* *hsflp,act>CD2>Gal4,UASRFP,UAS SypRNAi,UAS E93-WT*
Figure S2A,D,E. Related to Figure 3	*worGal4,UAS E93RNAi (*#HMC04773)
Figure S2B,D,E. Related to	*worGal4,UAS InRRNAi,UAS E93RNAi (*#HMC04773)
Figure S2C,D,E. Related to	*worGal4,UAS AlkRNAi,UAS E93RNAi (*#HMC04773)
Figure S3A. Related to Figure 4	*worGal4,UAS GFP-mCh-Atg8* *worGal4,UAS GFP-mCh-Atg8,UAS E93RNAi (*#HMC04773)
Figure S4A. Related to Figure 6	*worGal4/+ (OregonR)*
Figure S4B. Related to Figure 6	*worGal4,UAS EcRRNAi*
Figure S4C. Related to Figure 6	*hsflp,act>CD2>Gal4,UASRFP,UAS EcRRNAi*
Figure S4D,F. Related to Figure 6	*worGal4,UAS SypRNAi*
Figure S4E,F. Related to Figure 6	*worGal4,UAS EcRRNAi*
Figure S4F. Related to Figure 6	*worGal4/+ (OregonR)*